LA-UR-21-29906

Title: Producing ENDF/B-quality Evaluations of 239Pu(n,f) and 235U(n,f) Average Prompt Neutron Multiplicities using the CGMF Model

Author(s): Neudecker, Denise
Lovell, Amy Elizabeth
Talou, Patrick

Intended for: Report

Issued: 2021-10-06 (Draft)

Producing ENDF/B-quality Evaluations of ^{239}Pu(n,f) and ^{235}U(n,f) Average Prompt Neutron Multiplicities using the CGMF Model

D. Neudecker, A.E. Lovell, P. Talou
Los Alamos National Laboratory, Los Alamos, NM, 87545, USA

October 4, 2021

Contents

Abstract

This report documents evaluations of the neutron-induced ^{239}Pu and ^{235}U average prompt neutron multiplicities, $\overline{\nu}_p$, using the `CGMF` model developed at LANL. These evaluations are not updates of existing ENDF/B-VIII.0 nuclear data, but were both re-done from "scratch". That is, all experimental data were extracted from EXFOR, re-normalized to the newest nuclear data representing monitor observables, and detailed uncertainties were estimated from information in EXFOR as well as from templates of expected measurement uncertainties. We also included experimental data that were not yet available for ENDF/B-VIII.0, for instance, the data of Marini *et al.* for ^{239}Pu(n,f) $\overline{\nu}_p$ or the data of Khoklov *et al.* for ^{235}U(n,f) $\overline{\nu}_p$. Finally, we include the `CGMF` model; it computes $\overline{\nu}_p$ based on model parameters that at the same time calculate fission fragments as a function of mass, $Y(A)$, the average total kinetic energy as a function of incident-neutron energy, $\langle TKE\rangle(E_{\mathrm{inc}})$, *etc.* Such a detailed fission model that ties together many fission quantities has not been used to date for any $\overline{\nu}_p$ evaluation in ENDF/B. Here, we show that we can get evaluated ^{235}U(n,f) and ^{239}Pu $\overline{\nu}_p$ that not only correspond well to experimental $\overline{\nu}_p$, but that the associated evaluated model parameters also yield parameterizations of $Y(A)$, $\langle TKE\rangle(E_{\mathrm{inc}})$, *etc.*, that correspond well to their respective experimental data. The new evaluated ^{239}Pu(n,f) $\overline{\nu}_p$ was also combined into a ^{239}Pu test file with

the newest nuclear data for the ^{239}Pu prompt-fission neutron spectrum and fission cross sections. This new ^{239}Pu file performed reasonably well in predicting PU-MET-FAST assemblies, reaction rates in Jezebel and Flattop and three LLNL pulsed spheres. Due to that, the new ^{239}Pu(n,f) $\overline{\nu}_p$ evaluation presented here is being considered for ENDF/B-VIII.1. Hence, we can show here that CGMF is able to produce ENDF/B quality $\overline{\nu}_p$ nuclear data.
Keywords: ^{239}Pu, ^{235}U, Average Prompt-fission Neutron Multiplicity, CGMF

LA-UR-21-

1 Introduction

This report documents our progress towards two FY21 NCSP (Nuclear Criticality Safety Program) milestones for LANL. The text for both milestones is the same, and states in each case: "Evaluate PFNS and multiplicity consistently, including angular information about prompt neutrons". In one case, this applies to the isotope ^{239}Pu, in the other to ^{235}U. The goal was to use the CGMF model [1] for consistently modeling the average prompt-neutron multiplicity, $\overline{\nu}_p$, and PFNS (Prompt Fission Neutron Spectrum). We did not succeed in modeling the PFNS consistently with $\overline{\nu}_p$ as there seems to be a major model defect in the prediction of PFNS. Progress towards reducing this model defect is documented in the companion report, Ref. [2].

However, we produced an evaluation of $\overline{\nu}_p$ for ^{239}Pu(n,f) using CGMF that is being considered for ENDF/B-VIII.1. This tool has not been used for $\overline{\nu}_p$ evaluations so far. So, it was not clear whether evaluated $\overline{\nu}_p$ with CGMF would correspond to experimental data of this observable, while favorably linking back to other input quantities of CGMF such as $Y(A)$, $\langle TKE \rangle(E_{\mathrm{inc}})$, *etc.* However, such an evaluated $\overline{\nu}_p$ was achieved for ^{239}Pu(n,f). Moreover, the ^{239}Pu(n,f) $\overline{\nu}_p$ performs well when used simultaneously with a new PFNS [3] and fission cross sections [4] for simulations of criticality, reaction rates and LLNL pulsed sphere neutron-leakage spectra. Hence, this report shows for the first time how CGMF can be used to produce ENDF/B-quality nuclear data for ^{239}Pu $\overline{\nu}_p$. First results for ^{235}U $\overline{\nu}_p$ are also shown.

Section 2 discusses the input to the evaluations and Section 3 the evaluation algorithms used. Several types of results are shown in detail in Section 4. On the one hand, we compare the evaluated $\overline{\nu}_p$ to experimental data of the same quantity but also show in how far the evaluated model parameters link back to $Y(A)$, $\langle TKE \rangle(E_{\mathrm{inc}})$, *etc.* On the other hand, we show validation results calculated with these new data compared to the experimental validation responses. All of this information is assembled to showcase that an evaluation of $\overline{\nu}_p$ can be achieved that includes detailed fission modeling while yielding reasonable predictions of validation experiments representing application calculations in the field of criticality and safety, shielding, *etc.*

2 Input to the Evaluation

2.1 Model Input

There are several models and data needed for a complete CGMF calculation. Because we have already described these models in detail in our FY20 report [5] (along with the full CGMF publication [1]), we will not repeat the full information here but instead give an overview of the model.

Since CGMF spans incident neutrons from thermal to 20 MeV, we first need to know what compound nucleus is fissioning. The multi-chance fission probabilities are tabulated and sampled at the given incident energy to determine the reaction. If any neutrons are emitted before fission occurs, they can either be emitted from the equilibriated compound nucleus or inelastically scattered from the target (only energetically possible after approximately the opening of third-chance fission). In the first case, the neutron energies are sampled from an evaporation spectrum and are distributed uniformly in the center-of-mass frame of the compound nucleus. In the second case, the neutron energy and angular distribution is more representative of inelastically scattered neutrons.

Once any pre-fission neutrons have been emitted, the excitation energy of the resulting compound nucleus is determined, and the split into the heavy and light fission fragment is determined based on distributions in mass and charge that were phenomenologically modeled and fit to available experimental data. The total kinetic energy of the fragment pair is sampled from a similarly constrained distribution, then this mass split—and the Q value of the resulting reaction—determines the total excitation energy. The total excitation and kinetic energies are split between the heavy and light fragments. The spin and parity of each fragment are also sampled. The initial conditions of the fission fragments, $(A, Z, \mathrm{TKE}, J, \pi)$, are used to initiate the Hauser-Feshbach statistical decay of prompt neutrons and γ rays, which conserves energy, spin, and parity at each step in the decay.

For each fission event, we keep track of the initial conditions of the fission fragments, along with their momenta before and after neutron emission. We also record the energies and directions of all of the emitted neutrons and γ rays. From these history files, we can reconstruct both average quantities, their distributions, and correlations among them. Particularly in this study, we focus on the average number of neutron emitted from each event, $\overline{\nu}_p$. We construct the sensitivities using an approximation that changes in model output $\overline{\nu}_i$ (observable of interest) are related linearly to small changes in each parameter p_j, $R_{ij} = \Delta\overline{\nu}_i/\Delta p_j$. This approximation is valid as long as the final parameter set is not too far from the initial parameter set; since `CGMF` has already been pretty closely optimized to experimental values for $\overline{\nu}_p$, this approximation should be a fairly good one, as we will show later in this report.

From previous studies, we know that $\overline{\nu}_p$ is most sensitive to the $\langle TKE\rangle$; just by varying the magnitude and slope of $\langle TKE\rangle$ as a function of incident energy, we can closely reproduce the available experimental data of $\overline{\nu}_p$ up to 20 MeV using `CGMF`. Still for this work, we include in the optimization all of the parameters for $Y(A)$, $\mathrm{TKE}(E_{\mathrm{inc}})$, $\mathrm{TKE}(A)$, $\sigma_{\mathrm{TKE}}(A)$, and $\alpha(E_{\mathrm{inc}})$ (the energy dependence of the spin cutoff parameter). There is one important note that we have to make, especially due to differences between the inputs for ^{235}U(n,f) and ^{239}Pu(n,f) in `CGMF`: There is distinctly more data available for $^{233-235}$U(n,f) than for $^{237-239}$Pu(n,f). While there are separate parametrizations for the incident energy dependence of $\langle\mathrm{TKE}\rangle$ on each of these six reactions, for the three Pu reactions, $Y(A)$, $\langle\mathrm{TKE}\rangle(A)$, and $\sigma_{\mathrm{TKE}}(A)$ are repeated for each of the compounds, just changing the compound mass where necessary. Also, the default spin cutoff parameter is used for ^{238}Pu and ^{237}Pu. For ^{235}U(n,f), ^{234}U(n,f), and ^{233}U(n,f), however, the fission fragment initial conditions were optimized individually. Although it is impossible to tell for certain without starting with the same initial conditions for each evaluation, these differences could be the cause for some differences that are seen in how much the parameters change as well as the differences between the parameters at each chance fission.

For the Kalman filter evaluation (see Sec. 3), in addition to prior model parameters, we also need parameter uncertainties. Ideally, these are calculated at the same time as the optimization of the parameters; however, since this did not happen with `CGMF`, we now have to calculate them separately. The most straightforward way to calculate parameter uncertainties (albeit not the most accurate [6]) is to calculate the parameter covariance matrix around the best-fit set of parameters, which can be done in an approximate way through the Jacobian. Where there are experimental data, we can fit our `CGMF` parametrizations and perform this calculation (additionally, many python routines calculate the covariance through the optimization procedure). When we follow this procedure, we end up with parametric uncertainties—particularly for the $Y(A)$ parameters—that are orders of magnitude larger than the parameters themselves. In this case, the parameters are essentially unconstrained, which should not be true.

Instead, we perform a Markov Chain Monte Carlo sampling of the parameters that is constrained by the Bayesian condition

$$\frac{\exp[-\chi_f^2]}{\exp[-\chi_i^2]} \geq R, \tag{1}$$

where $R \in [0,1]$. This condition allows us to sample the parameter space, accepting parameter sets that lead to a worse fit than the initial parameter set, while still providing a reasonable description of the data. We make two estimations of the uncertainties: the first where we approximate the resulting parameter distribution as a Gaussian distribution (not a good approximation in many cases) and use the standard deviation as the one-σ uncertainty; and the second where we calculate the full width of the parameter distribution and use this as the three-σ uncertainty. Optimizations of $\overline{\nu}_p$ were performed with both uncertainties for ^{239}Pu, and it was found that the three-σ uncertainty lead to a more robust optimization.

The only outliers in this procedure were for the magnitude of $\langle \mathrm{TKE} \rangle (E_{\mathrm{inc}})$ and the spin cutoff parametrization. Although we can directly fit the $\langle \mathrm{TKE} \rangle$ as a function of incident neutron energy, the data sets span several MeV which was not captured by the Monte Carlo sampling. Here, we set the 1σ uncertainty to 2 MeV and the 3σ uncertainty to 4 MeV. Also, because the spin cutoff parameters cannot be directly fit to data, we use the same percent uncertainty from the magnitude of $\langle \mathrm{TKE} \rangle$ and its slope. Finally, the parametric uncertainties for each chance fission are taken to be the same, as there is generally less data available away from the major actinides. Because of the lack of data, we should really increase the uncertainties on the parameters for second- and third-chance fission, but we found that this increase was not necessary.

2.2 Experimental Input

For the evaluations of $\overline{\nu}_p$, all ^{235}U(n,f) and ^{239}Pu(n,f) $\overline{\nu}_p$ experimental data listed in Tables I and II were extracted from EXFOR. The EXFOR entry and, if available, the literature of each data set was studied in enough detail to decide whether it should be adopted or not. Some data sets in Tables I and II were rejected because of the energy range of their data; the nuclear data resulting from our evaluations are only anticipated to span an incident-neutron energy range from 100 keV to 30 MeV. Hence, any experimental data set that was in its entirety outside the energy range of the evaluation, was rejected. Other data sets had to be rejected for physics reasons or because of inadequate uncertainty information on the data set. The reasons for rejecting individual ^{235}U(n,f) and ^{239}Pu(n,f) $\overline{\nu}_p$ experimental data sets are briefly summarized in Appendix B and Appendix C, respectively.

Table I: Measured $\overline{\nu}$ data sets for ^{235}U(n,f) found in EXFOR. The EXFOR No., first author, year of publication and E_{inc} are given. In the second-last column, it is listed whether these data were accepted for the evaluations presented here (yes) or not (no). The last column tabulates all uncertainty sources that were added to those uncertainties found in the literature of the respective data set. The variable names are defined in Table III.

EXFOR #	First Author & Year	Monitor	E_{inc} (MeV)	Acc.	Added Unc.
41673.003	Apalin 1962	N/A	2.53e^{-8}	no	-
41397.01	Apalin 1965	N/A	2.53e^{-8}	no	-
21139.003	Barnard 1965	N/A	2.53e^{-8}	no	-
12397.002	Bethe 1955	N/A	4–4.5	no	-
40158.006	Bljumkina 1964 [7]	^{235}U(n,f) $\overline{\nu}_t$	0.08–0.99	yes	δc_{DG}, δb, $\delta \omega$ $\delta \tau$, $\delta \chi$, δa δd
41110.006	Boikov 1991 [8]	^{252}Cf(sf) $\overline{\nu}_p$	2.9–14.7	yes	δc_{ff}, δb, $\delta \omega$ $\delta \tau$, δa, δd $\delta d_{s/m}$
30772.003	Boldeman 1985	^{252}Cf(sf) $\overline{\nu}_p$	2.53e^{-8}	no	-

21454.005 007+008	Colvin 1965 [9]	^{252}Cf(sf) $\overline{\nu}_p$	2.53e^{-8}–2.57	yes	δc_{DG}, δb, δc_{ff} $\delta\omega$, $\delta\tau$, $\delta d_{s/m}$
20025.002	Conde 1965 [10]	^{252}Cf(sf) $\overline{\nu}_p$	7.5–14.8	yes	δc_{DG}, δa $\delta d_{s/m}$
14294.002	DeVolpi 1966	N/A	2.53e^{-8}	no	-
12337.003	Diven 1956 [11]	^{235}U(n,f) $\overline{\nu}_p$	0.08	yes	δc_{DG}, $\delta\omega$ $\delta\tau$, δa, δd $\delta d_{s/m}$
12436.002	Diven 1957	N/A	1.25–4.8	no	-
14297.007	Diven 1961 [12]	^{252}Cf(sf) $\overline{\nu}_p$	4	yes	δc_{DG}, δc_{ff} $\delta\omega$, $\delta\chi$, δa δd, $\delta d_{s/m}$
14297.006	Diven 1961(2)	^{252}Cf(sf) $\overline{\nu}_t$	2.53e^{-8}	no	-
21252.005	Fieldhouse 1966 [13]	^{252}Cf(sf) $\overline{\nu}_t$	0.075–14.2	yes	δc_{DG}, δb δc_{ff}, $\delta\omega$, $\delta\tau$ $\delta\chi$, δa, δd
21252.006	Fieldhouse 1966(2) [13]	^{252}Cf(sf) $\overline{\nu}_t$	0.04–7.96	yes	δc_{DG}, δb δc_{ff}, $\delta\omega$ $\delta\tau$, $\delta\chi$ δa, δd
40806.003	Flerov 1958	N/A	14.1	no	-
22592.003	Frehaut 1973	^{252}Cf(sf) $\overline{\nu}_t$	2.00e^{-6}–4.46e^{-5}	no	-
20506.002	Frehaut 1980 [14]	^{252}Cf(sf) $\overline{\nu}_t$	1.36–14.79	yes	δc_{DG}, δb δc_{ff}, $\delta\omega$ $\delta\tau$, $\delta\chi$, δa δd, $\delta d_{s/m}$
21685.002	Frehaut 1980(2)	^{252}Cf(sf) $\overline{\nu}_t$	2.279–2.828	no	-
21785.003	Frehaut 1982 [15]	^{252}Cf(sf) $\overline{\nu}_t$	1.14–14.66	yes	δc_{DG}, δb δc_{ff}, $\delta\omega$ $\delta\tau$, $\delta\chi$, δa δd, $\delta d_{s/m}$
12345.003	Fultz 1966	N/A	2.53e^{-8}	no	-
12833.001/3 12906.003	Gwin 1984	^{252}Cf(sf) $\overline{\nu}_t$	2e^{-8}–4.1e^{-5}	no	-
13101.003	Gwin 1986 [16]	^{252}Cf(sf) $\overline{\nu}_p$	0.0005–9	yes	$\delta\chi$, δa $\delta d_{s/m}$
12326.004	Hopkins 1963 [17]	^{252}Cf(sf) $\overline{\nu}_t$	2.53e^{-8}–14.5	yes	δc_{DG}, δc_{ff} $\delta\omega$, $\delta\chi$, δa δd, $\delta d_{s/m}$
10574.003	Howe 1976	^{235}U(n,f) $\overline{\nu}_t$	5.20e^{-7}–8.43e^{-5}	no	-
14051.002	Howe 1976(2) [18]	^{252}Cf(sf) $\overline{\nu}_t$	8.90e^{-2}–23.3	yes	δc_{DG}, δb δc_{ff}, $\delta\omega$ $\delta\tau$, $\delta\chi$, δa δd, $\delta d_{s/m}$
12870.004	Howe 1984	^{235}U(n,f) $\overline{\nu}_p$	17–48.9	no	-
21696.004	Johnstone 1956	^{235}U(n,f) $\overline{\nu}_t^M$	2.5–14.1	no	-
20427.002	Kaeppeler 1975 [19]	^{235}U(n,f) $\overline{\nu}_p$	0.225–1.363	yes	δc_{ff}, $\delta\tau$
40356.003	Kalashnikova 1957	^{235}U(n,f) $\overline{\nu}_t^M$	2.53e^{-8}	no	-
33102.004	Kappor 1963	N/A	2.53e^{-8}	no	-
41378.002	Khoklov 1994 [20]	^{252}Cf(sf) $\overline{\nu}_p$	0.048–14.122	yes	$\delta\chi$, δa

12419.002	Meadows 1962 [21]	^{252}Cf(sf) $\overline{\nu}_p$	0.03–1.76	yes	δc_{DG}, δb, δc_{ff} $\delta\omega$, $\delta\tau$, δa, δd
12391.002	Meadows 1965 [22]	^{252}Cf(sf) $\overline{\nu}_t$	3.91–6.36	yes	δc_{DG}, δb, δc_{ff} $\delta\omega$, $\delta\tau$, δa, δd
12399.002/4	Meadows 1967 [23]	^{252}Cf(sf) $\overline{\nu}_t$	0.039–1	yes	δc_{DG}, δb, δc_{ff} $\delta\omega$, $\delta\tau$, δa, δd
30022.002	Nadkarni 1967	N/A	0.37–2.13	no	-
40871.003	Nefedov 1983	^{252}Cf(sf) $\overline{\nu}_p$	2.53e^{-8}	no	-
40033.002 004/6/8	Nesterov 1970 [24]	^{252}Cf(sf) $\overline{\nu}_p$	2.53e^{-8}–1.51	yes	δc_{DG}, δb, δc_{ff} δa, δd, $\delta d_{s/m}$
40132.002	Prokhorova 1967 [25]	^{235}U(n,f) $\overline{\nu}_p$	0.37–3.25	yes	δc_{DG}, δb, δc_{ff} $\delta\omega$, $\delta\tau$, $\delta\chi$ δa, δd, $\delta d_{s/m}$
40392.002/3	Protopopov 1958 [26]	^{235}U(n,f) $\overline{\nu}_p^M$	14.8	yes	δb, δc_{ff}, $\delta\omega$ $\delta\tau$, $\delta\chi$, δa δd, $\delta d_{s/m}$
10427.003	Reed 1973	^{235}U(n,f) $\overline{\nu}_p^M$	1.20e^{-8}–2.64e^{-5}	no	-
21456.005	Sanders 1956	N/A	2.53e^{-8}	no	-
40058.004	Savin [27]	^{252}Cf(sf) $\overline{\nu}_p$	0.65–6.6	yes	δc_{DG}, δc_{ff}, $\delta\omega$ $\delta\tau$, δa, δd $\delta d_{s/m}$
40262.002	Savin 1972 [28]	^{252}Cf(sf) $\overline{\nu}_p$	0.86–5.35	yes	δc_{DG}, δc_{ff}, $\delta\omega$ $\delta\tau$, δa, δd $\delta d_{s/m}$
40493.002	Savin 1979 [29]	^{252}Cf(sf) $\overline{\nu}_p$	0.198–0.985	yes	δc_{DG}, δc_{ff}, $\delta\omega$ $\delta\tau$, δa, δd $\delta d_{s/m}$
20600.002	Simon 1976	^{252}Cf(sf) $\overline{\nu}_p$	2.03e^{-6}–7.46e^{-5}	no	-
40388.006	Smirenkin 1958 [30]	^{235}U(n,f) $\overline{\nu}_p^M$	4–15	yes	δb, δc_{ff}, $\delta\omega$ $\delta\tau$, $\delta\chi$, δa δd
12395.002	Snyder 1944	N/A	2.53e^{-8}	no	-
20568.002	Soleihac 1970 [31]	^{252}Cf(sf) $\overline{\nu}_p$	0.223–1.87	yes	δc_{DG}, δb, δc_{ff} $\delta\omega$, $\delta\tau$, $\delta\chi$ δa, δd
40785.002	Vasilev 1960	N/A	14.3	no	-
41597.004	Vorobyev 2013	N/A	3.63e^{-8}	no	-
30006.002	Walsh 1971 [32]	^{252}Cf(sf) $\overline{\nu}_p$	0.11–1.9	yes	$\delta\omega$, δa, δd
20113.003	Widen 1973	^{252}Cf(sf) $\overline{\nu}_p$	2.53e^{-8}	no	-

Table II: Measured $\overline{\nu}$ data sets for ^{239}Pu(n,f) found in EXFOR. The EXFOR No., first author, year of publication, main reference and E_{inc} are given. In the second-last column, it is listed whether these data were accepted for the evaluations presented here (yes) or not (no). The last column tabulates all uncertainty sources that were added to those uncertainties found in the literature of the respective data set. The variable names are defined in Table III.

EXFOR no.	First Author & Year	Monitor	E_{inc} (MeV)	Acc.	Added Unc.
41397.008	Apalin 1965	N/A	2.53e^{-8}	no	-
30772.004	Boldeman 1980 [33]	^{252}Cf(sf) $\overline{\nu}_p$	2.53e^{-8}	no	-
20052.002	Conde 1968 [34]	^{252}Cf(sf) $\overline{\nu}_p$	4.22–14.8	yes	δc_{DG}, $\delta\chi$, δa $\delta d_{s/m}$
12337.004	Diven 1956 [11]	^{235}U(n,f) $\overline{\nu}_p$	0.08	yes	δc_{DG}, $\delta\omega$, $\delta\tau$ δa, δd, $\delta d_{s/m}$
14279.009/10	Diven 1961 [11]	^{252}Cf(sf) $\overline{\nu}_t$	2.53e^{-8}–4	no	-
20490.003	Frehaut 1973 [14]	^{252}Cf(sf) $\overline{\nu}_p$	1.36–14.79	yes	δc_{DG}, δb, δc_{ff} $\delta\omega$, $\delta\tau$, $\delta\chi$, δa, δd
21685.004	Frehaut 1980 [14]	^{252}Cf(sf) $\overline{\nu}_p$	22.79–28.28	no	-
10759.004	Gwin 1978 [16]	^{252}Cf(sf) $\overline{\nu}_p$	5e^{-5}–6.4	no	-
12906.002	Gwin 1984 1 [16]	^{252}Cf(sf) $\overline{\nu}_p$	5e^{-9}–6e^{-5}	no	-
12833.004	Gwin 1984 2 [16]	^{252}Cf(sf) $\overline{\nu}_p$	5e^{-9}–1e^{-5}	no	-
13101.004	Gwin 1986 [16]	^{252}Cf(sf) $\overline{\nu}_p$	5e^{-4}–10	yes	$\delta\chi$, δa, $\delta d_{s/m}$
12326.005/6	Hopkins 1963 [17]	^{252}Cf(sf) $\overline{\nu}_p$	2.53e^{-8}–14.5	yes	δc_{DG}, δc_{ff}, $\delta\omega$ δa, δd, $\delta d_{s/m}$
30600.002	Huanqiao 1980 [35]	^{1}H(n,el) cs	0.186–1.44	no	-
21696.006	Johnstone 1965 [36]	^{235}U(n,f) $\overline{\nu}_t^M$	14.1	no	-
40757.002	Kalashnikova 1955 [37]	N/A	2.53e^{-8}	no	-
40523.002	Khoklov 1976 [38]	^{252}Cf(sf) $\overline{\nu}_t$	1.06–1.81	yes	δc_{DG}, δc_{ff}, $\delta\omega$ $\delta\chi$, δa, δd, $\delta d_{s/m}$
21453.004	Leroy 1960 [39]	^{238}U(n,f) $\overline{\nu}_p$	14.2	no	-
-	Marini 2021 [40]	^{252}Cf(sf) $\overline{\nu}_p$	0.97322–19.8958	yes	δc_{DG}, δc_{ff}, $\delta\omega$ δa, δd, $\delta d_{s/m}$
21135.007/8	Mather 1965 [41]	^{252}Cf(sf) $\overline{\nu}_t$	2.53e^{-8}–4.02	yes	δc_{DG}, $\delta\omega$, $\delta\tau$
20453.003	Mather 1970 [42]	^{252}Cf(sf) $\overline{\nu}_p$	0.0775–1.15	yes	δc_{DG}, $\delta\omega$, $\delta\tau$ δa, δd, $\delta d_{s/m}$
20453.002					
40871.002	Nefedov 1983	^{252}Cf(sf) $\overline{\nu}_p$	2.53e^{-8}	no	-
4033.003/7	Nesterov 1970 [24]	^{252}Cf(sf) $\overline{\nu}_p$	2.53e^{-8}–1.607	no	-
23012.009	Nishio 1988	N/A	2.53e^{-8}	no	-
40429.004	Nurpeisov 1975 [43]	^{252}Cf(sf) $\overline{\nu}_p$	0–4.89	yes	δc_{DG}, $\delta\omega$, $\delta d_{s/m}$
21456.007	Sanders 1956	^{235}U(n,f) $\overline{\nu}_p^M$	2.53e^{-8}	no	-
40058.003	Savin 1970 [27]	^{252}Cf(sf) $\overline{\nu}_p$	0.89–4.7	yes	δc_{DG}, δc_{ff}, $\delta\omega$ $\delta\tau$, δa, δd, $\delta d_{s/m}$
40388.007	Smirenkin 1959 [30]	^{239}Pn(n,f) $\overline{\nu}_p^M$	4–15	no	-
20568.004	Soleihac 1970 [31]	^{252}Cf(sf) $\overline{\nu}_p$	0.21–1.375	yes	δc_{DG}, δb, δc_{ff} $\delta\omega$, $\delta\tau$, $\delta\chi$, δa, δd
40148.003	Volodin 1970 (1) [44]	^{252}Cf(sf) $\overline{\nu}_p$	2.53e^{-8}–1.6	yes	δc_{ff}, $\delta\omega$, $\delta\tau$ $\delta\chi$, δa, δd, $\delta d_{s/m}$

40148.005	Volodin 1970 (2) [44]	^{239}Pu(n,f) $\overline{\nu}_p^M$	0.08–0.7	yes	δc_{ff}, $\delta\omega$, $\delta\tau$ $\delta\chi$, δa, δd, $\delta d_{s/m}$
41611.008	Vorobyev 2016	N/A	thermal spect.	no	-
30006.004	Walsh1970 [32]	^{252}Cf(sf) $\overline{\nu}_p$	0.2–1.9	yes	δd

Table III: Typical uncertainty sources expected to apply to ratio liquid-scintillator measurements of $\overline{\nu}_p$ are listed. The variable names defined in this table are used for the last columns of Tables I and II.

Variable	Uncertainty Source
δc_{DG}	Delayed Gamma-ray Uncertainties
δb	Random-background Uncertainties
δc_{ff}	False-fission Uncertainties
$\delta\omega$	Impurity Uncertainties
$\delta\tau$	Deadtime Uncertainties
$\delta\chi$	PFNS Uncertainties
δa	Uncertainties of Angular Distribution of Fission Neutrons
$\delta\overline{\nu}^m$	Monitor Uncertainties
δd	Uncertainty due to Thickness of Sample
$\delta d_{s/m}$	Sample-displacement Uncertainty
$\Delta E_{\rm inc}$	Energy Uncertainty

A detailed uncertainty estimate and literature review was undertaken for all remaining data sets. Appendix B and Appendix C concisely summarizes some key concerns on each data set and comments on the individual uncertainty estimate.

In general, care was taken to apply the same uncertainty procedure for each data set and to assume consistent uncertainty values for those that were missing in the literature or EXFOR or both. To this end, a module was developed in the code package ARIADNE [45] to estimate experimental covariances for $\overline{\nu}$ measurements. Codes were developed that estimated total covariances, ${\rm Cov}_{i,j}^{tot}$, for absolute measurements and ratio measurements by

$$ {\rm Cov}_{i,j}^{tot} = \sum_k \delta_i^k {\rm Cor}_{i,j}^k \delta_j^k, \tag{2} $$

accounting for individual uncertainty values, δ_i^k, and correlation coefficients, ${\rm Cor}_{i,j}^k$, for each expected uncertainty source k at incident-neutron energy i or j. This implicitly assumes hat the individual uncertainty sources k are partitioned such that they be independent.

The typical uncertainty uncertainty sources encountered in a $\overline{\nu}_p$ measurement are listed in Table III and were based on information in Ref. [46]. It can be seen in Tables I and II that uncertainty values were missing for at least one or more uncertainty sources for each measurement adopted for the evaluation. These missing uncertainties and their correlations were estimated following templates of expected uncertainties for ratio $\overline{\nu}$ measurements [46]. The values assumed for a particular δ_i^k and ${\rm Cor}_{i,j}^k$ are described in Appendix A.

Correlation coefficients between total uncertainties of different experiments are usually low as the dominant contribution to the uncertainty of many measurements is statistical in nature. To be more explicit, systematic uncertainties range from typically 0.5–0.9%, while statistical uncertainties often assume values of 1–2%. Also, many systematic uncertainties are only weakly correlated across measurements (see, *e.g.*, δb, δc_{ff}, δa as shown in Table XIII of Ref. [46]). The one exception is when multiple data sets were undertaken at the same facility by the same team using similar equipment.

Hence, correlations between uncertainties of different experiments were estimated for groups of data that were correlated. For instance, uncertainties between data of various Meadows data sets, all

Savin data sets, all adopted Frehaut data sets and Diven 1961 and Hopkins 1963 data were estimated for ^{235}U(n,f) $\overline{\nu}_p$.

In addition to that, a monitor uncertainty of 0.42% with full correlation across all data sets was applied to account for uncertainties in the current ^{252}Cf(sf) $\overline{\nu}$ put forth by the Neutron Data Standards committee [47]. While not all data were measured in ratio to this particular reaction, all of them were ratio measurements that tie back to a monitor reaction that either relies itself on ^{252}Cf(sf) $\overline{\nu}$ if it isn't ^{252}Cf(sf) $\overline{\nu}$ to begin with.

Phil Young's experimental database was still available for his ^{239}Pu(n,f) $\overline{\nu}_p$ evaluation which allows us to point out the main differences of his and our work. Phil adopted uncertainties mostly as given from EXFOR, *i.e.*, without estimating missing uncertainty sources. If he did not trust a data set (*e.g.*, in the case of Huanqiao ^{239}Pu(n,f) $\overline{\nu}_p$ experimental data), he doubled the uncertainties. He did not account for energy uncertainties which are mostly a minor uncertainty source given the smooth behavior of $\overline{\nu}_p$. It was unclear to the first author whether he accounted for any correlations between different uncertainties at different $E_{\rm inc}$ or across experiments, but given that he mentioned in a journal publication a covariances analysis [48], I assume that he at least accounted for correlations for uncertainties of individual experiments. But, it is questionable if he accounted for correlations between experiments.

Contrary to Phil Young, the data of Huanqiao and Nesterov were rejected for this evaluation based on physics reasons (too low efficiency in both cases, Nesterov data were actually rejected by its own experimental team in a later publication), while he rather chose to double their uncertainties given his own suspicions on the data. The first author also rejected the data by Johnstone, Smirenkin and Leroy as described in Appendix C, while Phil Young took them into account. These latter three data sets are highly uncertain.

As will be shown in Section 4, these above choices had little impact on the evaluated results and the new evaluated results with only experimental data were rather close to ENDF/B-VIII.0. However, the data of Marini et al. [40] obtained with the Chi-Nu array at LANSCE became recently available through a collaboration between the CEA and NNSA. These data are of very low statistical uncertainty and comparable systematic uncertainties to previous data sets. Due to that their overall uncertainty and variation over $E_{\rm inc}$ are distinctly reduced and these data provide decisive information for the evaluation. While they are very close to ENDF/B-VIII.0, they do lead to more distinct differences to ENDF/B-VIII.0 than any of the above changes in the experimental database as shown in Section 4.

Unfortunately, the experimental database for Phil Young's ^{235}U(n,f) $\overline{\nu}_p$ evaluation was not available at LANL anymore. Also, the first author was unable to find any detailed description of this evaluation, despite going back through decades of LANL reports. A few paragraphs of information were found in Ref. [48] and in MF=1 entries. From there, we know today that Khoklov and Boikov data were not included in the current ENDF/B-VIII.0 evaluation as these data were published after the evaluation. It was mentioned in an MF=1 entry that a re-evaluation is not necessary as the data were in fair agreement with his evaluation. However, Khoklov data are systematically lower than the current ENDF/B-VIII.0 evaluation below 0.8 MeV leading to changes in the evaluated results. From Ref. [48], one can conclude that the evaluation is based on a statistical analysis only including all experimental data at the time and using covariances for individual data sets. Likely included are data of Frehaut, 1982, Howe 1984, Gwin 1986, Savin 1972 & 1979 and Soleihac 1970.

3 Evaluation Methods

We use two evaluation techniques here, the generalized least squares algorithm and the Kalman filter method. Both can be encoded in one and the same set of equations, that give a vector of evaluated mean values $\boldsymbol{N}$ and Cov^N,

$$\begin{aligned} \boldsymbol{N} &= \boldsymbol{p} + \mathbf{Cov}^N \boldsymbol{S}^t (\mathbf{Cov}^e)^{-1} (\boldsymbol{e} - \boldsymbol{S}\boldsymbol{p}) \,, \\ \mathbf{Cov}^N &= \mathbf{Cov}^p - \mathbf{Cov}^p \boldsymbol{S}^t Q^{-1} \boldsymbol{S} \mathbf{Cov}^p , \end{aligned} \tag{3}$$

where

$$Q = \boldsymbol{S}\mathbf{Cov}^p \boldsymbol{S}^t + \mathbf{Cov}^e . \tag{4}$$

The variables $\boldsymbol{e}$ and $\mathbf{Cov}^e$ encode all experimental data used for the evaluation and their covariances estimated as described in Section 2.2.

If we apply the equations above in the sense of **generalized least squares** (GLS), $\boldsymbol{p}$ and $\mathbf{Cov}^p$ contain non-informative prior information in the $\overline{\nu}_p$ space, *i.e.*, ENDF/B-VIII.0 mean values with 100% uncertainty and a diagonal covariance matrix. The design matrix $\boldsymbol{S}$ and its transpose $\boldsymbol{S}^t$ were calculated in Ref. [49] by linear interpolation to bring experimental data onto the E_{inc} grid of the prior data. Hence, this generalized least squares approach as applied here gives evaluated results based on only experimental data. This approach is in essence the same that Phil Young took for his evaluation of ^{239}Pu(n,f) $\overline{\nu}$. The evaluated mean values $\boldsymbol{N}$ and Cov^N correspond in this case to evaluated $\overline{\nu}$ and their covarinaces.

If we want to bring into the evaluation the `CGMF` model, we need to apply Eq. (3) as a **Kalman filter**. To this end, $\boldsymbol{p}$ are model-parameter values and $\mathbf{Cov}^p$ are their covariances. The design matrix needs to convert experimental data into model-parameter space. This is achieved by taking as $\boldsymbol{S}$ the sensitivity vectors R_{ij} as discussed in Section 2.1. The evaluated mean values $\boldsymbol{N}$ and Cov^N correspond in this case to evaluated model parameters of `CGMF` that are then fed again into the model code to obtain an evaluated $\overline{\nu}^p$.

These two approaches are taken here in order to get two kinds of evaluated results: On the one hand, we get via GLS evaluated results based on only experimental data. This is the approach taken by Phil Young, and, hence, we can compare our results to those of Phil and see if we come reasonably close to his values. This is an important step to guarantee overall consistency of our first results. On the other hand, we can include the `CGMF` model via the Kalman filter technique. We gain an understanding of the impact of the model on the evaluation by comparing GLS and Kalman filter evaluated $\overline{\nu}_p$. This comparison is an equally important step in our analysis to guarantee that the model does not have an adverse impact on our evaluated results. It is expected to smooth out unphysical structures in the evaluation caused by statistical variations in the experimental data, but if the evaluated results with `CGMF` would have a very different trend than GLS results, one might question the impact of the model.

It should be noted that the experimental covariances were corrected for an effect termed "Peelle's Pertinent Puzzle", where the evaluated mean value of strongly correlated experimental data lies outside of the range of the experimental data due to an improperly formulated covariance matrix [50]. This effect has been observed for the evaluated results here. This is not surprising as a common, fully correlated uncertainty source was applied across the whole experimental covariances matrix, namely that one related to the ^{252}Cf(sf) $\overline{\nu}_p$. The covariance matrix was corrected following Ref. [50] in order to minimize the impact of "Peelle's Pertinent Puzzle".

4 Results

4.1 Evaluated Results of ^{239}Pu(n,f) $\overline{\nu}_p$

Two types of evaluations were performed here, a GLS evaluation including only experimental data and a second one using the Kalman filter to include the `CGMF` model. The first type of evaluation was undertaken to better compare to ENDF/B-VIII.0 as Phil Young evaluated his $\overline{\nu}$ based on only experimental data.

Evaluated Results of ^{239}Pu(n,f) $\overline{\nu}_p$ using Only Experimental Data As mentioned before, the evaluation presented here differs from that of Phil Young in:

- An updated uncertainty estimate for all adopted data sets,
- The first author rejected the data of Huanqiao, Nesterov, Smirenkin, Johnstone and Leroy. Phil Young doubled the uncertainties of the first two data sets and the uncertainties of the latter three are very high to begin with,
- Very recent data of Marini were included that were previously not available.

If we evaluate ^{239}Pu $\overline{\nu}_p$ with only experimental data minus the data of Marini (which were not available for the evaluation of Phil Young), the resulting $\overline{\nu}_p$ are very close in Fig. 1 to Phil's results despite the many changes to the experimental uncertainties. The reason for that lies in the fact that a dominant uncertainty source is δc, statistical uncertainties that was available for all data sets used (or could at least be backed out). Hence, our total uncertainties likely only differed little as did our total covariances. Our evaluated results only differ visibly from 0.1 to 0.4 MeV. In this energy range, experimental data are scarce and rather scattered. Looking at ENDF/B-VIII.0, I would assume that Phil did a linear fit to obtain a physical curve; as the two evaluations "touch" at specific E_{inc} nodes. I would assume that Phil used those nodes for the linear fit. Hence, while the two evaluations look like they disagree between 0.1 and 0.4 MeV, they are still in reasonable agreement taking into account that Phil likely post-processed his evaluation bearing in mind physics expected behavior.

While the evaluated mean values of this evaluation with only experimental data agree well with ENDF/B-VIII.0, the evaluated uncertainties differ distinctly in Fig. 2 from 0.5–15 MeV. One reason why a re-evaluation of the ^{239}Pu(n,f) $\overline{\nu}_p$ was proposed, was that it was shown via the PUBs methodology [51, 52] that the evaluated uncertainties in ENDF/B-VIII.0 were underestimated considering the differential information available for this evaluation. This is illustrated in Fig. 2, where ENDF/B-VIII.0 uncertainties are below the minimal realistic bound estimated via PUBs based on differential information. The new evaluated uncertainties without the data of Marini (i.e., the database that was taken into account for the assessment of PUBs bounds) lie well within PUBs bounds and are, therefore, indicated to be more realistic.

If we include Marini data into the above evaluation, small changes can be observed in Fig. 1 until 6 MeV. Above 7 MeV (*i.e.*, above the second-chance fission threshold), the ^{239}Pu(n,f) $\overline{\nu}_p$ is slightly smaller than ENDF/B-VIII.0. from 8–10 MeV, around 14 MeV and above 16 MeV. If we consider that second-chance fission opens up from 6–7 MeV, third-chance fission from 10–12 MeV and fourth-chance fission around 19 MeV, one could conclude that there are small structures in ^{239}Pu(n,f) $\overline{\nu}_p$ that slightly increase $\overline{\nu}$ at the respective thresholds compared to the more linear function of ENDF/B-VIII.0. The precise data of Marini et al. can capture such a behavior for the first time.

Figure 3 shows the ratio of the new evaluations to ENDF/B-VIII.0 and to each other and allow us to study in more detail where changes happened. The evaluation without Marini data agrees with ENDF/B-VIII.0 within 0.5% and meanders around ENDF/B-VIII.0 pointing to differences in the smoothing alogrithms chosen by Phil and the first author. When Marini data are introduced, the evaluation gets lower above 5 MeV.

It is also clear from Figs. 2 and 3 that the evaluated uncertainties including Marini data are lower again. That is justified given the low uncertainties of Marini data that were not considered in the PUBs analysis.

All in all, we were able to produce evaluated data with only experimental data that match ENDF/B-VIII.0 closely enough to show that the results are realistic. This evaluation is now the starting point for including the `CGMF` model.

Evaluated Results of ^{239}Pu(n,f) $\overline{\nu}_p$ Including CGMF Several test evaluations were performed before we zeroed in on one particular evaluation that corresponds to our final reported data. We are

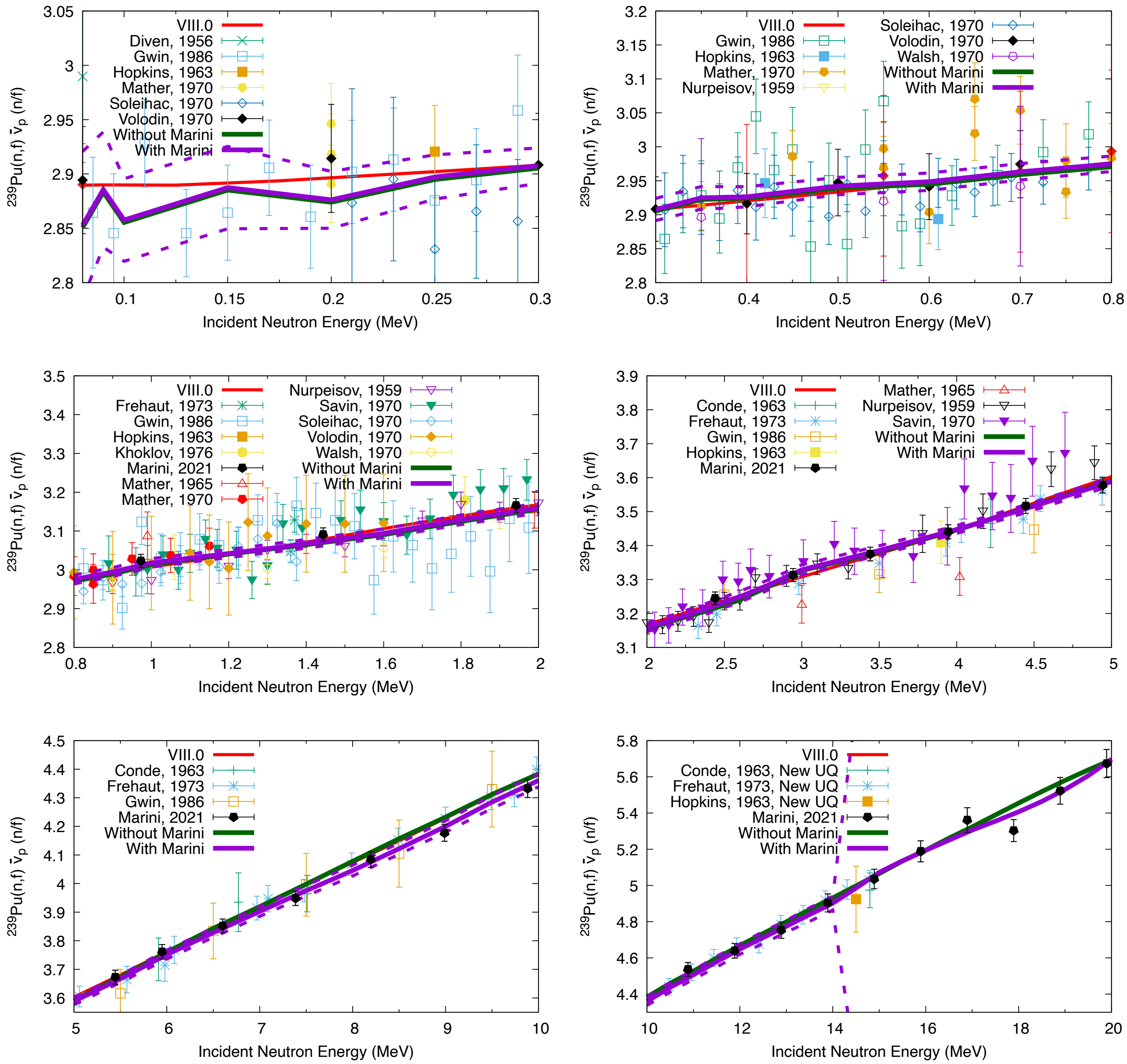

Figure 1: Evaluated ^{239}Pu(n,f) $\overline{\nu}_p$ are shown in comparison to ENDF/B-VIII.0 and experimental data that were used for the evaluation. The evaluated data were obtained with a statistical analysis of only experimental data. One evaluation is shown with and without Marini experimental data.

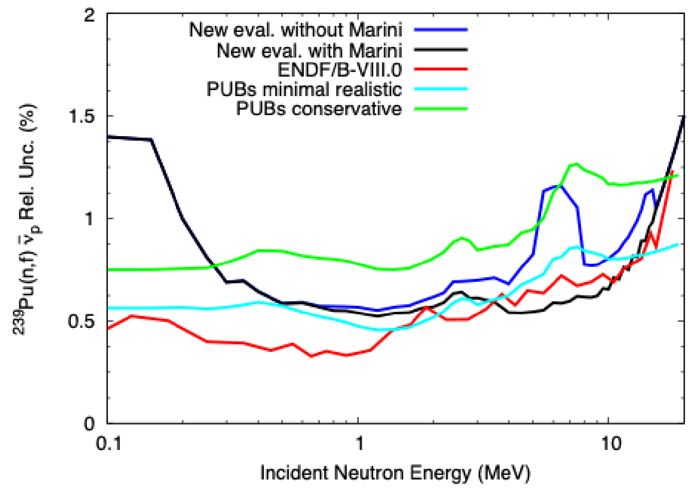

Figure 2: Evaluated uncertainties with and without Marini are compared to ENDF/B-VIII.0 uncertainties and PUBs bounds.

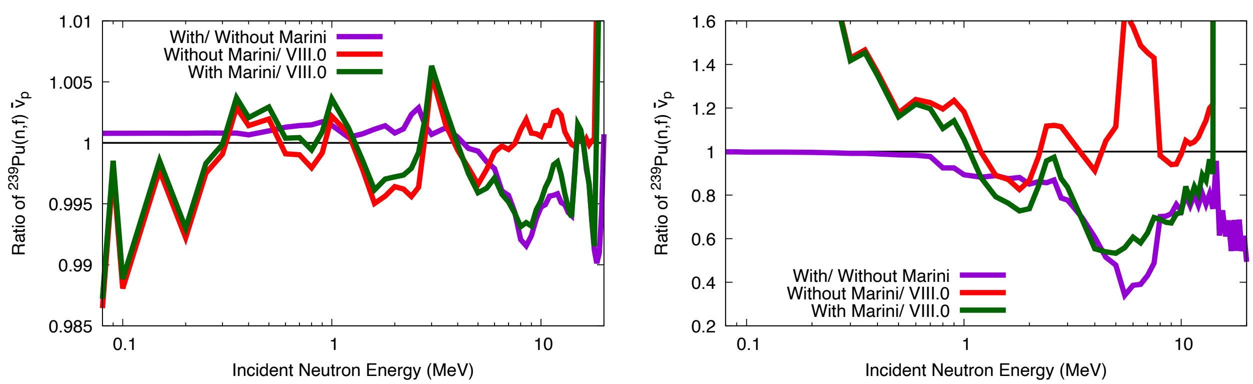

Figure 3: Ratios of evaluated mean values (left-hand side) and uncertainties (right-hand side) for ^{239}Pu(n,f) $\overline{\nu}_p$ are shown for ENDF/B-VIII.0 and the evaluations presented in Fig. 1.

only going to show a few of those example evaluations to illustrate why the selected evaluation was deemed the most appropriate one in the interest of length.

The evaluation described here was obtained by using all experimental data that were indicated as accepted in Table II and the `CGMF` model. The PPP effect was corrected for and the experimental data were used in the evaluation as is (*i.e.*, not brought to a common grid before the evaluation). The larger parameter uncertainties mentioned in Section 2.1 were assumed as one-σ bound. To be explicit, what the second author assumed to be covering the full distribution of parameters (*i.e.*, three sigma) was assumed as one-σ bound. That might sound like a large over-estimate of the prior parameter space.

However, as was already mentioned at the end of Section 2.1, the second- and third-chance fission parameters could not be well-defined due to missing experimental data. Hence, we assume that the parameter uncertainties were under-estimated to begin with. So, we enlarged the parameter space to allow for all necessary changes in the parameters. These changes in the parameter space are shown in ratio to the prior parameters in Figs. 4, 5 and 6. The first-chance fission parameter uncertainties all decrease indicating that the parameter space is large enough for the evaluation. That is true for most, but not all, second- and third-chance fission parameters.

Another issue, that is indicated in Figs. 4, 5 and 6 is the grid chosen for the evaluation. There is a lot of freedom in fitting the model parameters (more than 90 parameters are fitted to about 40 grid points). Hence, the model is prone to overfitting, especially in the energy range where we had scarce and scattered experimental data. To avoid over-fitting to statistical variations in experimental data, the grid was down-selected to (thermal, 0.1, 0.2, 0.5, 0.8, 1.3, 1.75, 2.5, 3.0, 3.5, etc.). The impact on the evaluated parameters can be seen in Figs. 4, 5 and 6. The changes in first-chance fission parameters is more modest while second-chance fission parameters change distinctly (and led to better predicted FY(A), *etc.*).

It is interesting to note that μ_1^a, μ_2^a and a for first-chance fission change very little in the evaluation. These parameters were tuned previously to predict a ^{239}Pu(n,f) $\overline{\nu}_p$ agreeing to experimental data. These tuned parameters entered the evaluation. This tuning was very successful as is indicated by the small changes from the Kalman filter. Instead we see changes in the width of FY(A), parameterization of $\langle TKE \rangle$ and the spin-parity distribution which is not well understood. It will be later shown that these evaluated parameters reproduce experimental data linked to them reasonably well.

When we use the evaluated parameters obtained by the Kalman filter and calculate ^{239}Pu(n,f) $\overline{\nu}_p$ with `CGMF` based on these parameters, we obtain the evaluated data in Fig. 7. These evaluated data agree very well with differential data and seemingly lie on top of ENDF/B-VIII.0 from 0.9 to 4 MeV. When one plots the evaluated results in ratio to ENDF/B-VIII.0 in Fig. 8, one sees that the changes are in the range of ± 0.5% up to the second-chance fission threshold.

When one compares Fig. 8 to Fig. 3, one sees that the general trend of changes is caused by the differential data but that `CGMF` has smoothing effects that perpetuate trends seen in the differential data. For instance, differential data indicate an increase in the evaluated data compared to ENDF/B-VIII.0 at 0.4, 0.5, 0.8 and 1 MeV that `CGMF` smoothes through and leads to an overall increase of ^{239}Pu(n,f) $\overline{\nu}$ below 1 MeV compared to ENDF/B-VIII.0. It is shown with criticality testing that this is not favorable and a slight tweak below 1 MeV might be needed. Changes from 1–5 MeV in Fig. 8 resemble those due to differential data but balance them out more. Criticality tests indicate that these changes are indeed favorable. Above 5 MeV, changes are coming from both Marini data and `CGMF`. These data cannot be validated with any of the integral data available.

4.2 Validation of ^{239}Pu(n,f) $\overline{\nu}_p$

Validation of Evaluated Parameters Against Various Fission Data The fitted parameter sets can be used as input to `CGMF`, not only to ensure the fitted $\overline{\nu}_p$ calculation matches the exact `CGMF` calculation, but also to understand whether the fission fragment initial conditions and other prompt observables have remained physical, even though they were not included in the optimization. Here, we

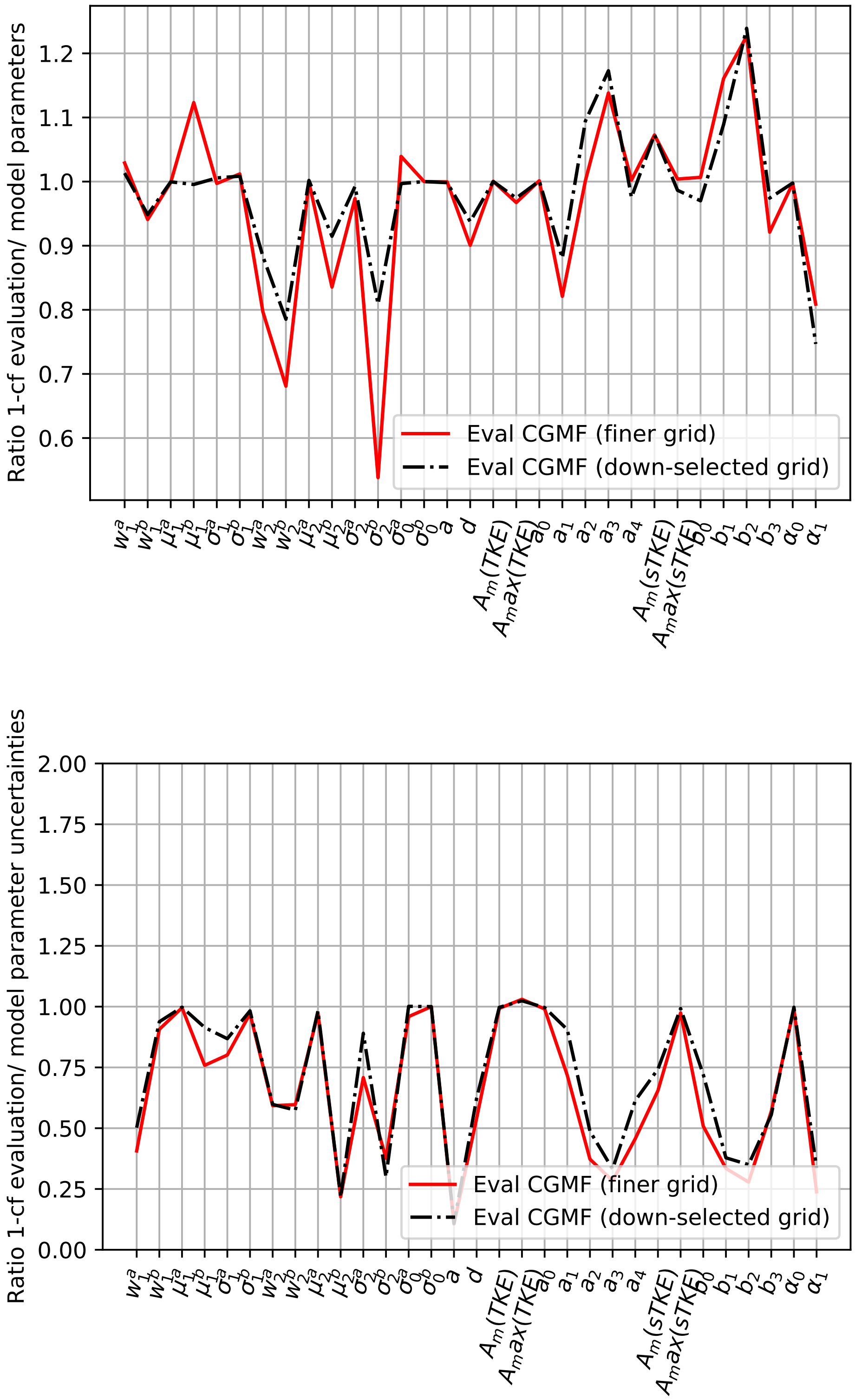

Figure 4: Impact on evaluated parameters and their uncertainties if all E_{inc} are fitted at once at a down-selected grid and 18-MeV point of Marini removed. Changes in first-chance fission parameters are shown.

show four different evaluated parameter sets: 1) the first-chance fission parameters are fit first then held constant while the remaining parameters were fit, 2) all parameters were fit simultaneously, 3)

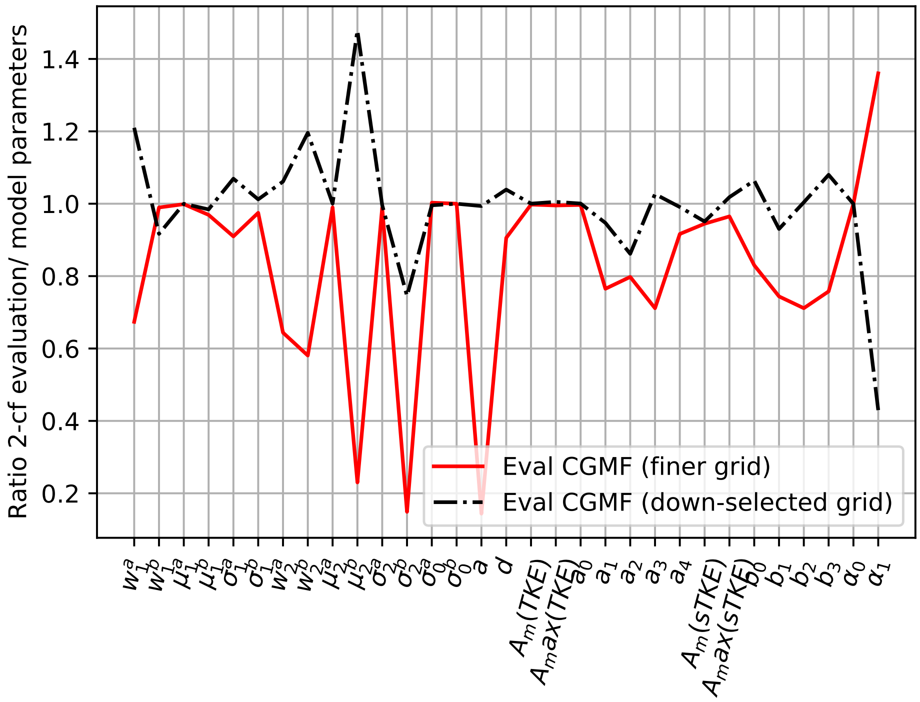

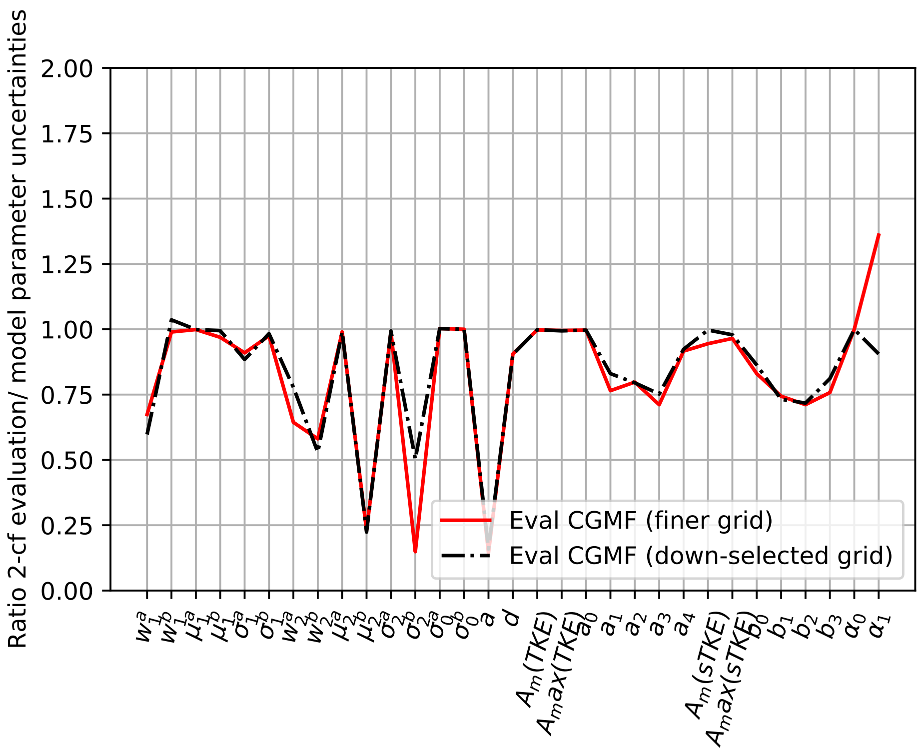

Figure 5: Impact on evaluated parameters and their uncertainties if all $E_{\rm inc}$ are fitted at once at a down-selected grid and 18-MeV point of Marini removed. Changes in second-chance fission parameters are shown.

the fit was performed to the ENDF/B-VIII.0 evaluation instead of experimental data, and 4) a finer but then down-selected energy grid was used in the optimization. The `CGMF` evaluation in Fig. 7

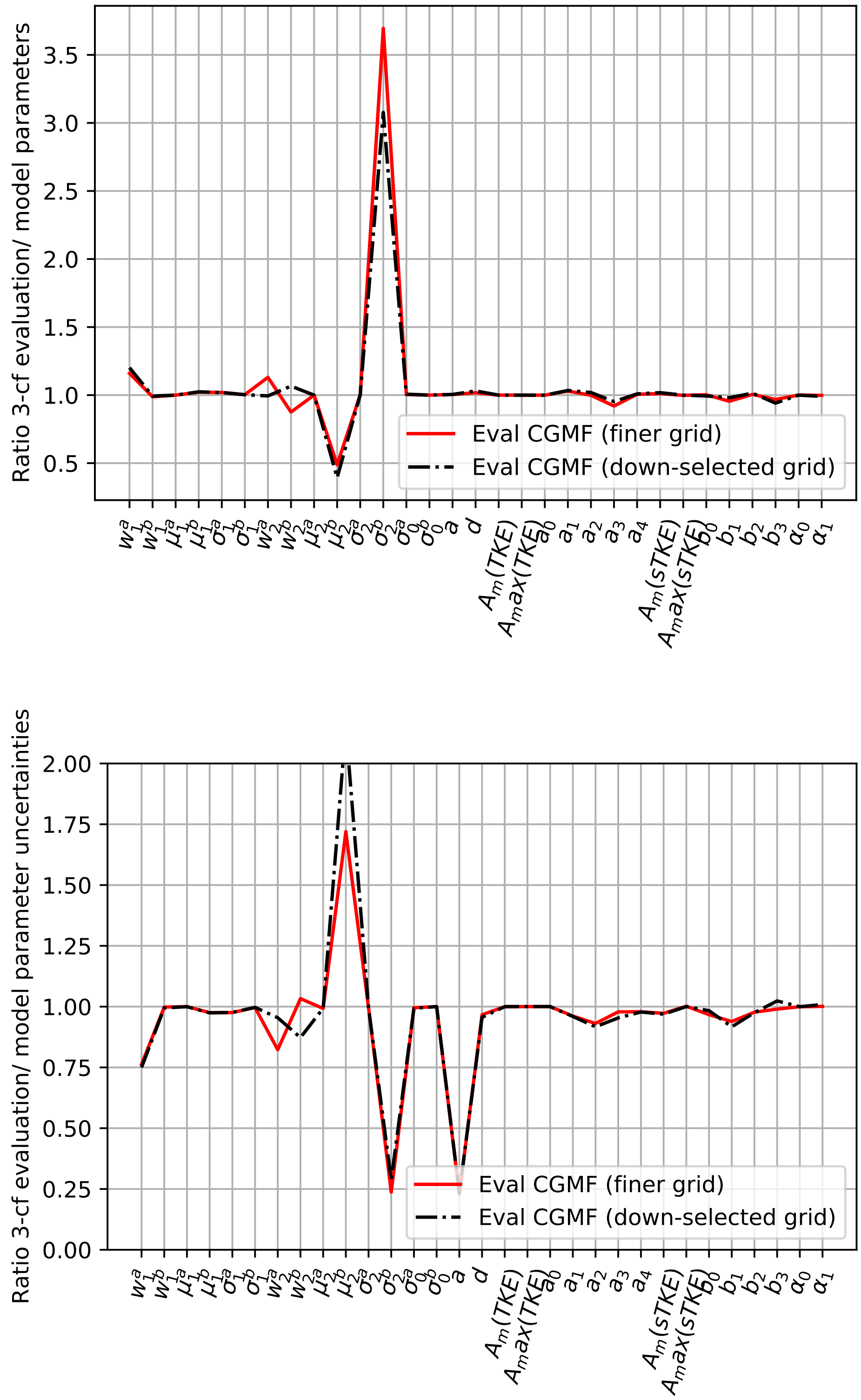

Figure 6: Impact on evaluated parameters and their uncertainties if all E_{inc} are fitted at once at a down-selected grid and 18-MeV point of Marini removed. Changes in third-chance fission parameters are shown.

corresponds to this fourth parameter set. Still, we show the comparison between all four parameter sets and experimental data to further justify the use of this fourth fit as the final evaluated value.

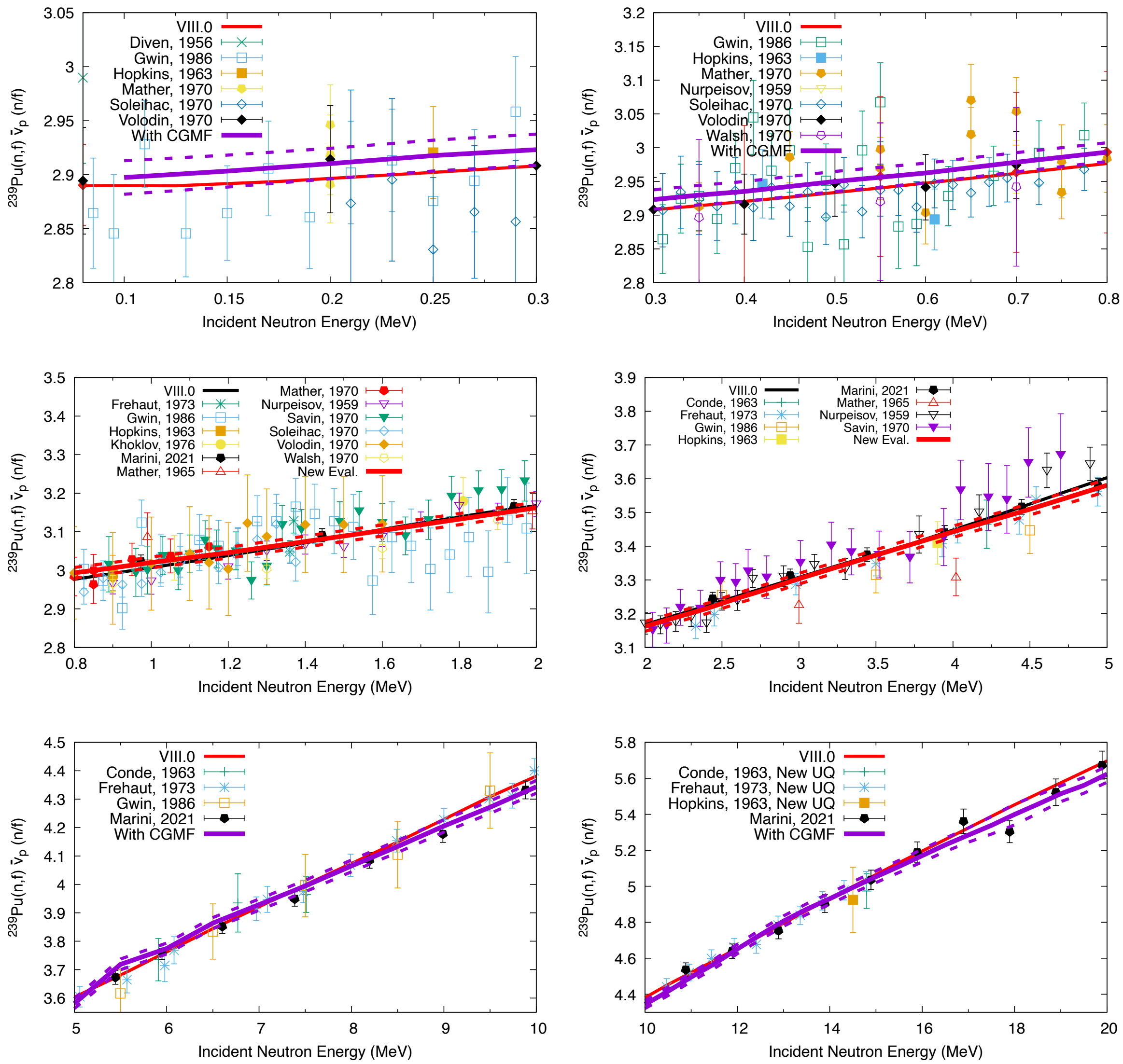

Figure 7: Evaluated ^{239}Pu(n,f) $\overline{\nu}$ are shown in comparison to ENDF/B-VIII.0 and experimental data that were used for the evaluation. The evaluated data were obtained with `CGMF`.

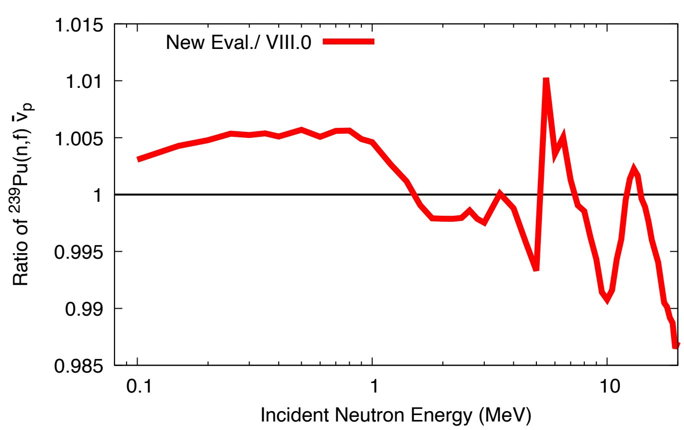

Figure 8: Ratios of evaluated mean values for ^{239}Pu(n,f) $\overline{\nu}$ are shown for the final evaluation presented here to ENDF/B-VIII.0.

First, we show the pre-neutron mass yield, $Y(A)$, for the four parametrizations at specific incident energies where there is available experimental data in Fig. 9. We see that the fit with the finer and then down-select grid (green dot-dashed) is the only parameter set that is not above the experimental data in the valley of $Y(A)$. Additionally, if we were to plot $Y(A)$ for each incident energy on the same plot (not shown here), we would see that the finer and then down-selected grid evaluation is the only one where the symmetric valley is filled as the incident energy increases, which is what is seen in experimental data as well. The other three optimizations have a less filled valley as the incident energy increases.

We then plot the total kinetic energy as a function of incident energy, $\langle\mathrm{TKE}\rangle(E_{\mathrm{inc}})$ in Fig. 10 (left). All three evaluations roughly follow the shape of $\langle\mathrm{TKE}\rangle(E_{\mathrm{inc}})$, when allowing for the approximately 2-MeV spread in the experimental data. The differences in magnitude are compensated by the spin cutoff parameter, which has an impact on the γ-ray observables (shown later but not explicitly a part of this milestone). The finer and then down-selected grid fit additionally smooths out the bump at the opening of second-chance fission that is seen in the other three parameter sets. In the right panel of Fig. 10, we show $Y(\mathrm{TKE})$ for thermal incident neutrons (the only incident energy where there is experimental data). The fit to ENDF clearly best reproduces the experimental data. However, the $\langle\mathrm{TKE}\rangle$ will always be renormalized to $\langle\mathrm{TKE}\rangle(E_{\mathrm{inc}})$—which has a large experimental uncertainty—and we typically find that we need to decrease σ_{TKE} by about 20% to be able to reproduced the neutron multiplicity distribution, $P(\nu)$. This observable will be discussed later in this report, but it does not necessarily mean that the ENDF optimization is better able to reproduce TKE observables—at least not based on our previous studies.

Next, we show the average prompt neutron and γ-ray multiplicities in Fig. 11. If we first look at $\overline{\nu}_p$ and disregard the fit to ENDF, we see that all three optimizations are able to reproduce the experimental data, as we would expect since `CGMF` was fit to these data. We can see that the two fits when first-chance fission was fixed and when all parameters were fit simultaneously (black solid and red dashed) are slightly below the data in the second-chance fission incident energy range. This difference is removed when the finer and then down-selected grid is used for the optimization. The fit to ENDF also has some challenges in the third-chance incident energy range, which was also seen in the output of the Kalman filter. The cause of this discrepancy is still under further investigation. For the average prompt γ-ray multiplicity, $\overline{N}_\gamma$, we have significantly different results when the four optimizations are performed. As had been mentioned when looking at the $\langle\mathrm{TKE}\rangle(E_{\mathrm{inc}})$, to keep $\overline{\nu}_p$ consistent with experimental data, the differences in the $\langle\mathrm{TKE}\rangle(E_{\mathrm{inc}})$ parametrizations are compensated by changes to the spin cutoff parameters. These parameter changes have a significantly larger impact on the γ-ray multiplicity. Therefore, in the right panel, even though the four optimizations give very similar results at thermal, the shape of the energy dependence varies greatly between the four calculations, and we once again see that there is something odd going on with the ENDF fit above third-chance fission. While we do not expect to reproduce the ENDF/B-VIII.0 evaluation with `CGMF`, since the shape is based on photon production data, we do expect the average multiplicity to increase with increasing incident energy. Once again, the multiplicity does not increase across the whole energy range for the fit to ENDF (again, compensation for the $\langle\mathrm{TKE}\rangle(E_{\mathrm{inc}})$ parametrization).

We then plot the average outgoing energies of the prompt neutrons and γ rays in Fig. 12. As expected based on our previous sensitivity studies, these optimizations have very little impact on the outgoing neutron energies, particularly above first-chance fission. We do see some differences coming from the spread in the $\langle\mathrm{TKE}\rangle(E_{\mathrm{inc}})$—causing a larger or smaller boost on the neutrons. The γ-ray energies are also very similar between the optimizations, not including the fit to ENDF, where we once again see unresolved problems in the third-chance energy range.

Figures 13 and 14 show the multiplicity distributions for the neutrons and γ rays where experimental data are available (significantly more incident energy values for $P(\nu)$ compared to $P(N_\gamma)$). For the neutron multiplicity, we see better agreement to the experimental data from each of the parametrizations except for the fit to ENDF. The disagreement between $P(\nu)$ and the ENDF fit is to be expected

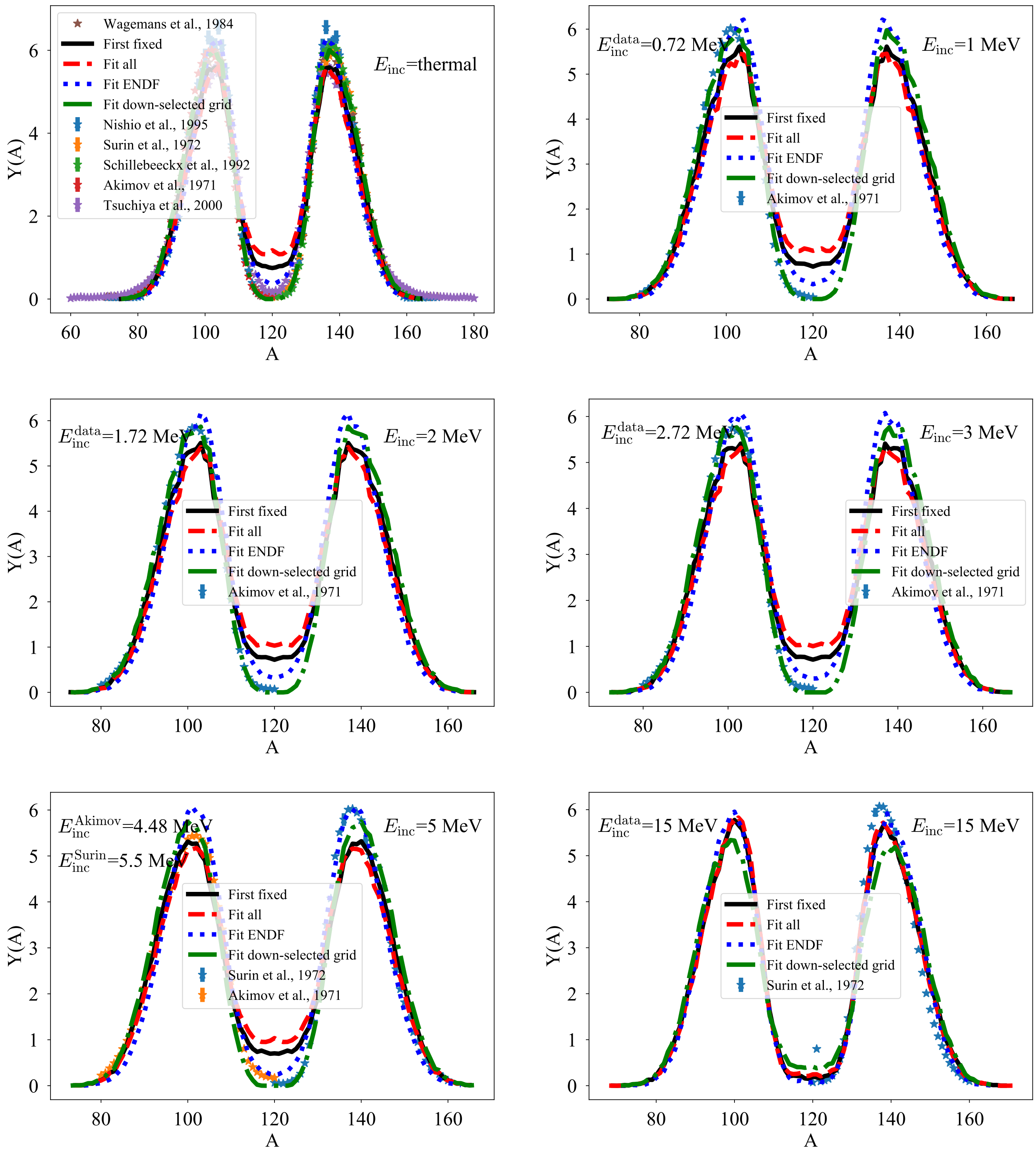

Figure 9: Comparison of the pre-neutron emission mass yield, $Y(A)$, among the four optimizations with CGMF and available experimental data.

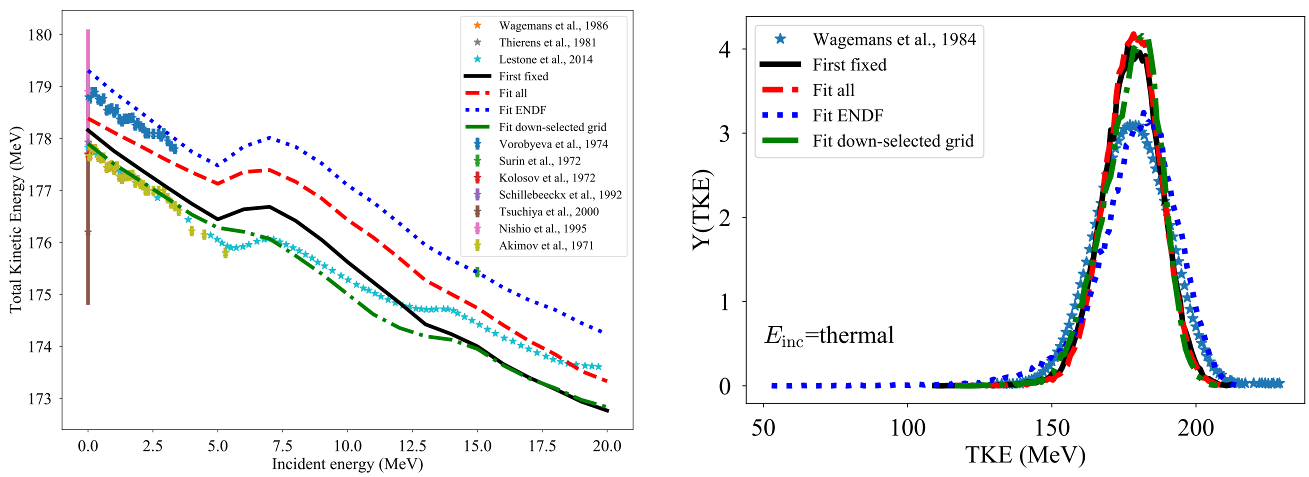

Figure 10: (Left) Comparison among the four CGMF optimizations and available experimental data for the total kinetic energy as a function of incident neutron energy, $\langle \text{TKE} \rangle (E_{\text{inc}})$. (Right) Same comparison for the distribution of TKE, $Y(\text{TKE})$, for thermal incident neutrons.

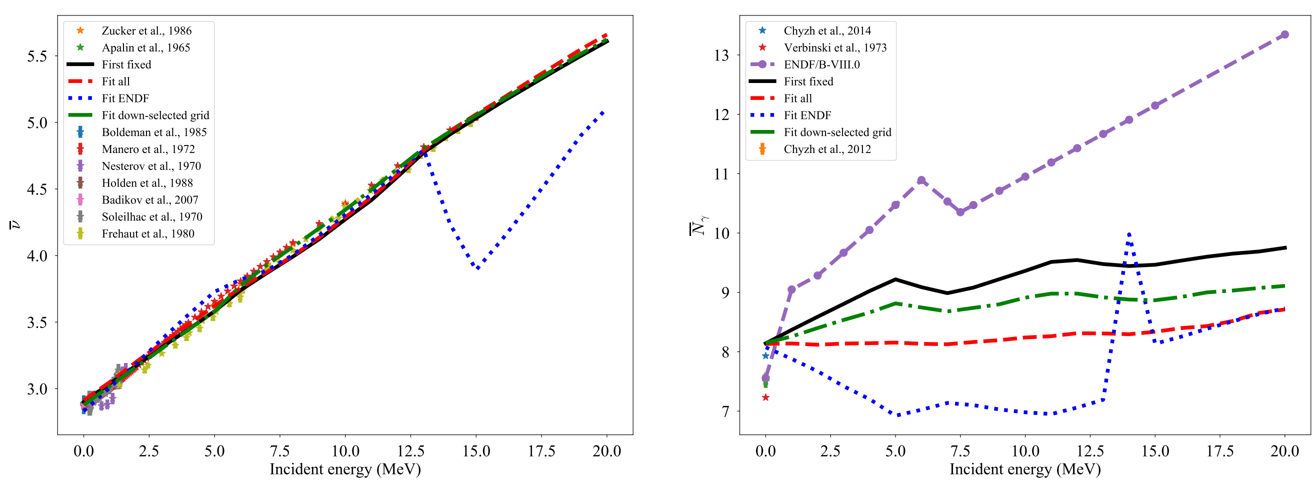

Figure 11: Comparison among the four optimizations with CGMF and available experimental data for (left) average prompt neutron multiplicity, $\overline{\nu}_p$ and (right) average prompt γ-ray multiplicity, $\overline{N}_\gamma$. For $\overline{N}_\gamma$, we also show the comparison to the ENDF/B-VIII.0 evaluation.

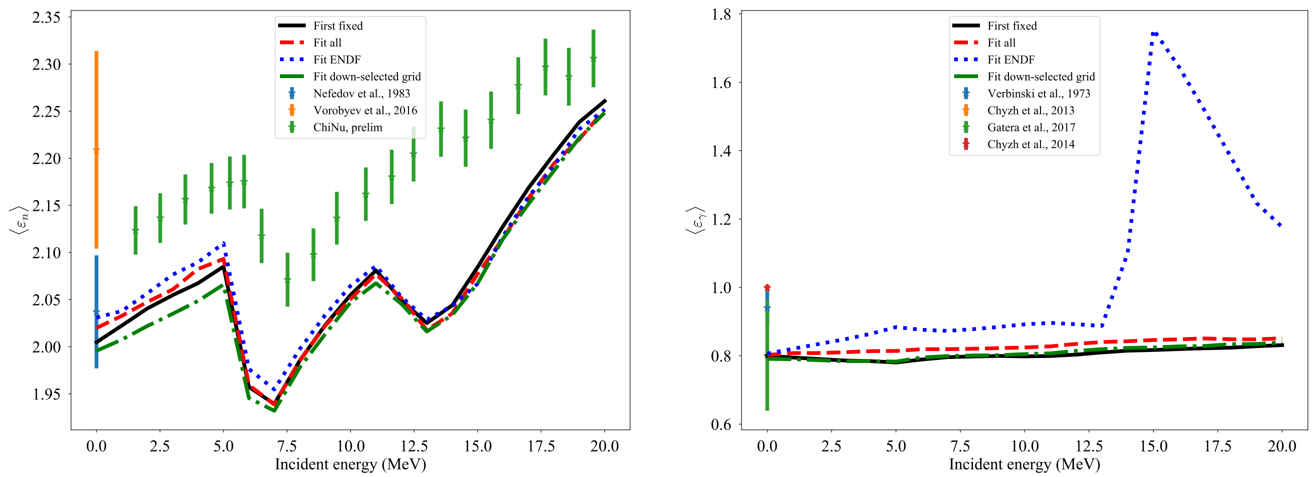

Figure 12: Comparison among the four optimizations with CGMF and available experimental data for (left) average outgoing neutron energy and (right) average outgoing γ-ray energy.

based on the difference between that fit and the others for $Y(\text{TKE})$. In each case, the peak of the multiplicity distribution is not quite reproduced, but we typically see slight discrepancies in this region between data and CGMF. As with the other γ-ray observables, there is not much difference in $P(N_\gamma)$ between the four calculations. We also should note that there is no γ-ray threshold energy taken into account in the CGMF calculations, which would shift the peak of the distribution to somewhat lower values for N_γ.

Overall, while each of the parameter sets besides the one that was fit to ENDF give reasonable observables compared to data, the fit with the down-selected grid produces the most physically sensible results. This calculation is ultimately what we propose for the new ENDF/B-VIII.I evaluation and what is included in all of the validation calculations.

Validation of Evaluated Nuclear Data Versus Validation Experiment Responses The final ^{239}Pu(n,f) $\overline{\nu}_p$ was also validated with respect to various integral responses. To this end, we included the new data (with the help of N. Gibson and W. Haeck, both XCP-5) into the ^{239}Pu ENDF/B-VIII.0 file. The only differences between the the ^{239}Pu ENDF/B-VIII.0 file are:

- The ^{239}Pu(n,f) $\overline{\nu}_p$,
- ^{239}Pu(n,f) $\overline{\nu}_t$ (which has to absorb changes in ^{239}Pu(n,f) $\overline{\nu}_p$ to maintain the sum-rule of $\overline{\nu}_t$ in the file),
- A new PFNS including Chi-Nu and CEA data from 0.5–30 MeV,
- The INDEN PFNS at thermal,
- A new ^{239}Pu(n,f) cross section including fissionTPC data [4] and updates due to the templates of expected measurement uncertainties in (n,f) measurements [53],
- An (n,el) cross section that absorbs changes in the (n,f) cross to ensure that the sum-rule of cross sections (all partials sum to total) is obeyed.

In short, we changed the observables of the fission-source term all at once. That is necessary because if one changes only one constituent of the fission-source term (like the cross section, PFNS or $\overline{\nu}_p$), criticality, k_{eff}, will invariably be off as they are balanced out against each other.

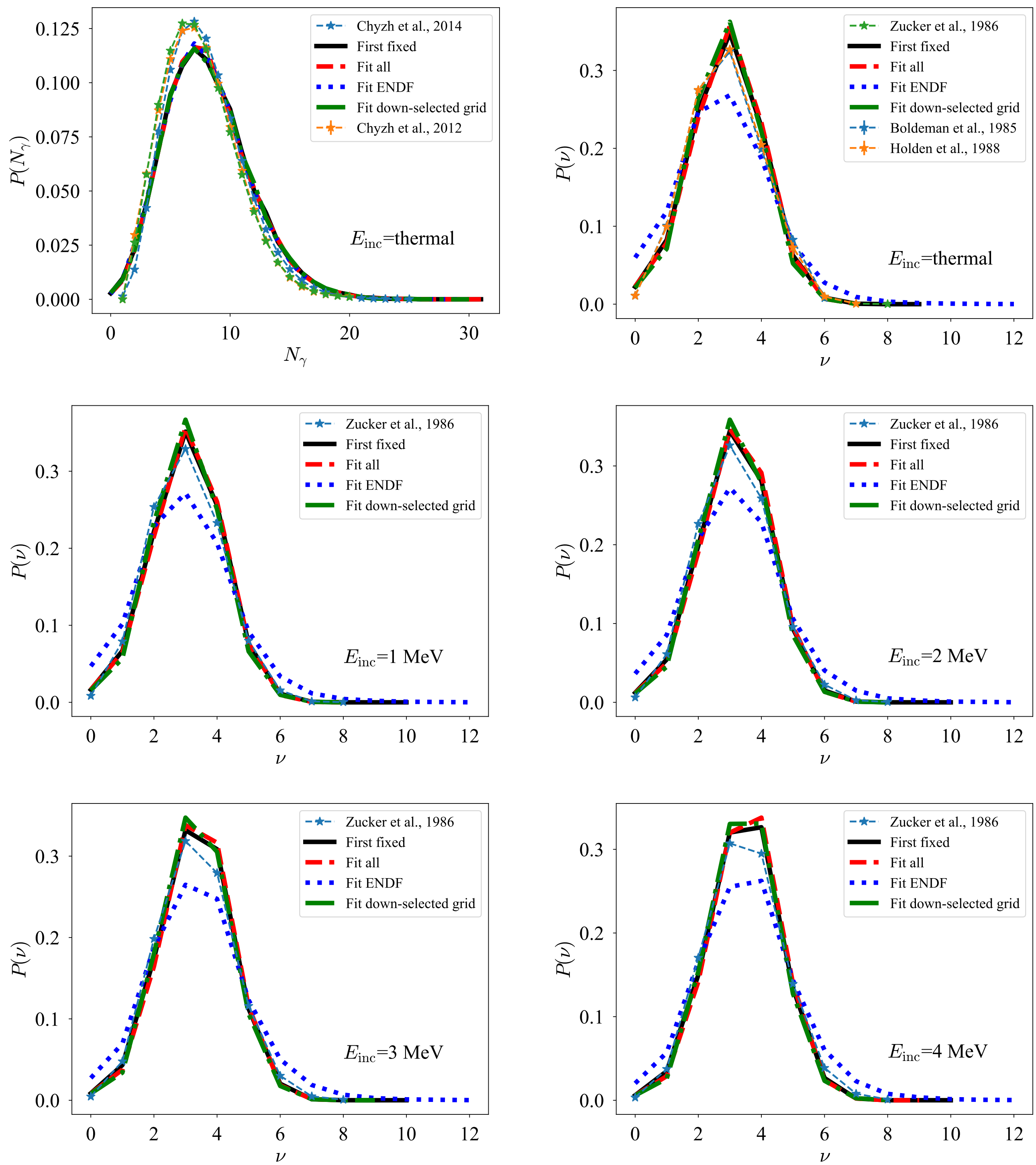

Figure 13: Comparison among the four optimizations with `CGMF` and available experimental data for the γ-ray multiplicity distribution, $P(N_\gamma)$ for thermal incident neutrons (upper left panel), and the neutron multiplicity distribution, $P(\nu)$, for incident neutrons between thermal and 4 MeV (remaining panels). Incident energies are given in the lower right corner of each panel.

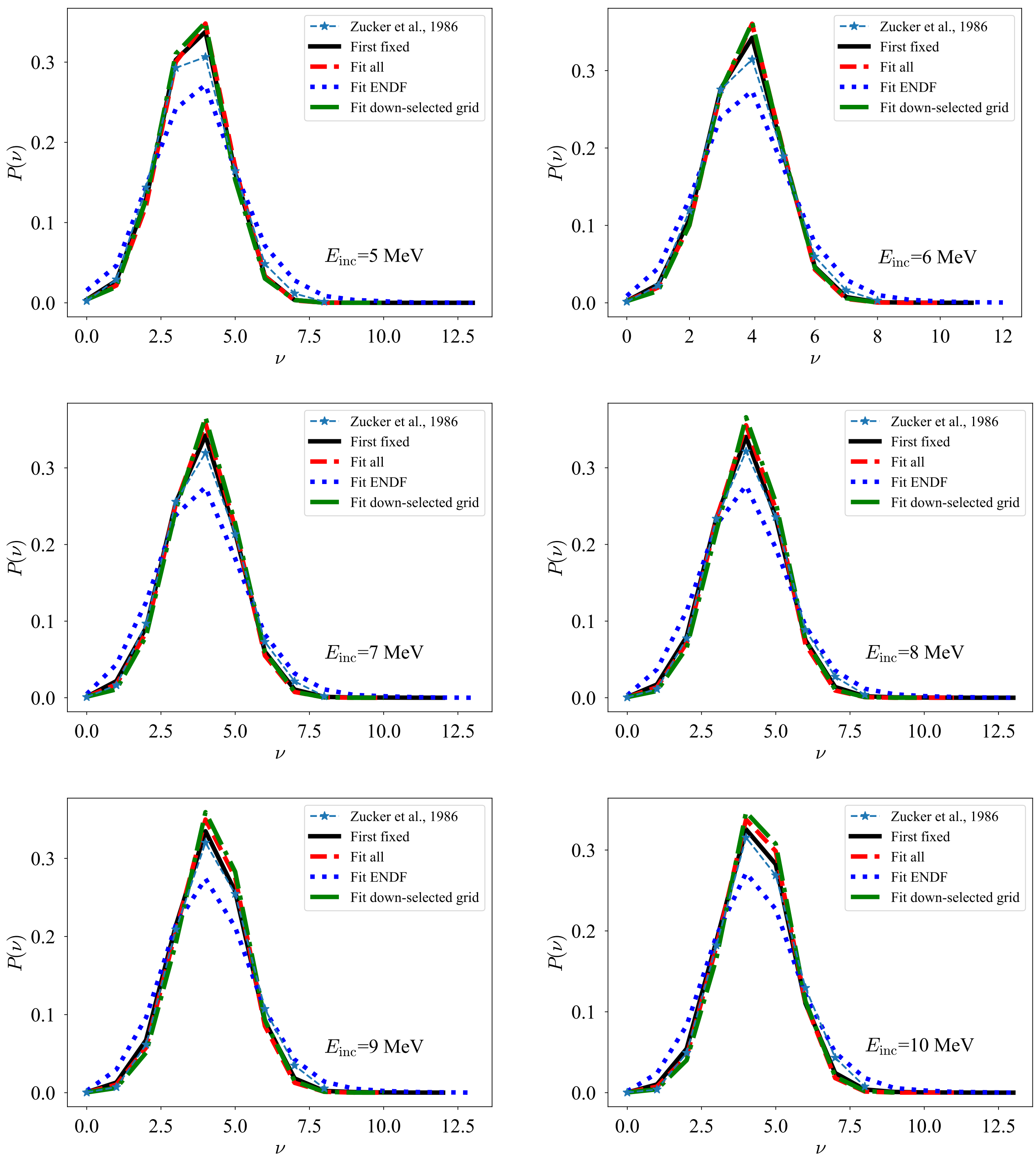

Figure 14: Same as Fig. 13 with $P(\nu)$ for incident energies between 5 MeV and 10 MeV.

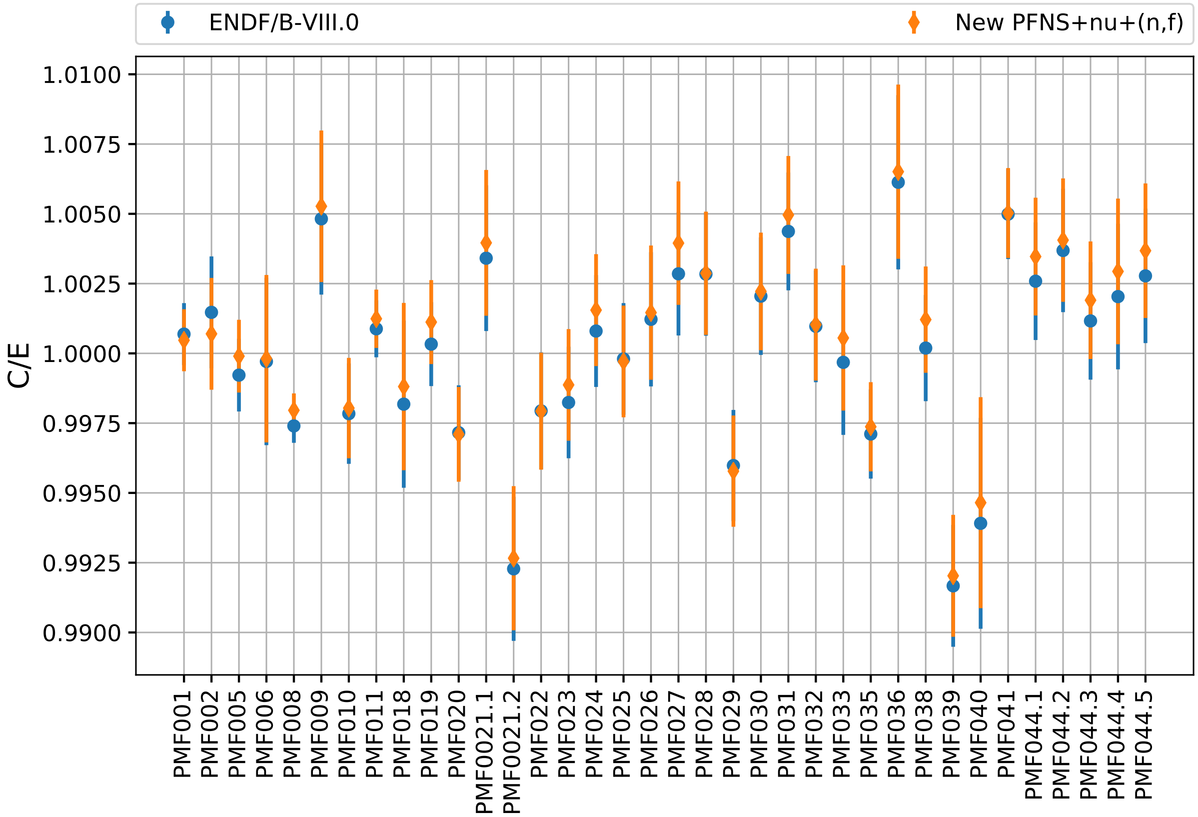

Figure 15: Calculated over experimental, C/E, values are shown for criticality, $k_{\rm eff}$, of PU-MET-FAST assemblies in ICSBEP. C/E values are given for ENDF/B-VIII.0 as well as the new ^{239}Pu files including new ^{239}Pu(n,f) cross sections, PFNS or $\overline{\nu}_p$.

However, and this should be emphasized, we did **NOT** balance out the (n,f) cross section, PFNS or $\overline{\nu}_p$ with each other here. We implemented all of them as obtained from the most recent analyses including a wealth of new, high-precision experimental data on all three observables simultaneously. So, all changes just reflect our improved understanding thanks to measurement campaigns and informed by other fission observables through `CGMF` for the case of the $\overline{\nu}_p$.

It was very surprising for us to see in Fig. 15 that the criticality, $k_{\rm eff}$, values of PU-MET-FAST assemblies of ICSBEP [54] simulated with the new ^{239}Pu files are reasonably close to the ENDF/B-VIII.0 file despite the fact that sizable changes happened in ^{239}Pu(n,f) cross sections, PFNS and $\overline{\nu}_p$. If one takes the mean bias over all ENDF/B-VIII.0 C/E values, it is 18 pcm, while it is slightly increased with 58 pcm for the new file. It is interesting to note here that those benchmarks with the hardest spectrum are in general simulating better. For instance, Jezebel (PMF001, v.4), dirty Jezebel (PMF002) and Falttop-Pu (PMF006) all move closer to their respective experimental values with the new value, while those PU-MET-FAST assemblies with a softer spectrum (011, 018, 019, 021.1, 021.2, 024, 027, 031, 032, 033, 036, 038 and all cases of 044) have worse C/E than when simulated with ENDF/B-VIII.0.

This trend can be also observed when simulating PU-MET-INT assemblies, which have an intermediate (even softer) spectrum. The C/E values with the new file are distinctly worse in Fig. 16 than when simulated with ENDF/B-VIII.0. The mean bias over PMI C/E goes from 601 pcm with ENDF/B-VIII.0 to 767 pcm with the new file.

All of this points to the fact that the new ^{239}Pu(n,f) $\overline{\nu}_p$ is performing well together with PFNS and (n,f) cross section from a few hundred keV to 5 MeV. However, a slight tweak in the ^{239}Pu(n,f)

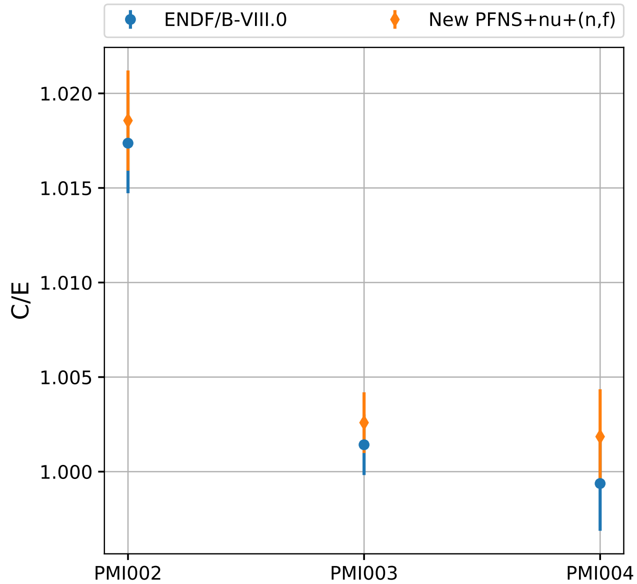

Figure 16: Calculated over experimental, C/E, values are shown for criticality, k_{eff}, of PU-MET-INT assemblies in ICSBEP. C/E values are given for ENDF/B-VIII.0 as well as the new ^{239}Pu files including new ^{239}Pu(n,f) cross sections, PFNS or $\overline{\nu}_p$.

$\overline{\nu}_p$ might be needed from 80 keV to a few hundred keV. This tweak will be undertaken at a later point as T-2 evaluators are currently working on updating other reaction cross sections.

Changes in nuclear data above 5 MeV cannot be validated with criticality benchmarks. However, LLNL pulsed spheres [55] allow us to validate ^{239}Pu from approximately 10–15 MeV, where we also observed changes in $\overline{\nu}_p$, PFNS and (n,f) cross sections. These changes did not significantly impact the simulation of Pu LLNL pulsed spheres as can be seen in Fig. 17. This can be attributed to the modest changes in all three observables compared to the significant C/E bias in the simulated values, but also to the fact that changes in a narrow energy range in (n,f) cross section and $\overline{\nu}$ lead mostly to a constant off-set of the simulated neutron-leakage spectra. As they are treated as shape data and are re-normalized to yield an integral of one over the entire spectrum, changes in $\overline{\nu}$ and (n,f) cross section have little effect.

The last integral response we study here are reaction rates in the center of the Jezebel and Flattop-Pu critical assemblies. The main objective here was to "do no harm" and be reasonably close to ENDF/B-VIII.0 values which was achieved as shown in Table IV.

All in all, the new ^{239}Pu file performed surprisingly well when simulating various integral responses, despite the fact that we did not tune any of the nuclear data with respect to each other. In addition to that, the evaluated parameters tied to the ^{239}Pu(n,f) $\overline{\nu}_p$ link back favorably to various fission data through `CGMF`. Hence, the new evaluated $\overline{\nu}_p$ is being considered as a potential candidate for ENDF/B-VIII.1.

4.3 Evaluated Results of ^{235}U(n,f) $\overline{\nu}_p$

Again, two types of evaluations were performed here, a GLS evaluation including only experimental data and a second one using the Kalman filter to include the `CGMF` model. The first type of evaluation was undertaken to better compare to ENDF/B-VIII.0 as we assume that Phil Young evaluated his $\overline{\nu}$ based on only experimental data and a covariance analysis.

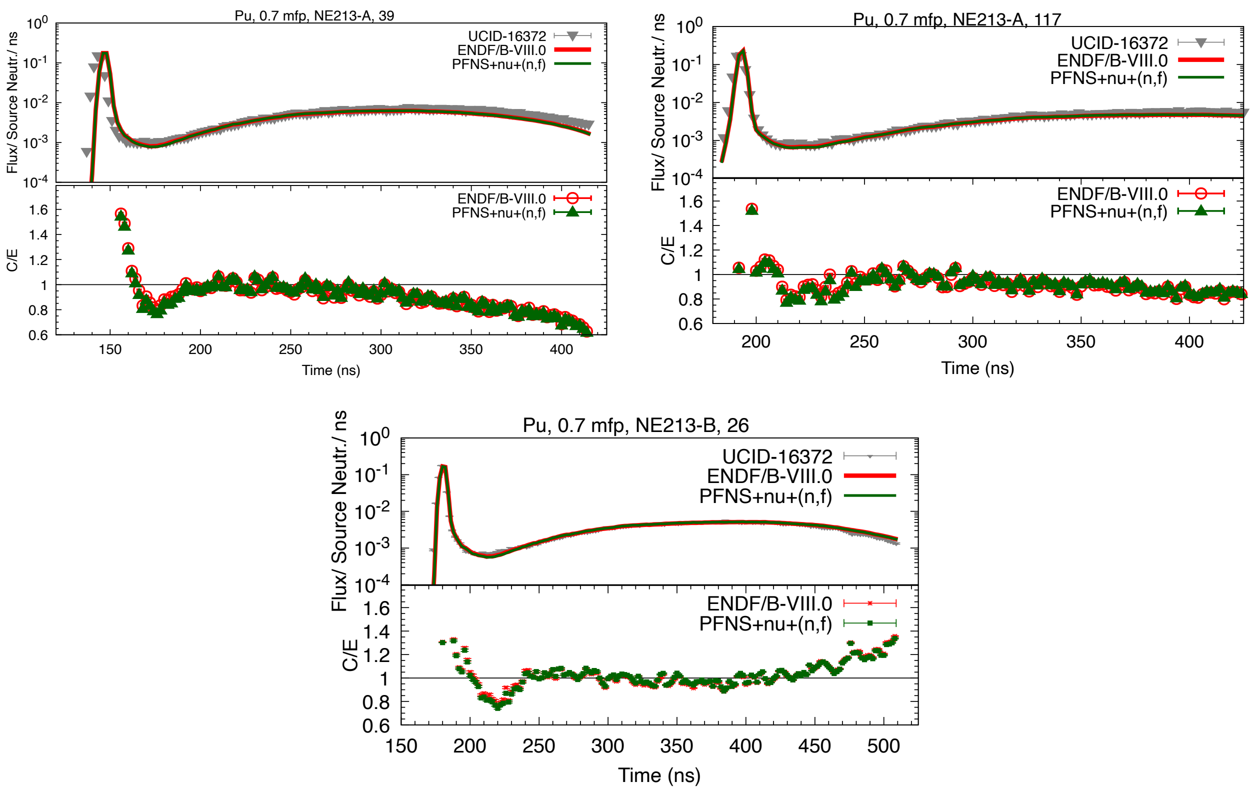

Figure 17: Calculated and experimental values are shown for Pu LLNL pulsed spheres. Calculated values are given for ENDF/B-VIII.0 as well as the new ^{239}Pu files including new ^{239}Pu(n,f) cross sections, PFNS or $\overline{\nu}_p$.

Table IV: Calculated values are shown for reaction rates of various reactions in the Jezebel and Flattop-Pu critical assemblies. Calculated values are given for ENDF/B-VIII.0 as well as the new ^{239}Pu files including new ^{239}Pu(n,f) cross sections, PFNS or $\overline{\nu}_p$.

Assembly	Oservable	ENDF/B-VIII.0	VIII.0+PFNS+(n,f) cs+ $\overline{\nu}$
Jezebel	$k_{\rm eff}$	1.00069(1)	1.00047(1)
Jezebel	^{239}Pu(n,2n)/^{239}Pu(n,f)	0.00230(5)	0.00224(5)
Jezebel	^{239}Pu(n,γ)/^{239}Pu(n,f)	0.0345(2)	0.355(2)
Jezebel	^{238}U(n,f)/^{235}U(n,f)	0.212(1)	0.209(1)
Jezebel	^{237}Np(n,f)/^{235}U(n,f)	0.9768(5)	0.9662(5)
Jezebel	^{233}U(n,f)/^{235}U(n,f)	1.566(7)	1.566(7)
Jezebel	^{239}Pu(n,f)/^{235}U(n,f)	1.427(6)	1.423(6)
Flattop-Pu	$k_{\rm eff}$	0.99971(1)	0.99981(1)
Flattop-Pu	^{239}Pu(n,2n)/^{239}Pu(n,f)	0.00197(4)	0.00193(4)
Flattop-Pu	^{239}Pu(n,γ)/^{239}Pu(n,f)	0.0455(1)	0.0464(1)
Flattop-Pu	^{238}U(n,f)/^{235}U(n,f)	0.1800(9)	0.1774(9)
Flattop-Pu	^{237}Np(n,f)/^{235}U(n,f)	0.8581(4)	0.8497(4)

Evaluated Results of ^{235}U(n,f) $\overline{\nu}_p$ using Only Experimental Data As mentioned before, we know only a little in how far the ^{235}U(n,f) $\overline{\nu}_p$ evaluation presented here differs from that currently in ENDF/B-VIII.0. The ENDF/B-VIII.0 evaluation is based on a covariance analysis using differential experimental data, possibly, nearly all the data available at the time of the evaluation if one extrapolates from what was done for the ^{239}Pu(n,f) $\overline{\nu}_p$ evaluation. We also know that Boikov and Khoklov data were not included in the evaluation of ENDF/B-VIII.0 given that they were released after the time of the evaluation. Hence, we show two evaluated results with GLS in Fig. 18: (a) one with all accepted data of Table I, and (b) one excluding Boikov and Khoklov data.

The evaluation with Boikov and Khoklov is noticeably lower than the one without the data below 800 keV. This decrease of the evaluated data is likely caused by Khoklov data because Boikov data are only provided at 4 and 14 MeV. This corresponds to the fact that Khoklov data are systematically lower than the bulk of the data until about 2 MeV. The evaluation without Boikov and Khoklov data, however, meanders around ENDF/B-VIII.0 and one can assume that some of the differences observed, especially up to 5 MeV, could be eradicated by smoothing the evaluation without Boikov and Khoklov data.

Also, differences in the evaluation with only exerimental data and ENDF/B-VIII.0 are observed around multiple-chance fission thresholds, at 6.5 MeV and 13 MeV. ENDF/B-VIII.0 has a strictly linear behavior, while the GLS evaluation shows small enhancements in $\overline{\nu}_p$ around the threshold. This trend in the data is actually expected from physics point of view and it is encouraging that the experimental data are precise enough to resolve these structures.

Hence, differences between ENDF/B-VIII.0 and the GLS evaluation (only experimental data) are caused by:

- Khoklov data that lead to an overall lower trend in $\overline{\nu}_p$ until 800 keV,
- Smoothing assumptions that remove statistical fluctuations in the data for ENDF/B-VIII.0 but also removed structures in $\overline{\nu}_p$ around the second- and third-chance fission thresholds.

It can be also seen from Fig. 19 that the evaluated uncertainties are distinctly higher for the new evaluation than ENDF/B-VIII.0. ENDF/B-VIII.0 uncertainties are so low because they were not enlarged commensurate with the enlarged ^{252}Cf(sf) $\overline{\nu}$ uncertainties.

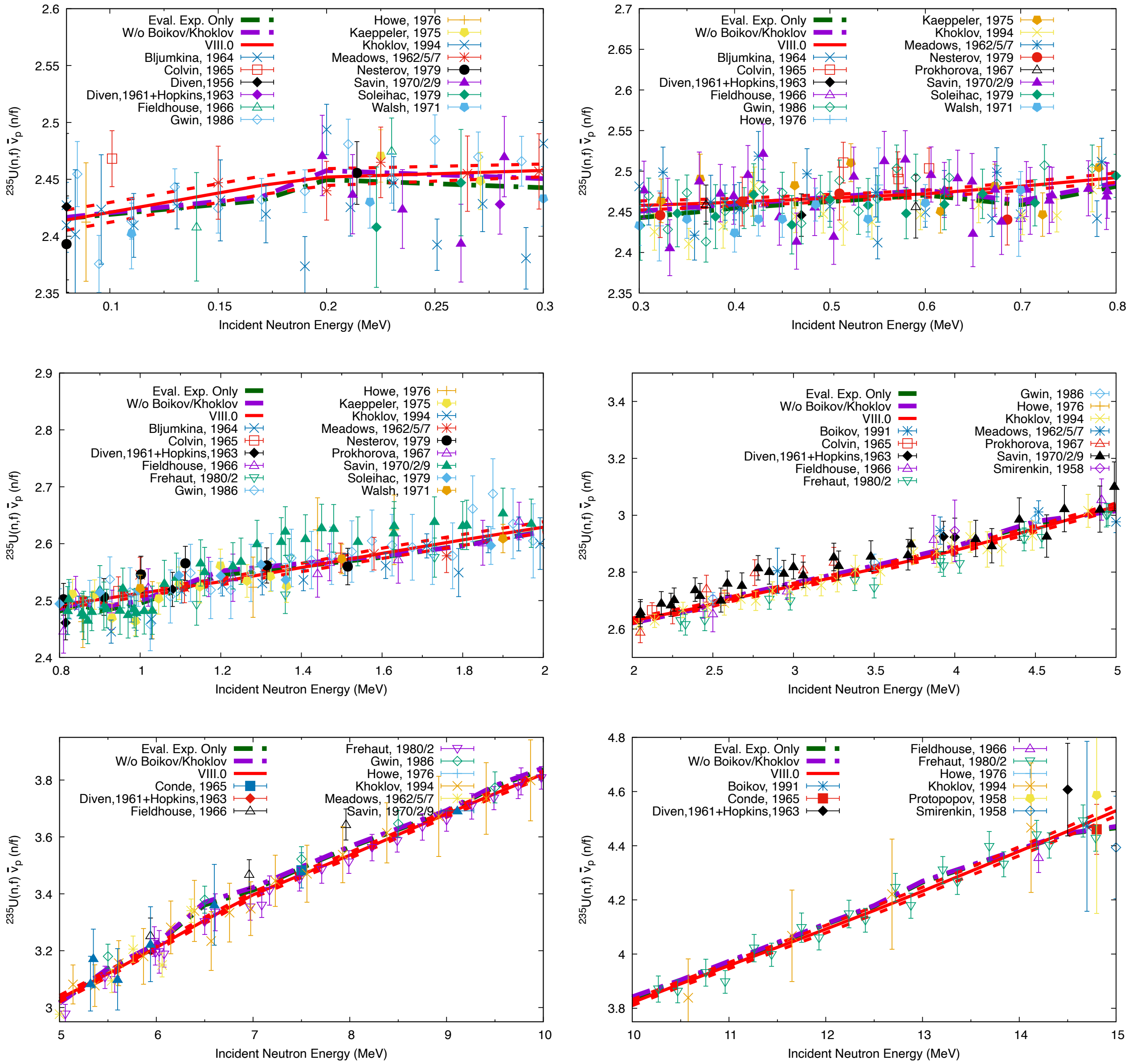

Figure 18: Evaluated ^{235}U(n,f) $\bar{\nu}_p$ are shown in comparison to ENDF/B-VIII.0 and experimental data that were used for the evaluation. The evaluated data were obtained with a statistical analysis of only experimental data. One evaluation is shown with and another without Boikov and Khoklov experimental data.

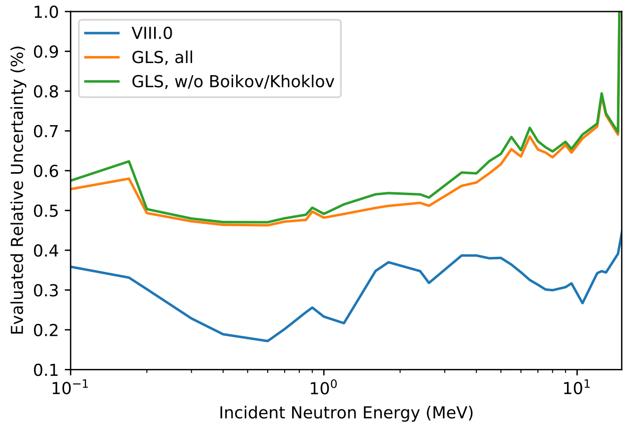

Figure 19: Evaluated uncertainties with and without Marini are compared to ENDF/B-VIII.0 uncertainties and PUBs bounds.

Evaluated Results of ^{235}U(n,f) $\overline{\nu}_p$ Including CGMF Again several evaluations of the ^{235}U(n,f) $\overline{\nu}_p$ including the `CGMF` model via the Kalman filter were undertaken; we show in Fig. 20 the results obtained with two different scenarios:

1. A denser or a smaller grid; the latter takes into account points at {thermal, 0.1, 0.2, 0.5, 0.6, 1.2, 1.3, 1.4, 1.5, 1.75, 2.25}, then every half MeV until 7 MeV and then every MeV,
2. Allowing or excluding a bend in the $\langle TKE \rangle$.

As can be seen in the upper two rows of Fig. 20, the evaluated results until 2 MeV are closer to our baseline, the evaluation based on only experimental data, when one down-selects the grid. The reason for that lies in the fact that differential data, especially below 800 keV have a wide spread and some data show wave-like structures around 0.7 MeV (see data of Savin, Kaeppeller, Nesterov and Gwin), while others are smoother (Khoklov) and again others show random behavior (Meadows, Soleihac, Walsh) that are difficult to reproduce by a model that predicts a straight line. Down-selecting the grid allows for an averaging of these structures in the data where they are not predicted by the model and give more stable results. Therefore, we show in the following only results for a down-selected grid.

The second consideration concerns the $\langle TKE \rangle$. The data of Duke et al. in the left-hand side lower row of Fig. 30 show a distinct bend in the $\langle TKE \rangle$ below 1 MeV, while this effect is less clear in the data of Vorobyeva and Meadows. Preliminary data from the fissionTPC also do not support this bend. The default parameterization of `CGMF` models this bend in $\langle TKE \rangle$ and perpetuates it for the second- and third-chance fission threshold parameters.

When we use this parameterization for the evaluation, including the bend in $\langle TKE \rangle$, the Kalman filter changes the parameters related to this bend (E_0 and b) significantly for first-chance fission in Fig. 21. Moreover, it drives the parameter E_0 either to zero or negative values for second- and third-chance fission (Figs. 22 and 23), which effectively removes the bend for parametrizing $\langle TKE \rangle$ for these two regimes.

Given that behavior of evaluated parameters and the fact that the bend in $\langle TKE \rangle$ is supported only by a part of the data sets, and it is somehow unclear at what exact energy it is situated, we decided to try a second parameterization of $\langle TKE \rangle$ without the bends. If we do that, changes in $\langle TKE \rangle$-related parameters (a and d) are more modest in Figs. 24–26. It should also be mentioned that evaluated parameter uncertainties are less erratic, when we take the bends out of $\langle TKE \rangle$ for the second- and third-chance fission parameters.

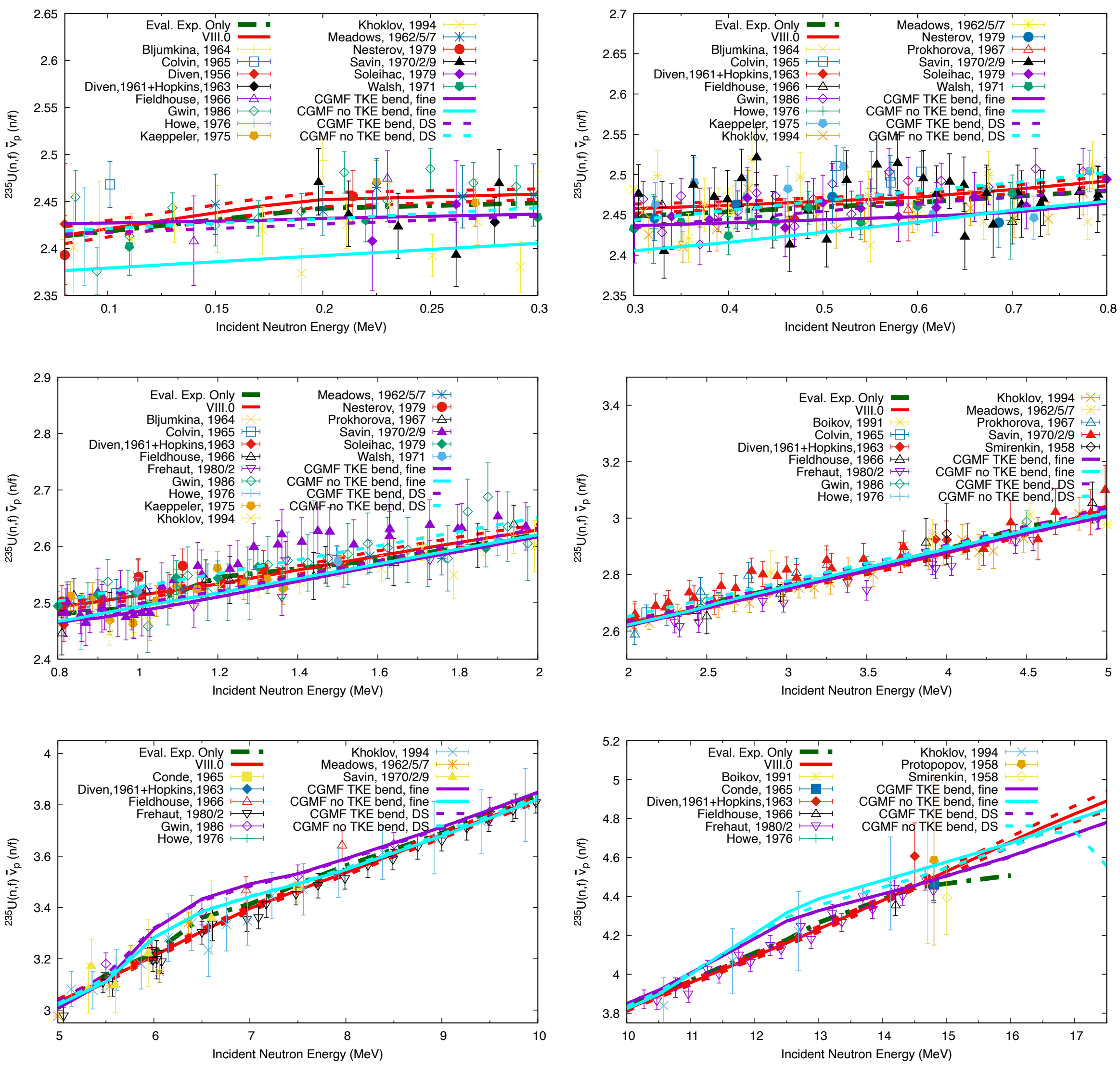

Figure 20: Evaluated ^{235}U(n,f) $\overline{\nu}_p$ are shown in comparison to ENDF/B-VIII.0 and experimental data that were used for the evaluation. The evaluated data were obtained with CGMF and only experimental data.

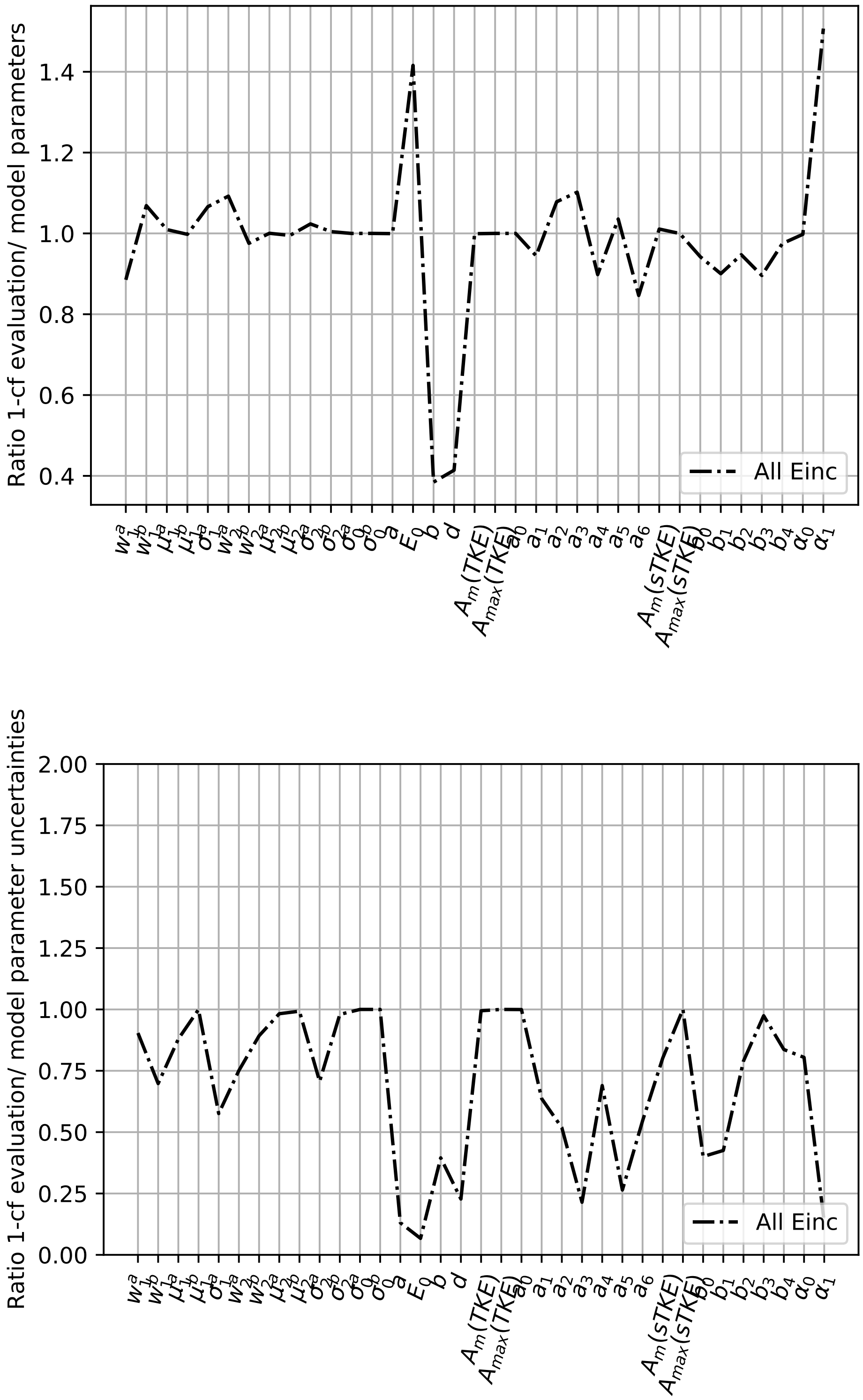

Figure 21: Impact on evaluated parameters and their uncertainties if all E_{inc} are fitted at once using ENDF/B-VIII.0 nuclear data above 14 MeV. Changes in first-chance fission parameters are shown.

However, evaluated $\overline{\nu}_p$ in Fig. 20 agree overall better up to 2 MeV if we consider the bend in $\langle TKE \rangle$ as part of the CGMF modeling, while the agreement at second-chance fission is better if we take the bends out. From that we conclude that it might be best to just consider a bend in $\langle TKE \rangle$ for

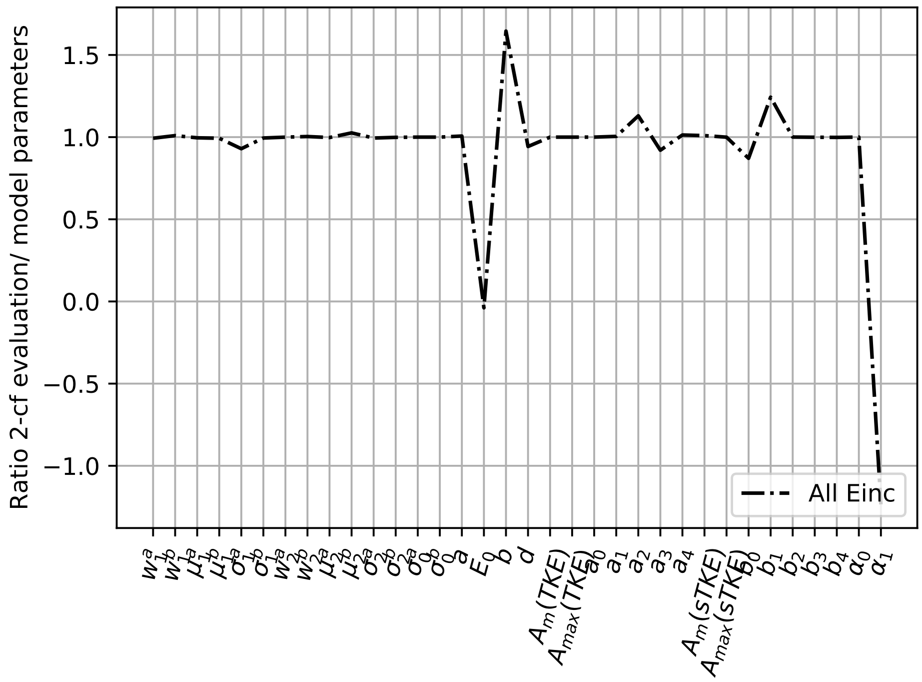

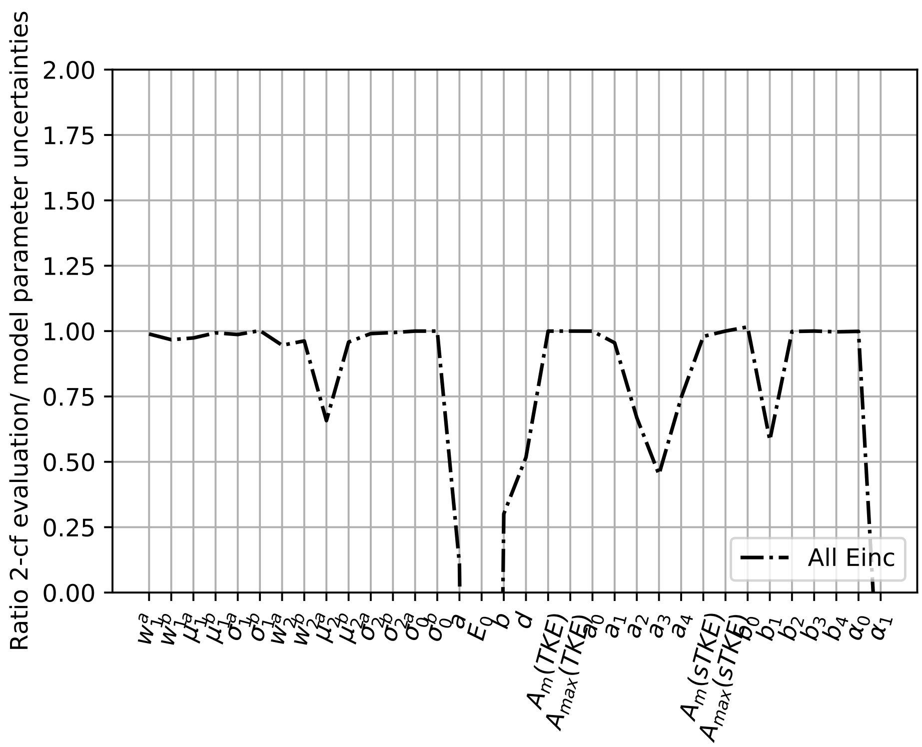

Figure 22: Impact on evaluated parameters and their uncertainties if all E_{inc} are fitted at once using ENDF/B-VIII.0 nuclear data above 14 MeV. Changes in second-chance fission parameters are shown.

first-chance fission and otherwise not. Work is currently under-way to try this out.

Another feature that is worth noticing is the dip in the evaluated data at 17 MeV for $\langle TKE \rangle$ without a bend and a down-selected grid; also, problems in fitting third-chance fission can be observed. This could be related to the spin-parity parameter α_1 that varies widely. We will try to constrain this

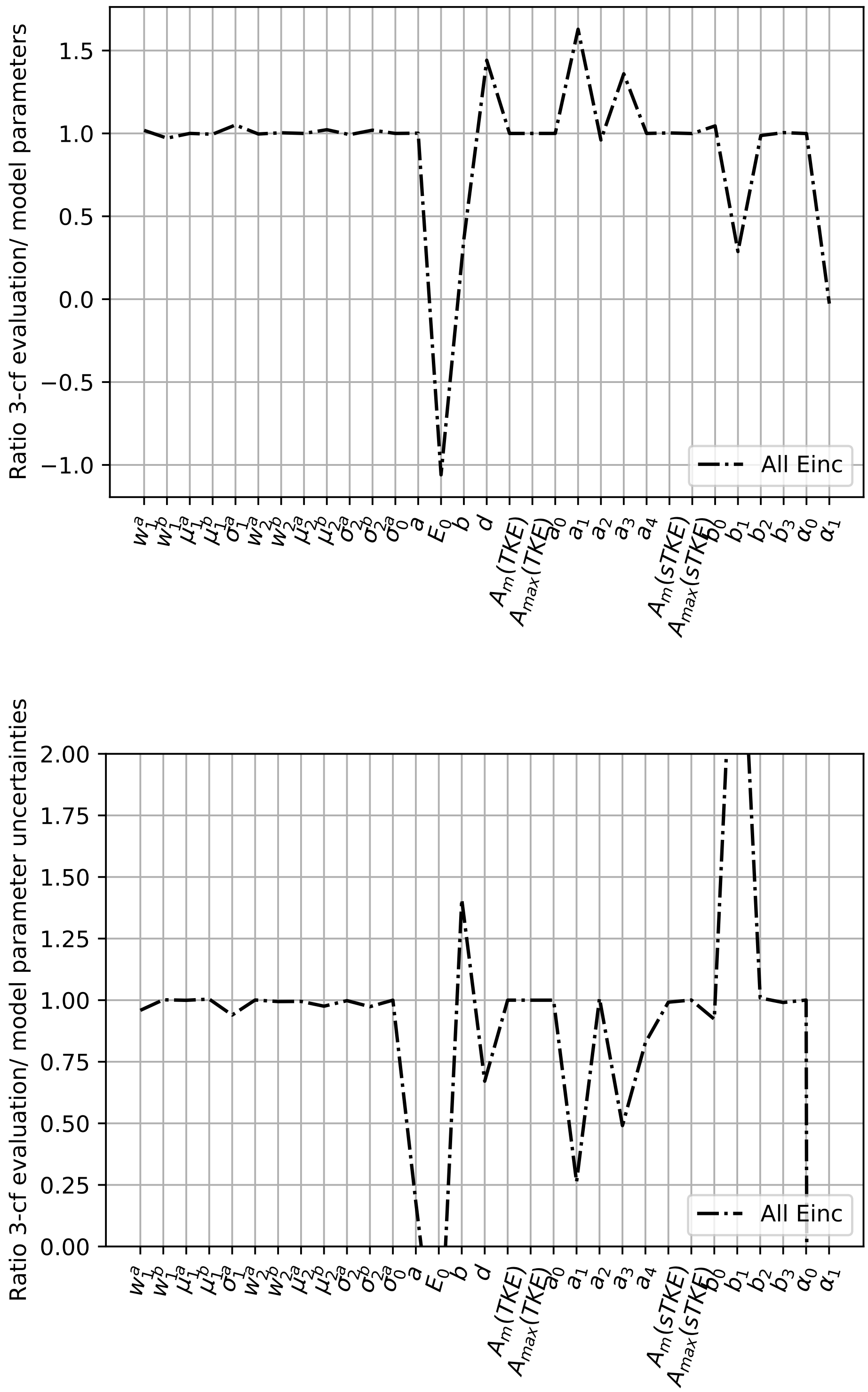

Figure 23: Impact on evaluated parameters and their uncertainties if all E_{inc} are fitted at once using ENDF/B-VIII.0 nuclear data above 14 MeV. Changes in third-chance fission parameters are shown.

parameter more tightly and see if the features in the evaluated data will then vanish.

Lastly, it should be mentioned that the evaluated uncertainties obtained with `CGMF` are reasonably close in Fig. 27 to the evaluation with only experimental data (our baseline) to conclude that the evaluated uncertainties are not adversely impacted by the `CGMF` model.

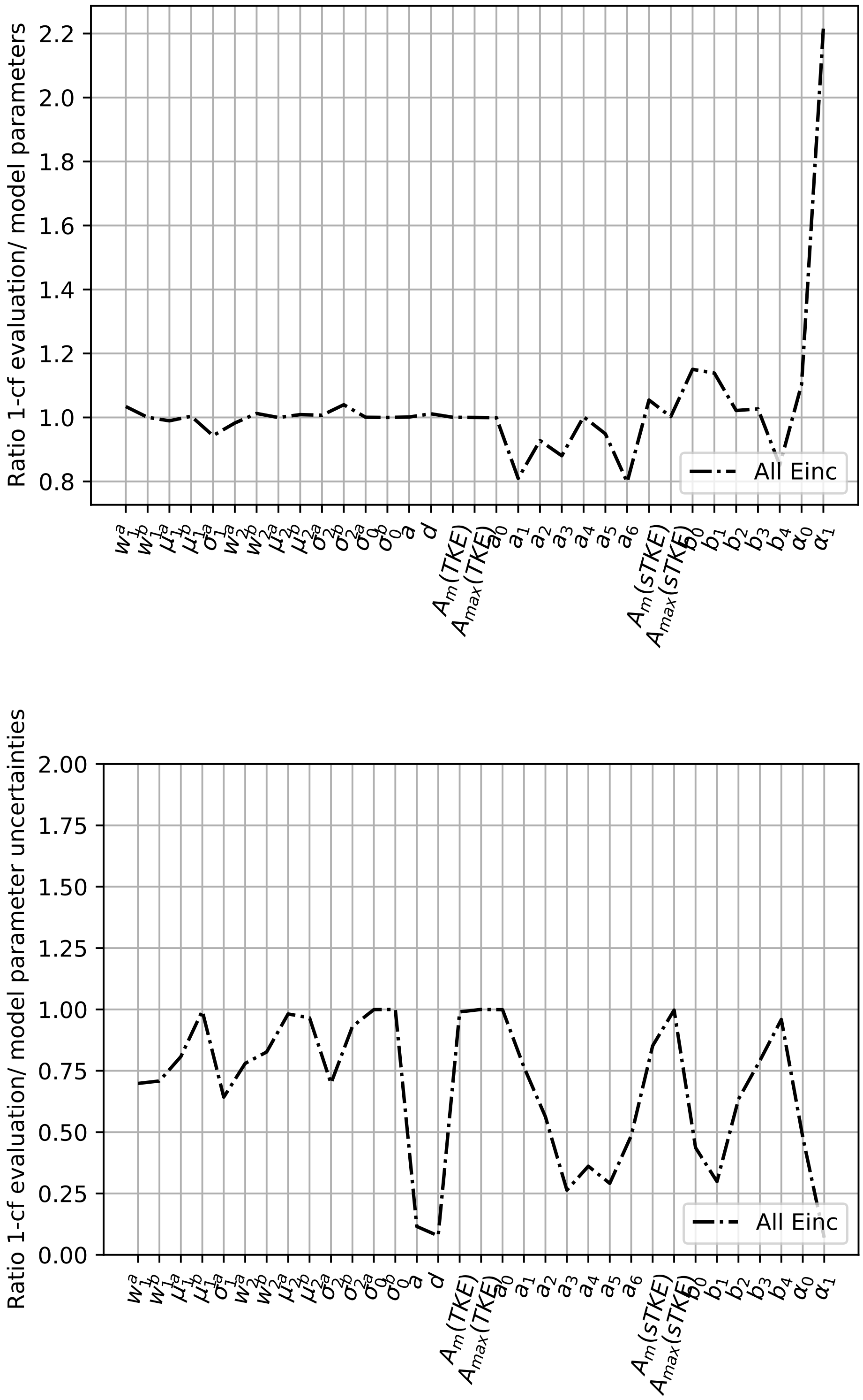

Figure 24: Impact on evaluated parameters and their uncertainties if all $E_{\rm inc}$ are fitted at once on a down-selected grid and taking out a bend in $\langle TKE \rangle$ at approximately 1 MeV. Changes in first-chance fission parameters are shown.

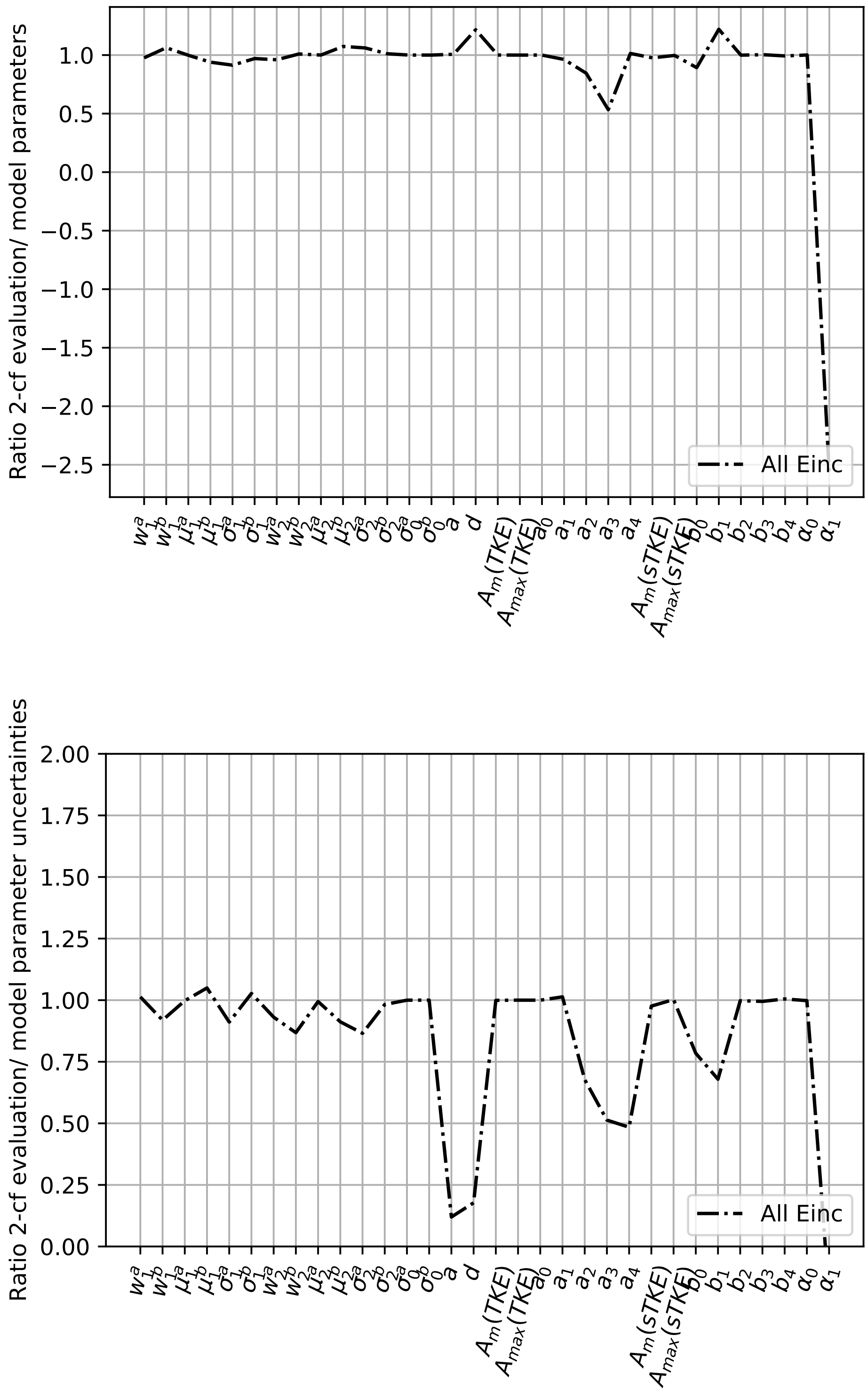

Figure 25: Impact on evaluated parameters and their uncertainties if all E_{inc} are fitted at once on a down-selected grid and taking out a bend in $\langle TKE \rangle$ at approximately 1 MeV. Changes in second-chance fission parameters are shown.

4.4 Validation of Evaluated Parameters Against Various Fission Data

We again compare the `CGMF` calculations to a variety of prompt-fission observables beyond $\overline{\nu}_p$, that were not included in the optimization. Here, we show the comparison of two optimizations; the first keeping

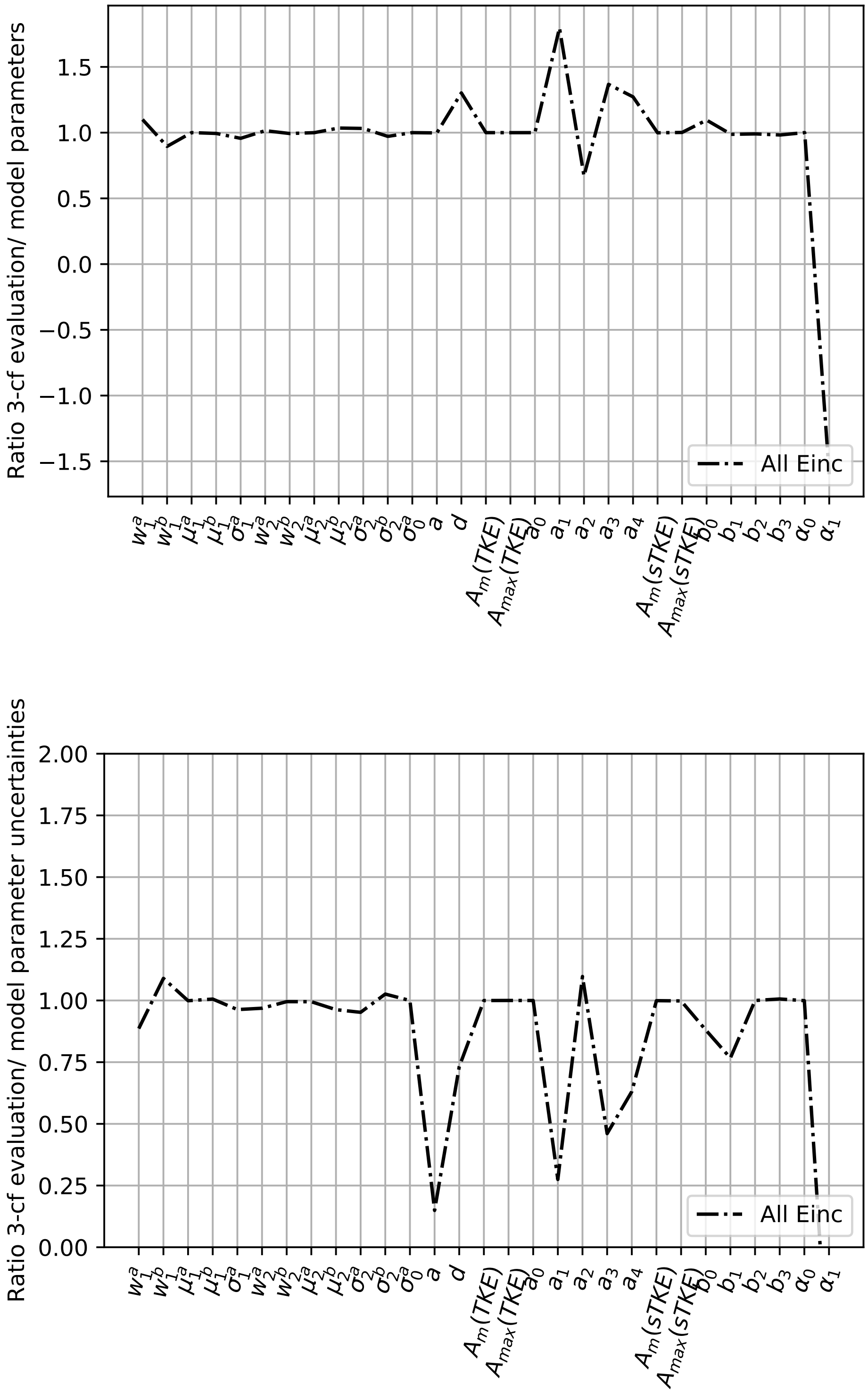

Figure 26: Impact on evaluated parameters and their uncertainties if all $E_{\rm inc}$ are fitted at once on a down-selected grid and taking out a bend in $\langle TKE \rangle$ at approximately 1 MeV. Changes in third-chance fission parameters are shown.

the slope change in the TKE parametrization for each chance fission and the second removing the slope change (having a more similar shape of $\langle$TKE$\rangle$($E_{\rm inc}$) to that of ^{239}Pu(n,f)). For both calculations, the parametrization from the down-selected grid is used.

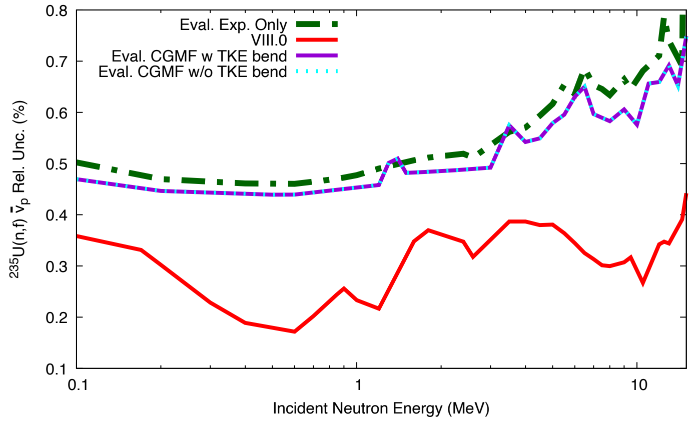

Figure 27: Evaluated ^{235}U(n,f) $\overline{\nu}$ uncertainties are shown in comparison to ENDF/B-VIII.0. The evaluated data were obtained with `CGMF` and only experimental data.

First, in Figs. 28 and 29, we show $Y(A)$ for the two calculations compared to available experimental data at the incident energy listed on each subplot. The parametrization with the slope change (red dashed) has is narrower as well as higher in the peak region, above the data. The higher peaks also cause fewer events in the symmetric mass region, which, due to the current statistics, causes $Y(A)$ to be flat in this region. On the other hand, the parametrization without the slope change better reproduces the magnitude of the experimental data in the peaks of the mass distributions. For both parametrizations, the symmetric mass region is filled in as the incident energy is increased, following the expected trend (unlike what was seen for many of the parametrizations with ^{239}Pu(n,f)).

We then compare directly the average TKE as a function of incident energy (left) and the distribution of TKE values (right) in Fig. 30. When the bend in the average TKE is included, the $\langle \mathrm{TKE}(E_{\mathrm{inc}}) \rangle$ is much flatter in the first-chance fission incident energy range than for the parametrization without the bend, even though the TKE at thermal is essentially identical. For both parametrizations, there is a slight upturn in the TKE near where fourth-chance fission comes in. For the distribution of TKE at thermal, $Y(\mathrm{TKE})$, it is wider without the bend included, more similar to the available experimental data for $\sigma_{\mathrm{TKE}}(A)$. However, as we will see in the neutron multiplicity distribution, this wider TKE distribution leads to a worse comparison in $P(\nu)$ between experiment and the `CGMF` calculations. Still, it is interesting to see that this fit leads to a larger σ_{TKE}.

In Fig. 31, we show the comparison between the two TKE parametrizations for the average prompt neutron and γ-ray multiplicities, $\overline{\nu}_p$ and $\overline{N}_\gamma$. These are compared to available experimental data and, in the case of $\overline{N}_\gamma$, the ENDF/B-VIII.0 evaluation. For $\overline{\nu}_p$, it is not surprising that the `CGMF` calculations go through the experimental data, as this observable was fitted; however, we see a large discrepancy in the third-chance fission energy region; this change is still under investigation. For $\overline{N}_\gamma$, we do not expect to reproduce ENDF, as the shape comes from γ-ray production data, but we do notice that both parametrizations cause an increase in the average γ-ray multiplicity up through the first-chance energy region, then is flat–or even decreasing–at higher incident energies. The decrease is due to a negative slope for $\alpha(E_{\mathrm{inc}})$, which is probably unphysical, as the multiplicity should increase.

Next, we show the average neutron and γ-ray energies in Fig. 32. The shape and magnitude of the neutron energies is nearly identical for the two parametrizations (although TKE should have an impact on the neutron energies in the lab frame, from the boost of the fragments), there is almost no difference seen after first-chance fission. However, at the lowest incident energies, we see that the parametrization without the bend in TKE reproduces the preliminary Chi-Nu measurement–which we have not seen before. On the other hand, the average γ-ray energies are nearly identical until the opening of third-chance fission, where the TKE parametrization without the bend causes a drastic increase in the average energy. This feature again indicates that there is something wrong with the

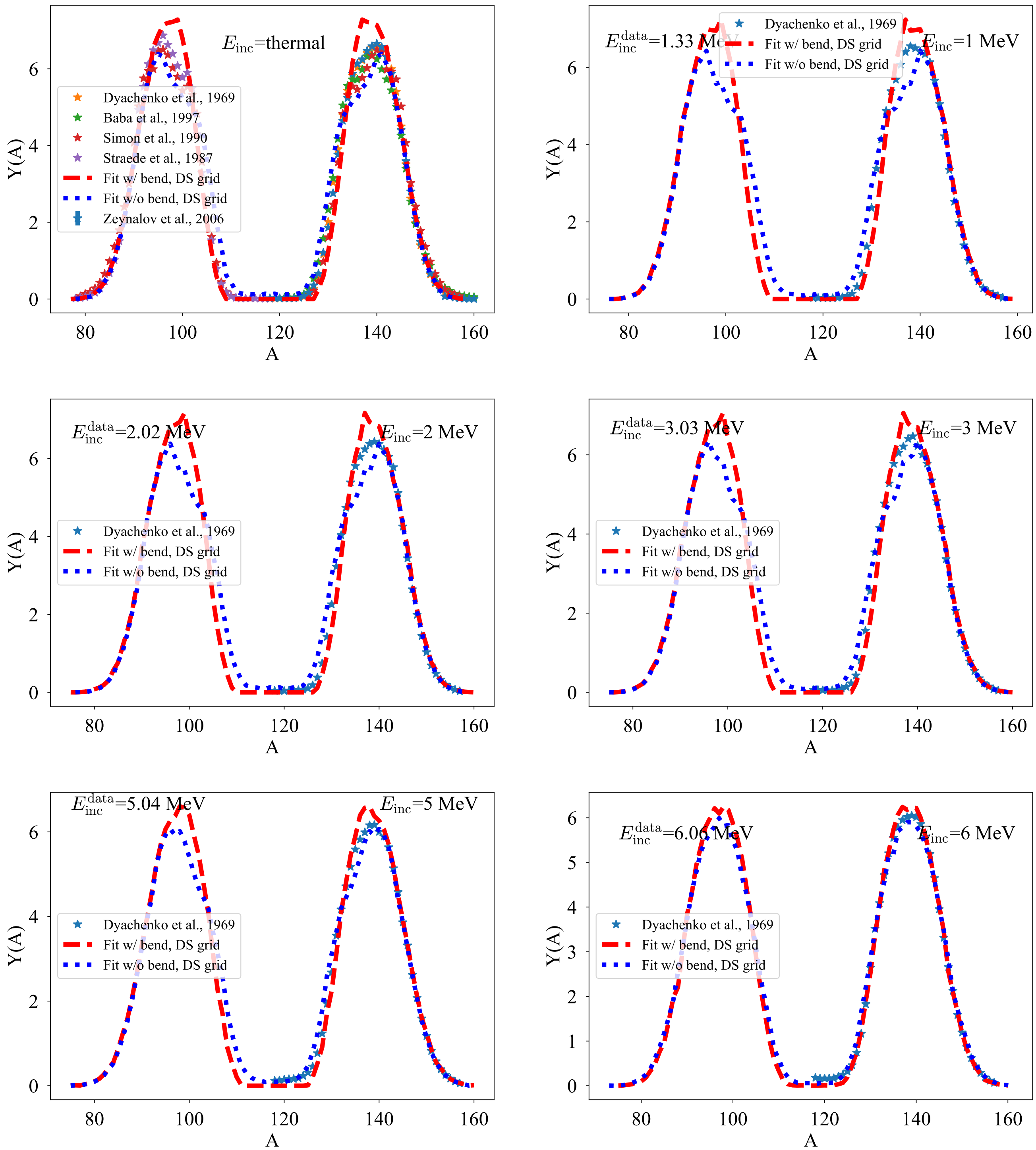

Figure 28: Comparison of the pre-neutron emission mass yield, $Y(A)$, among the two optimizations with `CGMF` and available experimental data.

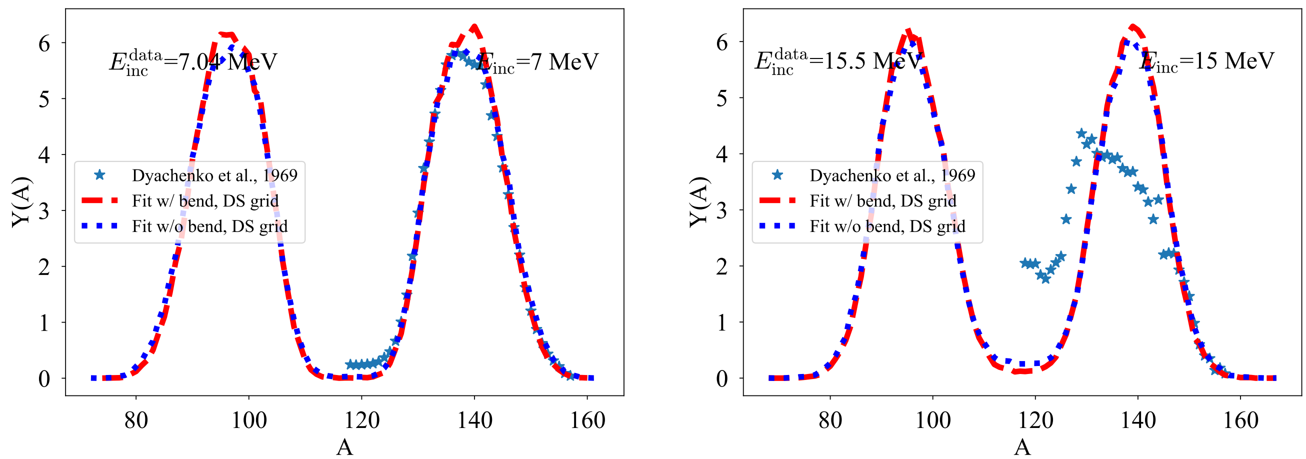

Figure 29: Comparison of the pre-neutron emission mass yield, $Y(A)$, among the two optimizations with CGMF and available experimental data.

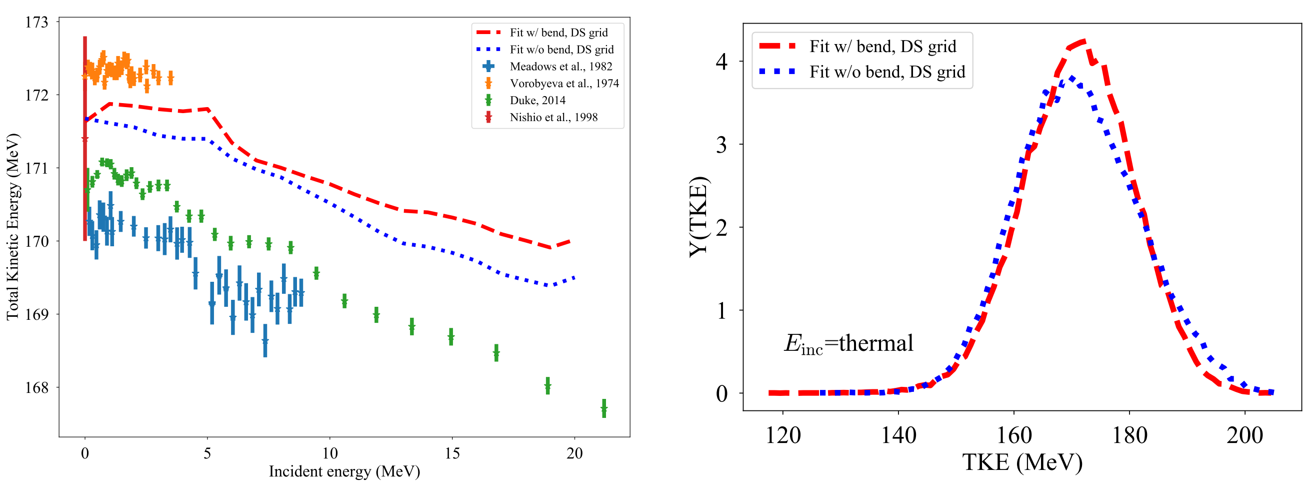

Figure 30: (Left) Comparison among the two CGMF optimizations and available experimental data for the total kinetic energy as a function of incident neutron energy, $\langle \mathrm{TKE} \rangle (E_{\mathrm{inc}})$. (Right) Same comparison for the distribution of TKE, $Y(\mathrm{TKE})$, for thermal incident neutrons.

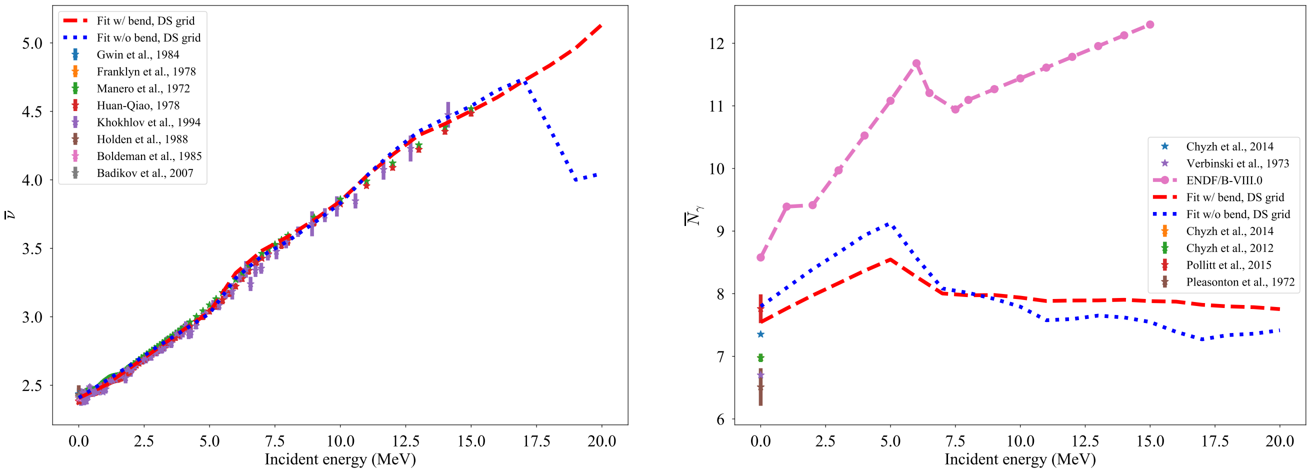

Figure 31: Comparison among the two optimizations with CGMF and available experimental data for (left) average prompt neutron multiplicity and (right) average prompt γ-ray multiplicity, $\overline{N}_\gamma$. For $\overline{N}_\gamma$, we also show the comparison to the ENDF/B-VIII.0 evaluation.

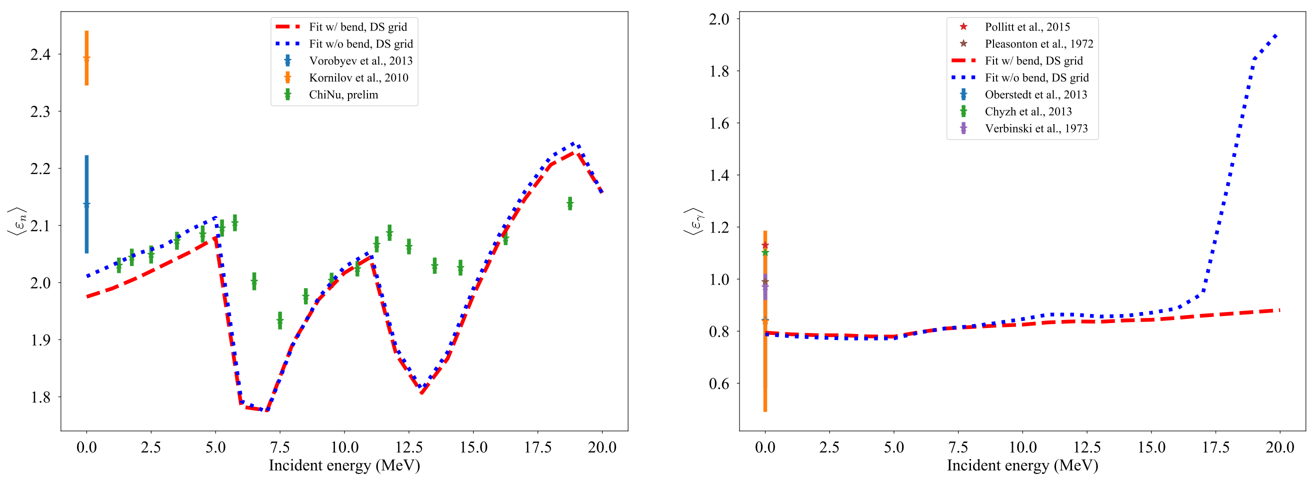

Figure 32: Comparison among the two optimizations with CGMF and available experimental data for (left) average outgoing neutron energy and (right) average outgoing γ-ray energy.

spin cutoff parametrization.

Finally, in Fig. 33, we show the comparison between the two parametrizations and experimental multiplicity distributions. On the right, $P(N_\gamma)$, we see very little difference between the two parametrizations. The average experimental multiplicity is slightly lower than the calculated one, but there is no energy threshold considered in the CGMF calculation, which would lower the average multiplicity. If we look at $P(\nu)$ instead (left), we see a significant difference between the two parametrizations, which, as mentioned before, is due to the 20% difference in $\sigma_{\rm TKE}$. In this case, we trust more the parametrization with the bend, as the best comparison to the data is to Holden. These differences are typically why we need to lower $\sigma_{\rm TKE}$ compared to experimental data.

5 Conclusions and Outlook

This report is in answer to a FY21 NCSP (Nuclear Criticality Safety Program) milestones for LANL that aims to evaluate PFNS and multiplicity, $\overline{\nu}_p$, consistently for ^{235}U and ^{239}Pu. While we did not

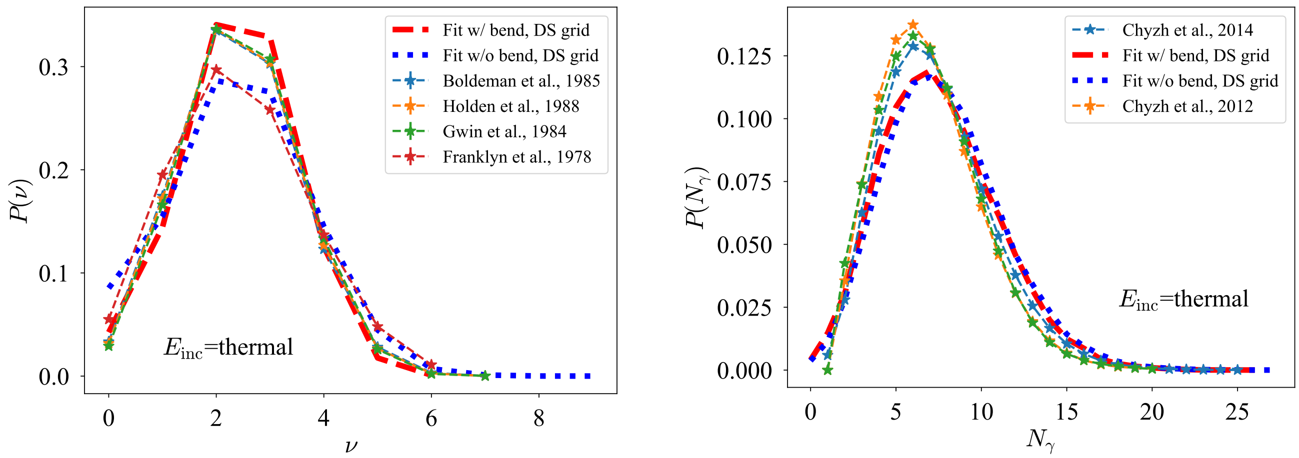

Figure 33: Comparison among the four optimizations with CGMF and available experimental data for (left) average outgoing neutron energy and (right) average outgoing γ-ray energy.

succeed in obtaining consistent evaluated data of PFNS and $\overline{\nu}_p$ due to significant model defects in PFNS, we were able to show that CGMF can be used to produce ENDF/B-quality $\overline{\nu}_p$ data.

This was shown by performing an evaluation of the ^{239}Pu(n,f) $\overline{\nu}_p$ that was started from scratch. We started out by a re-assessment of all experimental data and obtained evaluated data in line with previous evaluations that were also based on only experimental data showing that the approach worked this far. When we included the CGMF model in the evaluation, the evaluated results did not change drastically but were smoother showing the physics constraints introduced through the model.

In addition to that, we could show that the evaluated model parameters link favorably back to other fission data like FY(A), TKE, *etc.* when parameterized through these evaluated parameters. Hence, our evaluated ^{239}Pu(n,f) $\overline{\nu}_p$ ties back well to other fission data. Moreover, this new ^{239}Pu(n,f) $\overline{\nu}_p$ performed well when used in integral testing of various validation responses ($k_{\rm eff}$ of PU-MET-FAST and PU-MET-INT ICSBEP assemblies, various reaction rates in Jezebel and Flattop-Pu, Pu LLNL pulsed spheres) if considering at the same time changes in the PFNS and (n,f) cross section coming from new high-precision experiments. Given the good performance of these new $\overline{\nu}_p$ in validation testing, it is being considered as candidate for ENDF/B-VIII.1.

So, in short, one can produce ENDF/B-quality nuclear data for $\overline{\nu}$ with the CGMF model.

In the near future, we will finalize the evaluation of the ^{235}U(n,f) $\overline{\nu}_p$ and commence then with integral testing. The next step is extending this approach to ^{238}U(n,f) and Pu minor isotope $\overline{\nu}_p$.

Acknowledgments

DN thanks N. Gibson and W. Haeck (both XCP-5) for their help in assembling the new ^{239}Pu file. Work at LANL was carried out under the auspices of the National Nuclear Security Administration (NNSA) of the U.S. Department of Energy (DOE) under contract 89233218CNA000001. We gratefully acknowledge partial support of the Advanced Simulation and Computing program at LANL and the DOE Nuclear Criticality Safety Program, funded and managed by NNSA for the DOE.

References

[1] P. Talou, T. Kawano, I. Stetcu et al. , "Fission Fragment Decay Simulations with the CGMF Code," Comp. Phys. Comm. **269**, 108087 (2021).

[2] A.E. Lovell and D. Neudecker, "Correcting the PFNS for more consistent fission modeling," Los Alamos National Laboratory Report LA-UR-21- (2021).

[3] D. Neudecker, O. Cabellos, A.R. Clark, "Informing Nuclear Physics via Machine Learning Methods with Differential and Integral Experiments," Phys. Rev. C **104**, 034611 (2021).

[4] D. Neudecker, V.G. Pronyaev and L. Snyder, "Including ^{238}U(n,f)/^{235}U(n,f) and ^{239}Pu(n,f)/^{235}U(n,f) NIFFTE fissionTPC Cross-sections into the Neutron Data Standards Database," Los Alamos National Laboratory Report LA-UR-21-24093 (2021).

[5] A.E. Lovell, D. Neudecker, P. Talou, et al. , "Consistent Evaluation of the Prompt-Fission Neutron Spectrum and Multiplicity for n+^{235,238}U and n+^{239}Pu," Los Alamos National Laboratory Report LA-UR-20-26932 (2020).

[6] G.B. King, A.E. Lovell, L. Neufcourt, and F.M. Nunes et al. , "Direct Comparison between Bayesian and Frequentist Uncertainty Quantification for Nuclear Reactions," Phys. Rev. Lett **122**, 232502 (2019).

[7] Ju.A. Bljumkina, I.I. Bondarenko, V.F. Kuznetsov, V.G. Nesterov, V.N. Okolovitch, G.N. Smirenkin, L.N. Usachev, "Channel effects in the energy dependence of the number of prompt neutrons and the kinetic energy of fragments in the fission of U^{235} and U^{233} by neutrons," Nucl. Phys., **52** 648 (1964).

[8] G. S. Boykov, V. D. Dmitriev, G. A. Kudyaev, Yu. B. Ostapenko, M. I. Svirin, G. N. Smirenkin, "Spectrum of Neutrons Accompanying Fission of ^{232}Th,^{235}U, and ^{238}U by 2.9-MeV and 14.7-MeV Neutrons (Below and Above the Threshold of Emission Fission)", Yad. Fiz. **53**, 628–648 (1991) [Sov. J. Nucl. Phys. **53**, 392–406 (1991)].

[9] D.W. Colvin, M.G. Sowerby, "Boron pile nu-bar measurements," Proc. of Nuclear Data For Reactors Conf., Paris 1966 **1**, 307 (1966).

[10] H. Conde, "Average number of neutrons from the fission of U-235," Arkiv foer Fysik **29**, 293 (1965).

[11] B.C. Diven, H.C. Martin, R.F. Taschek, "Multiplicities of Fission Neutrons," Phys. Rev. **101** 1012–1016 (1956).

[12] B.C. Diven, J.C. Hopkins, "Numbers of prompt neutrons per fission for U^{233}, U^{235}, Pu^{239} and Cf^{252}," Proc. Reactor Physics Sem., Vienna 1961 **1**, 149 (1961).

[13] D.S. Mather, M.H. Mctaggart, A. Moat, "Revision of the Harwell ^{240}Pu source strength and nu for ^{235}U and ^{252}Cf," J.Nuclear Energy A&B **20**, 549 (1966).

[14] M. Soleihac, J. Frehaut and J. Gauriau, "Energy Dependence of $\overline{\nu}_p$ for Neutron-induced Fission of ^{235}U, ^{238}U and ^{239}Pu from 1.3 to 15 MeV," J. of Nucl. Energy **23**, 257–282 (1969); J. Frehaut, G. Mosinski and M. Soleihac, "Recent Results in $\overline{\nu}_p$ Measurements between 1.5 and 15 MeV," Topical Conference on $\overline{\nu}_p$ The Average Number of Neutrons Emitted in Fission, France, 1972, Report EANDC(E)-15 "U" (1973).

[15] J. Frehaut, A. Bertin, R. Bois, "Mesure de $\overline{\nu}_p$ et E-bar$_\gamma$ pour la fission de ^{232}Th, ^{235}U et ^{237}Np induite par des neutrond d'energie comprise entre 1 et 15 MeV," Centre d'Etudes Nucleaires **2196**, (1981).

[16] R. Gwin, R.R. Spencer and R.W. Ingle, "Measurements of the Energy Dependence of Prompt Neutron Emission from ^{233}U, ^{235}U, and ^{239}Pu for E_n =0.0005 to 10 MeV Relative to Emission from Spontaneous Fission of ^{252}Cf," NUCL. SCI. ENG. **94**, 365–379 (1986); R. Gwin, R.R. Spencer and R.W. Ingle,"Measurements of the Energy Dependence of Prompt Neutron Neutron Emission from ^{233}U, ^{235}U, ^{239}Pu, and ^{241}Pu for E_n =0.0005 to 10 eV Relative to Emission from Spontaneous Fission of ^{252}Cf," NUCL. SCI. ENG. **87**, 381–404 (1984); R. Gwin, R.R. Spencer, R.W. Ingle et al. ,"Measurements of the Average Number of Prompt Neutrons Emitted per Fission of ^{239}Pu and ^{235}U," Oak Ridge National Laboratory ORNL/TM-6246 (1978).

[17] J.C. Hopkins and B.C. Diven, "Prompt neutrons from fission," NUCLEAR PHYSICS, **48**, 433 (1963).

[18] R.E. Howe, T.W. Phillips, "Fission nu-bar measurements," BROOKHAVEN NATIONAL LABORATORY REPORTS **21501**, 66 (1976).

[19] F. Kaeppeler, R.E. Bandl, "The average number of prompt neutrons from neutron induced fission of U-235 between 0.2 and 1.4 MeV," PROC. OF CONF.ON NUCL. CROSS-SECT. AND TECHN.,WASHINGTON 1975 **2**, 549 (1975).

[20] Yu.A. Khokhlov, I.A. Ivanin, V.I. Inkov, Yu.I. Vinogradov, L.D. Danilin, B.N. Polynov, "Measurements Results of Average Neutron Multiplicity From Neutron Induced Fission of Actinides in 0.5-10 MeV Energy Range," PROC. OF CONF. ON NUCL. DATA FOR SCI. AND TECHN., GATLINBURG 1994 **1**, 272 (1994).

[21] J.W. Meadows, J.F. Whalen, "Energy Dependence Of Prompt $\overline{\nu}$-For Neutron-Induced Fission Of U^{235}," PHYS. REV. **126**, 197 (1962).

[22] J.W. Meadows, "MEASUREMENT OF NU BAR(P) FOR U-235," U.S. REPORT TO EANDC **70**, 9 (1964).

[23] J.W. Meadows, J.F. Whalen, "Energy dependence $\overline{\nu}_p$ for neutron-induced fission of U^{235} below 1.0 MeV," J. NUCL. ENERGY **21**, 157 (1967).

[24] L.I. Prokhorova, R.E. Bagdasarov, I.I. Kotukhov et al. , "Yield of Prompt Neutrons $\overline{\nu}_{\rm tot}$ in the Fission of U^{235} by Neutrons with Energies up to 1.5 MeV," ATOMNAYA ÉNERGIYA **30**, 250–257 (1971).

[25] L.I. Prokhorova, G.N. Smirenkin, "Average Number of Prompt Neutrons from U^{235} and Th^{232} Fission Induced by Neutrons Having Energies up to 3.3 MeV," YADERNAYA FIZIKA **7**, 961 (1968).

[26] A.N. Protopopov, M.V. Blinov, "Mean number of neutrons emitted in U^{235} fission induced by 14.8-MeV neutrons," ATOMNAYA ENERGIYA **4**, 374 (1958).

[27] M.V. Savin,Yu.A. Khokhlov,Yu.S. Zamjatnin et al. , "The Average Number of Prompt Neutrons in Fast Neutron Induced Fission of U-235, Pu-239 and Pu-240," IAEA Report IAEA-CN-26/40 (1970).

[28] M.V. Savin, Y.A. Khokhlov, A.E. Savelev, I.N. Paramonova, "Energy Dependence of $\overline{\nu}$ in the Fission of U^{235} by Fast Neutrons," PROC. OF THIRD ALL UNION CONF. ON NEUTRON PHYS., KIEV, 9-13 JUN 1975 **5**, 186 (1975).

[29] M.V. Savin, Ju.A. Khokhlov, V.N. Ludin, "AVERAGE NUMBER OF PROMPT NEUTRONS AT THE U-235 FISSION BY THE NEUTRONS IN THE ENERGY INTERVAL 0.2 - 1.0 MEV," PROC. OF SEC. CONF. ON NEUTRON PHYSICS, KIEV 1973 **4**, 63 (1973).

[30] G.N. Smirenkin, I.I. Bondarenko, L.S. Kutsaeva et al. , "Mean Number of Prompt Neutrons in the Fission of U^{233}, U^{235}, Pu^{239} by 4 and 15 MeV Neutrons," Sov. Atomic Energy **4**, 253–255 (1958).

[31] M. Soleihac, J. Fréhaut, J. Gauriau et al. , "Average Number of Prompt Neutrons and Relative Fission Cross-Sections of U-235 and Pu-239 in the 0.3 to 1.4 MeV Range," Proc. of the Conference for Nuclear Data for Reactors, Helsinki, **2**, 145– (1970); J.W. Boldeman, J. Fréhaut and R.L. Walsh, "A Reconciliation of Measurements of $\overline{\nu}_p$ for Neutron-induced Fission of Uranium-235," Nucl. Sci. Eng. **63**, 430–436 (1977).

[32] R.L. Walsh and J.W. Boldeman, "The Energy Dependence of $\overline{\nu}_p$ for ^{233}U, ^{235}U and ^{239}Pu below 5.0 MeV," J. Nucl. Energy **25**, 321–330 (1971).

[33] J.W. Boldeman and M.G. Hines, "Prompt Neutron Emission Probabilities Following Spontaneous and Thermal Neutron Fission," Nucl. Sci. Eng. **91**, 114–116 (1985); J.W. Boldeman and R.L. Walsh, "The Energy Dependence of $\overline{\nu}_p$ for Neutron Induced Fission of ^{235}U below 2.0 MeV," J. Nucl. Energy **24**, 191–205 (1970).

[34] H. Condé, J. Hansén and M. Holmberg, "Prompt $\overline{\nu}_{\text{tot}}$ in Neutron-induced Fission of ^{239}Pu and ^{241}Pu, " J. of Nucl. Energy **22**, 53–60 (1968).

[35] Z. Huanqiao, X. Jincheng, L. Zuhua et al. , "The Dependence of Average Numbers of Prompt Fission Neutron of Pu-239 on Incident Fast Neutron Energies," Chin. J. of Nucl. Phys. **2**, 29 (1980).

[36] I. Johnstone, "A Measurement of the Average Number of Prompt Neutrons Emitted in Fission at High Energy,"Atomic Energy Research Establishment Report A.E.R.E NP/R 1912 (1956).

[37] V.I. Kalashnikova, V.I. Lebedev, P.E. Spivak et al. , "Absolute Evaluation of the Average Number of Neutrons Emitted in the Fission of some Isotopes of Uranium and Plutonium," Proc. of the USSR Conf. peaceful Uses of Atomic Energy, USSR 1955, 156 (1955).

[38] M.V. Savin, Yu.A. Khokhlov, A.E. Savelév et al. , "Energy Dependence of $\overline{\nu}_{\text{tot}}$ in the Fission of U^{235} by Fast Neutrons," Soviet J. of Nucl. Physics **16**, 638–640 (1973).

[39] P.J. Leroy, "Nombres Moyens de Neutrons Prompts Èmis Dans La Fission de ^{238}U, ^{239}Pu, ^{232}Th," Le Journal de Physique et le Radium **21**, 617–628 (1960).

[40] P. Marini, J. Taieb, D. Neudecker, "Energy Dependence of Prompt Fission Neutron Multiplicities in the ^{239}Pu(n,f) Reaction," Phys. Rev. L. **xx**, submitted (2021).

[41] D.S. Mather, P. Fieldhouse and A. Moat, "Measurement of Prompt $\overline{\nu}_{\text{tot}}$ for the Neutron-induced Fission of Th^{233}, U^{233}, U^{234}, U^{238} and Pu^{239}," Nucl. Phys. A **66**, 149–160 (1965).

[42] D.S. Mather, P. Fieldhouse, A. Moat, "Measurement Of Prompt $\overline{\nu}$ For The Neutron-Induced Fission Of Th^{232}, U^{233}, U^{234} And Pu^{239}," Nucl. Phys. **66**,149 (1965).

[43] B. Nurpeisov, K.E. Volodin, V.G. Nesterov et al. , "Dependence of $\overline{\nu}_{\text{tot}}$ on Neutron Energies up to 5 MeV for ^{233}U, U^{235}, and ^{239}Pu," Atomnaya Énergiya **39**, 199–205 (1975).

[44] K.E. Bolodin, V.F. Kuznetsov, V.G. Nesterov et al. , "Average Number of Prompt Neutrons in Pu^{239} Fission," Atomnaya Énergiya **33**, 901–906 (1972).

[45] D. Neudecker, "ARIADNE—a program estimating covariances in detail for neutron experiments," EPJ-N **4**, 34 (2018).

[46] D. Neudecker, A. Lewis, E. Matthews *et al.*, "Templates of Expected Measurement Uncertainties," Los Alamos National Laboratory Report LA-UR-19-31156 (2019).

[47] A.D. Carlson *et al.* , "Evaluation of the Neutron Data Standards," Nucl. Data Sheets **148**, 143 (2018).

[48] P.G. Young, M.B. Chadwick, R.E. MacFarlane *et al.*, "Evaluation of Neutron Reactions for ENDF/B-VII: $^{232-241}$U and ^{239}Pu," Nuc. Data Sheets **108**, 2589–2654 (2007).

[49] D. Neudecker, P. Talou, T. Kawano et al. , "Evaluations of Energy Spectra of Neutrons Emitted Promptly in Neutron-induced Fission of ^{235}U and ^{239}Pu," Nucl. Data Sheets **148**, 293 (2018).

[50] D. Neudecker, R. Frühwirth and H. Leeb, "Peelle's Pertinent Puzzle: A Fake due to Improper Analysis," Nuc. Sci. Eng. **170**, 54–60 (2012).

[51] D. Neudecker et al. , "Validating Nuclear Data Uncertainties Obtained from a Statistical Analysis of Experimental Data with the "Physical Uncertainty Bounds" Method," EPJ Nuclear Sci. Technol. **6**, 19 (2020).

[52] D.E. Vaughan and D.L. Preston, "Physical Uncertainty Bounds (PUB)," Los Alamos National Laboratory Report LA-UR-14-20441.

[53] D. Neudecker, V.G. Pronyaev and L. Snyder, "Including ^{238}U(n,f)/^{235}U(n,f) and ^{239}Pu(n,f)/^{235}U(n,f) NIFFTE fissionTPC Cross-sections into the Neutron Data Standards Database," Los Alamos National Laboratory Report LA-UR-21-24093 (2021).

[54] J. Bess (editor), "International Handbook of Evaluated Criticality Safety Benchmark Experiments (ICSBEP)," Organization for Economic Co-operation and Development-Nuclear Energy Agency Report NEA/NSC/DOC(95)03 (2019).

[55] C. Wong, J.D. Anderson, P. Brown et al. , "Livermore Pulsed Sphere Program: Program Summary through July 1971," Lawrence Livermore Laboratory Report UCRL-ID-51144 (1972); C. Wong, E.F. Plechaty, R.W. Bauer et al. , "Measurements and Calculations of the Leakage Multiplication from Hollow Beryllium spheres," Lawrence Livermore Laboratory Report UCRL-ID-91774 (1985); W. Webster and C. Wong, "Measurements of the neutron emission spectra from spheres of N, O, W, ^{235}U, ^{238}U, and ^{239}Pu, pulsed by 14-MeV neutrons," Lawrence Livermore Laboratory Report UCID-17332 (1976); A.A. Marchetti and G.W. Hedstrom, "New Monte Carlo Simulation of the LLNL Pulsed-Sphere Experiments," Lawrence Livermore Laboratory Report UCRL-ID-131461 (1998); E.R. Plechaty and R.J. Howerton, "Calculation Models for LLL Pulsed Spheres (CSEWG Shielding Benchmark Collection No. SDT 10)," Lawrence Livermore Laboratory Report UCID-16372 (1973).

A Definition of Template Uncertainties

Total covariances had to be estimated for each data set in Tables I and II that was accepted for the evaluation. Unfortunately, specific uncertainty sources were missing (i.e., no uncertainty values defined) for all accepted data sets, although they would have been expected to occur for a $\overline{\nu}_p$ measurement. However, one also has to estimate these missing uncertainties. Otherwise, one data set with many missing uncertainties might have an unjustified higher weight in the evaluation than one where the author provided many uncertainty sources adequately. Also, a complete uncertainty estimate of all input experimental data is the basis to obtain a realistic evaluated uncertainty.

We took recourse to templates of expected measurement uncertainties in ratio and absolute liquid-scintillator measurements of Ref. [46] in order to estimate the missing uncertainty sources. In Table XIII of Ref. [46], uncertainty values and correlation coefficient are estimated for these types of experiments for all pertinent uncertainty sources. These values were used here and are summarized in Table V and Fig. 34. If one particular uncertainty source is listed in the last columns of Tables I and II for a measurement entering any of the evaluations presented here, the uncertainty values and correlation coefficients defined in Table V and Fig. 34 are used.

Table V: Uncertainty values and correlation coefficients are provided based on templates of expected measurement uncertainties of Ref. [46] for those uncertainty sources typically encountered in $\overline{\nu}_p$ measurements (defined in Table III). These values are used if values for a specific uncertainty source are missing for a particular measurement. If one particular uncertainty source is listed in the last columns of Tables I and II, the uncertainty values and correlation coefficients defined in this table are used.

Unc. source	Ratio (%)	Cor(Exp$_i$,Exp$_i$)
δc_{DG}	0.12%	Full
δb	0.5%	Gaussian
δc_{ff}	0.22%	Gaussian
$\delta \omega$	^{235}U: 0.05%; ^{239}Pu: 0.07%	Full
$\delta \tau$	0.08%	Full
$\delta \chi$	See Fig. 34	Gaussian
δa	See Fig. 34	Full
$\delta \overline{\nu}^m$	0.42%	Full
δd	0.2%	Full
$\delta d_{s/m}$	0.05%	Full
ΔE_{inc}	Estimate from Similar Facilities	Full

B Experimental Data for ^{235}U(n,f) $\overline{\nu}_p$

Bljumkina, 1964 This is an unusual measurement in as far as the ratio of neutron and fission count rate is taken. They use a Th fission chamber and a scintillator as neutron detector. They provide correction factors (but not uncertainties) for deadtime, multiple scattering, angular disribution and PFNS. They are all reasonable compared to template information. I use template uncertainties for this measurement. Missing corrections: sample roughness (can play a role for the Th measurement!) and impurity.

Boikov, 1991 This is yet another unusual measurement. It is a PFNS measurement, from which they extracted a nu-bar. The experimental data agree well at 14 MeV and are high at 2.9 MeV, but within the spread of differential data. The "total" uncertainties are fairly high which is not surprising given that they extracted a nu-bar from PFNS. The only uncertainty they truly give is the time resolution (2.5 ns on a flight path of 205 cm). The PFNS uncertainty for ^{252}Cf is given with 3% but that applies to the PFNS part of the measurement. I would assume that one third of that applies to nu-bar and take 1.5% instead of 3% and the rest of the total uncertainties as statistical in nature. Missing corrections: multiple scattering, deadtime, false fission, sample thickness, beam stability. I am worried about their missing multiple-scattering correction as this can cause a sizable contribution on a PFNS measurement. However, they took the ratio to ^{252}Cf. The correction in their PFNS can amount to 2%. Hence, I add a 1.0% multiple scattering uncertainty for $\overline{\nu}_p$. Admittedly, I am wary about this measurement as their Pu-9 PFNS measurement at high E_{inc} was rejected, because they measure at one angle only, and hence, the PFNS is only good for one angle, which is not good for a PFNS at 14.5 MeV (pre-equilibrium component!). However, they considered that in their calculations and seem to have taken that into account for $\overline{\nu}_p$. There are two data sets given in EXFOR. I don't know why and what is the difference. I take the second one.

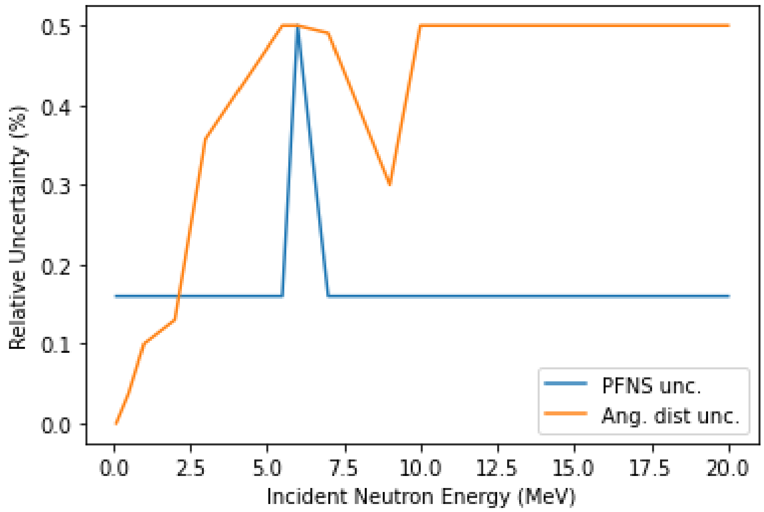

Figure 34: Uncertainty values assumed for $\delta\chi$, PFNS uncertainties, and δa, uncertainties in the correction for the angular distribution of fission neutrons, are shown as a function of E_{inc}. These values were used if $\delta\chi$ and δa are not provided for a particular experiment. These uncertainties were estimated based on Table XIII of Ref. [46].

Colvin, 1965 This is an unusual measurement that uses the Boron pile technique. This technique was pretty strongly criticized for ^{252}Cf(sf)$\overline{\nu}$ given that it produced lower results than Mn-baths and liquid scintillators on average. Hence, the experimentalist studied a lot of effects and provided many uncertainties. The data are systematically higher than VIII.0 until 1 MeV, but agree otherwise well. I adopt many of their uncertainties.

Conde, 1965 They measured with mono-energetic neutron sources but also performed TOF for energy determination to distinguish spontaneous fission. They used the ratio liquid-scintillator technique. A coincidence between FF and PF gammas in the scintillator was used as a start of the gate. First, background was corrected, then impurities. Corrections were given for PuncertaintiesFNS, angular distribution, $\overline{\nu}$ from impurities, background from thermal neutrons, deadtime, sample thickness and false fissions. I assumed half of the corrections as uncertainty except for PFNS and angular distribution uncertainties as these seem distinctly underestimated. This is not surprising as second-chance fission effects in PFNS likely were not well understood in the mid-60s, nor was the angular distribution. I used template values instead. Energy uncertainties were taken from EXFOR. I backed statistical uncertainties out by assuming the rest of uncertainties not accounted for were of random nature. I added uncertainties for delayed gammas and sample displacement from the template.

Diven, 1956 This is a very old measurement with short gate time (30 μs) and double coincidence as trigger. They measured the detector efficiency. Uncertainties encompass: statistics, detector efficiency and coincidences (background). Effects not mentioned to be corrected: geometry, neutron flux variations, delayed gammas, displacement of sample. The data are 3.5% away from VIII.0. I corrected their $\overline{\nu}_p$ value for sample thickness following Boldeman and Frehaut, NSE 76, p. 49 (1980).

Diven, 1961 & Hopkins, 1963 This measurement used the same equipment as for Diven 1956 (also same co-authors). The efficiency was determined by scattering d+d and T+d neutrons in the scintillator and a NE 102 plastic scintillator. I.e., the determined their detector efficiency experimentally like Diven, 1956. They counter-checked this measurement with simulations (1963!). The counting gate was opened by pulses in the fission chamber and prompt gammas in scintillator which could reduce the effect of false fissions? The gate is open for a reasonably long time (64 μs). The background is measured by a random gate several milliseconds after the main gate. Energy spread is explicitly given. Systematic uncertainties are due to pile-up and neutron-flux contamination (down-scattering to thermal). Not corrected for: impurities in the sample, displacement of the sample (definitely a problem because in the same time in the beam), angular distribution & forward-boost (definitely a problem at 14 MeV), sample thickness, delayed gammas. I corrected for sample thickness following Boldeman and Frehaut, NSE 76, p. 49 (1980). From the EXFOR entry alone and the journal article it was not clear if the monitor is prompt or total ^{252}Cf(0,f) $\overline{\nu}$. After considerable amount of digging it became clear that it is total.

Fieldhouse, 1966 The level of documentation and knowledge that went in this experiment of 1966 (!) is impressive. It is no wonder that Fieldhouse and Moat provided standard data. One data set is systematically high but still well within the spread of data while the 14-MeV point is systematically low. They had a neutron-detection efficiency of 0.89%, with 0.2% uncertainties explicitly given. The gate was open reasonably long (40 μs). They give PFNS uncertainties, but I rather take my own as they seem low. They were aware of many corrections and did a great job. They did an estimate of corrections needed for delayed gammas but could not calculate the correction factor. Not many uncertainties are given but templates fit well together with the reported sizes of their corrections.

Frehaut, 1980 to 1982 They measured with mono-energetic neutron sources but also performed TOF for energy determination to distinguish spurious neutron groups. They used the ratio liquid-scintillator technique. A coincidence between fission fragment and prompt-fission gammas in the scintillator (doped with Gd) was used as a start of the gate. Most uncertainties are take from the template as they are either missing or the template uncertainties are within a credible range given the corrections that Frehaut mentions in his journal articles. The level of documentation on these data sets is fair. Frehaut was aware of many necessary corrections, but his documentation is confusing at best. One example is that the monitor is 3.782 for 1980 and 3.732 for 1982 leading to a systematic off-set at high $E_{\rm inc}$ that is not explained. It is also not clear to me why he did less corrections for the 1982 than for the 1980 data set. The data seems systematically lower than the ENDF/B-VIII.0 evaluation but that might be caused by the a bit too low a monitor value that Frehaut used. I am not sure which data set is the final one, especially as fewer corrections were undertaken for the 1982 data set. I adopt both as Phil seems to have done looking at the final evaluated data (no input data found). The gate is open for a reasonably long time (50 μs). Julien Taieb mentioned there is an issue with the data because the (n,2n) and $\overline{\nu}_p$ competition was not correctly resolved. Frehaut cites a total systematic uncertainty of 0.2% in the 1982 paper which is too low.

Gwin, 1986 I adopted their statistical, deadtime, false-fission, impurity, background (considered in statistical), delayed-gamma, displacement of sample and sample thickness uncertainties. I replaced their PFNS and angular distribution uncertainties with template values as they did not take into account the effect of second-chance fission. One thing that seems missing is that the forward-boost was not corrected for. However, their data end at 10 MeV, where this effect should be smaller, so missing this particular correction could be fine. Energy uncertainties are also not provided and I adopt them from other data measured with ORELA at that time.

Howe, 1976 This is a really weird experiment. They did not use the typical liquid scintillator but rather a combination of shells (U, Li, Pb) going to a benzene liquid scintillator, where they had to correct for a lot of multiple scatters. They corrected multiple scattering via neutron-transport codes, in 1976! Their complete efficiency is on the order of 50% which is pretty low and reflects how many mistakes they could have. They did not corrections for angular distributions of fission fragments. You see that in their data. They are systematically high above 4 MeV. In a later publication (1984), they talk at considerable length about the need for this correction, which I assume is their way of saying that they should have done it. So, I reject the data above 1.6 MeV and remove one outlier at 2 MeV. I will generously add a multiple scattering uncertainty of 1.0% (expert judgment) given how many materials they had in the beam and that I don't believe that they can get it that right and it will matter for a 50%-detector-efficiency correction.

Käppeler, 1975 The data are measured with an absolute technique (neutrons versus fission rate) but re-normalized to an evaluation. I re-normalize to VIII.0. The measurement is fairly well described. Most pertinent corrections were undertaken, except for deadtime (maybe just not documented) and false fissions (likely forgotten). The uncertainties are realistic given the templates. All in all, a fairly good job and likely good data. I take from templates, deadtime and false fission uncertainties as these should apply as well.

Khoklov, 1994 The data are systematically below VIII.0 below 0.8 MeV. The data set is very well-documented. The gate is open for a reasonable time, maybe a bit too short for low energies? The uncertainties are all half of template uncertainties. I adopt all uncertainties except for PFNS and angular distribution which are much higher from the templates (0.1 and 0.2, respectively). The reason for that is that the authors do no comment on taking into account the E_{inc}-dependence of the PFNS and do not mention forward boost which can be substantial for this measurement). Impurity uncertainties times a factor of 0.5 are adopted from templates as they use rather pure samples. I took energy uncertainty from their ^{239}Pu measurement. The only missing correction is that due to forward-boost. This can matter at higher E_{inc}.

Meadows, 1962–1967 This is one of the earliest measurements. It is a coincidence measurement but the neutron-detector efficiency is incredibly (5-9%) LOW!! Alone for that I would have rejected that. But weirdly enough their data lie well within the bulk of the data if a bit high for the 1967 data set. So, they seem to have known what they are doing. It is fairly well documented but only two partial uncertainties are given (PFNS, sample displacement) which I adopt. I adopt template uncertainties otherwise. Statistical uncertainties are given for the 1965 and 1967 data sets. It is not specified what 1962 uncertainties are but the size suggests statistical uncertainties. Energy uncertainties are given for the 1965 and 1967 data sets. No uncertainties are given for the 1962 data set. I adopt the 1967 ones as those are for the same neutron beam.

Nesterov, 1970 This is a fairly well-documented data sets with many corrections and uncertainties described. I am worried about missing corrections for delayed gammas. Also, the neutron-detector efficiency is very low. The data lie pretty much on top of VIII.0. I rejected the data from the same group for ^{239}Pu which was clearly off and the authors attributed the problem to contaminations in their sample and published new ^{239}Pu results. However, no issue seems to affect the ^{235}U measurement. They explicitly give PFNS, background, deadtime, impurity, statistical and energy uncertainties. I assume uncertainties for false fissions, delayed gammas, sample displacement and sample thickness. The sample thickness is five times larger than that of Gwin which did not need a correction. However, for this experiment, one needs to correct for that. I re-normalize the data by a factor of 1.0013 following Boldeman & Frehaut, NSE 76, p. 49 (1980), Fig. 1.

Prokhorova, 1967 I could not find any of the publications. Hence, I don't know much. A lot corrections are missing: delayed gamma, deadtime, sample thickness, displacement of sample, energy spread. multiple scattering.

Protopopov, 1958 The data agree well within their uncertainties with ENDF/B-VIII.0. This measurement is more like an absolute measurement where one measures the fission and neutron count rates. They use an ionization chamber for neutron-detection measurements. It is very unusual but has the advantage of being insensitive to gammas and, therefore no delayed-gamma correction applies. They did correct for many effects. Exceptions are samples thickness, displacement of sample and deadtime. No uncertainty information is provided; total uncertainties are very large and statistical. The remaining uncertainties are adopted from the templates. While the measurement has little weight due to large uncertainties, it is amazing that such a good measurement was performed in 1958 and that they were aware of so many effects.

Savin, 1970–1979 The data lie systematically above the evaluation and have a wave-like structure that makes me wonder about their statistical uncertainties. One can calculate an energy uncertainty from the TOF length of 35 m and time resolution of 1 ns/m. I wonder if this data set could be correlated with Khoklov because they use the same flight-path length and Khoklov is the second author. Fission was detected by prompt gammas. They accounted for scattering in the sample holder/ backing (Pb) by doing measurements just with the sample holders/ backing. The neutron-detector efficiency assumes a value of 70%. That is not the best value but reasonable. The statistical uncertainty of the combined data set is 0.5-0.7%. The neutron-detection efficiency is given with 0.5% which replaces the PFNS uncertainty. Background uncertainty of 0.5% is provided. Weirdly enough in EXFOR ERR-3 is given with 1% citing background uncertainties. It seems that the total uncertainties in EXFOR consist of neutron-detection efficiency uncertainties, background uncertainties and statistical uncertainties. Hence, the latter can be backed out. The journal article is in Russian. Hence, I cannot be sure what was corrected and what not. No mention of delayed gammas, deadtime, sample thickness, displacement of sample, energy spread and beam-stability monitoring was made in the EXFOR entry. Uncertainties taken from template: delayed gamma, false fission deadtime, angular distribution, sample thickness, sample displacement and impurity uncertainties.

Smirenkin, 1958 This is an unusual measurement in as far as a double fission chamber is used. The first half is used to detect fission fragments, the second half is used to detect fission neutrons by registering fission. Hence, no delayed-gamma correction applies and no displacement of sample needs to be taken into account. Very scarce uncertainty information is provided. I take most uncertainties from templates. Missing corrections: thickness, forward boost, neutron flux.

Soleihac, 1970 This measurement used the same equipment as Frehaut 1983. They measured with mono-energetic neutron sources but also performed TOF for energy determination to distinguish spurious neutron groups. They used the ratio liquid-scintillator technique. A coincidence between fission fragments and prompt-fission gammas in scintillator (doped with Gd) was used as a start of the gate. Most uncertainties are estimated with the template following the procedure for Frehaut data as they are missing or the template uncertainties are within a credible range given the corrections that Frehaut mentions in his journal articles.

Walsh, 1971 The data agree partially with ENDF/B-VIII.0. Some of them are outlying but overall the agreement is fine. The counting gate was open for 40 μs which is reasonable. Many uncertainties were explicitly given. Background uncertainties seem low but maybe ok as many background related uncertainties are treated as separate uncertainties and give reasonable total background uncertainties The description of the measurement is very detailed and I do not see any red flags. They were aware of many pertinent effects.

Rejected Data Rejected data sets because measured at lower or larger E_{inc} than the evaluation (from 100 keV to 30 MeV):

- Apalin (1962) measured at thermal.
- Apalin (1965) measured at thermal.
- Barnard (1955) measured at thermal.
- Boldeman (1985) measured at thermal.
- DeVolpi (1966) measured at thermal.
- Diven (1961; 2) measured at thermal.
- Frehaut (1973) measured from 2.0e-6 to 4.45e-5 MeV.
- Fultz (1966) measured at thermal.
- Gwin (1984) measured from 2e-8 to 4.1e-5 MeV.
- Howe (1976) measured from 5.2e-7 to 8.43e-5 MeV.
- Kalashnikova (1955) measured at thermal.
- Kappor (1963) measured at thermal.
- Nefedov (1983) measured at thermal.
- Reed (1973) measured from 1.2e-8 tp 2.64e-5 MeV.
- Sanders (1956) measured at thermal.
- Simon (1976) measured from 2.03e-6 to 7.46e-5 MeV.
- Snyder (1970) measured at thermal.
- Vorobyev (2016) measured at 3.63e-8 MeV.
- Widen (1973) measured at thermal.

Rejected data sets because they were either clearly outlying, or for physics reasons, too large uncertainties or insufficient uncertainty information:

- Bethe (1955): The data are 8.2% off at 4.0 MeV and 9.5% at 4.5 MeV! The uncertainties are in the range of 10%. The information in EXFOR is extremely scarce. This measurement will have no impact on the evaluation and is clearly biased. While interesting from science history point of view, not useful for the evaluation.
- Frehaut (1980, 2), EXFOR-number: 2167.002: The experimental data are a factor 2 larger than ENDF/B-VIII.0. No information provided on the data. I am not sure what is going on. Maybe a wrong tabulation? Anyway, I have to reject those data. The other Frehaut data are much better documented.
- Nadkarni (1967): The data are only documented in an abstract according to the EXFOR entry. The information in the EXFOR entry is very scarce and do not contain critical points that encourage trust in the data. While they detect fission fragments, it is unclear how they count neutrons for starters. Not even the monitor is documented! The data are systematically off by 5% with an uncertainty of 5%. The data would have little impact and are biased.

- Johnstone (1965): The gate was open too long (500 μs); hence, they will measure a lot of background. The monitor is also not properly described in the EXFOR entry. (It seems to be natural uranium!) The statistical uncertainty is large (4.5%). The data will likely have no impact at all and are rejected. Not surprisingly, the data are outlying. Missing corrections: attenuation, sample thickness, angular distribution of fission fragments, forward boost (14 MeV), geometry, displacement of sample. The data point at 2.5 MeV is too low, at 14 MeV too high but uncertainties overlap. The problem is less severe than for ^{239}Pu as the effect of the wrong monitor (natural uranium) will wash out more in the ratio. Still, the data are problematic.

- Diven (1957): This data set is very, very scarcely described. Not even the monitor is given and in Diven's case this could be both ^{235}U(n,f$_{\rm th}$) or ^{252}Cf(sf) $\overline{\nu}$. The publication is a theoretical paper with no experimental details; the EXFOR entry is incredibly short. I cannot do anything with this. Also, the data are systematically high which could be due to an outdated monitor.

- Flerov (1958): This is a really weird experiment. They measure the total production of neutrons for 14.1-MeV neutrons in then subtsrate, (n,2), (n,inl) and divide through the fission cross section. They did not have an (n,inl) cross section, so they extrapolated it. We do not know (today, not 1958!) the cross section to better than 25%! It is amazing that the datapoint is only 6% lower than VIII.0. While conceptually interesting, this data set is much too uncertain and riddled with too many systematic unknowns to be considered.

- Howe (1984): The data are actually very well described and many important corrections were undertaken. The real problem with the data is the very complicated monitor: An average detector efficiency for the neutron detector (scintillator) was backed out by comparing the ^{235}U $\overline{\nu}_p$ from 1–15 MeV to Manero data from 1–15 MeV. I could not find Manero evaluated data to see how accurate that data are, they seem reasonably close to VIII.0 but that was only on a plot. They were also re-normalized to a new ^{252}Cf(sf) $\overline{\nu}_p$. So, in short they used an approximate detector efficiency that would be hard to correct for. In addition to that, the detector efficiency does change with incident energy because of the angular distribution but also the PFNS and is not the same averaged from 1–15 MeV and energies from 15–30 MeV. The angular distribution was corrected for but not the PFNS. The experimental data are systematically higher from VIII.0. One could, in principle, assign a pretty high detector-efficiency uncertainty. The reason I did not do that is that the data are systematically higher than ENDF/B-VIII.0. The same is true for 1976_2 Howe data and for those we can actually compare to other data.

- Vasilev (1960): I could not find the article (journal out of print) and the EXFOR entry is the barest skeleton I have seen so far. I have no clue what was corrected for, if there was a monitor used, what the uncertainties are. In addition to that, the data point is highly outlying and highly uncertain. I reject it given the lack of information.

C Experimental Data for ^{239}Pu(n,f) $\overline{\nu}_p$

Conde, 1968 They measured with mono-energetic neutron sources but also performed TOF for energy determination to distinguish spontaneous fissioning (important for ^{241}Pu and impurities). They used the ratio liquid-scintillator technique. A coincidence between fission fragments and prompt-fission gammas in scintillator was used as a start of the gate. First, background was corrected, then impurities. Corrections were given for PFNS, angular distribution, $\overline{\nu}_p$ from impurities, background from thermal neutrons, deadtime, sample thickness and false fissions. I assumed half of the corrections as uncertainties except for PFNS and angular distribution uncertainties as these seem distinctly underestimated. This is not surprising as second-chance fission effects in PFNS likely were not well understood in the mid-60s, nor was the angular distribution. I used template values instead. Energy uncertainties were taken from EXFOR. I backed statistical uncertainties out by assuming the rest of uncertainties not accounted for were of random nature. I added uncertainties for delayed gammas and sample displacement from the template.

Diven, 1956 This is a very old measurement with a short gate time (30 μs) and double coincidence as trigger. They measured the detector efficiency. Uncertainties encompass: statistics, detector efficiency and coincidences (background). Effects not mentioned to be corrected: geometry, neutron flux variations, delayed gammas, displacement of samples. The data are 3.5% from VIII.0. I corrected for sample thickness following Boldeman and Frehaut, NSE 76, p. 49 (1980).

Frehaut, 1973 They measured with mono-energetic neutron sources but also performed TOF for energy determination to distinguish spurious neutron groups. They used the ratio liquid-scintillator technique. A coincidence between fission fragments and prompt-fission gammas in the scintillator (doped with Gd) was used as a start of the gate. Most uncertainties are take from the template as they are either missing or the template uncertainties are within a credible range given the corrections that Frehaut mentions in his journal articles.

Gwin, 1986 I adopted their statistical, deadtime, false-fission, impurity, background (considered in statistical), delayed-gamma, displacement of sample and sample thickness uncertainties. I replaced their PFNS and angular distribution uncertainties with template values as they did not take into account the effect of second-chance fission. One thing that seems missing is that the forward-boost was not corrected for. However, their data ends at 10 MeV, where this effect should be smaller, so could be fine. Energy uncertainties are also not provided and I adopt them from other data measured with ORELA in the same time period.

Hopkins, 1963 This measurement used the same equipment as Diven 1956 (same co-authors). The efficiency was determined by scattering d+d and T+d neutrons in the scintillator and a NE102 plastic scintillator. They counter-checked this detector-efficiency measurement with simulations (1963!). The counting gate was opened by pulses in the fission chamber and prompt gammas in the scintillator. That could have possibly reduced false fissions? The gate is open for a reasonably long time (64 μs). The background is measured by a random gate several milliseconds after the main gate. The energy spread is explicitly given. Systematic uncertainties are due to pile-up and neutron-flux contamination (down-scattering to thermal). Not corrected for: impurities in the sample, displacement of the sample (definitely a problem because in the same time in the beam), angular distribution & forward-boost (definitely a problem at 14 MeV), sample thickness, delayed gammas. I corrected for sample thickness following Boldeman and Frehaut, NSE 76, p. 49 (1980).

Khoklov, 1976 This experiment is fairly well-documented for ^{235}U but not ^{239}Pu. A TOF length of 35 m and time resolution of 1 ns/m is given to calculate an energy uncertainty from. Fission registration was undertaken through detecting prompt gammas. The neutron-detection efficiency was 0.7 which is not great but not too bad either. Background from sample backing and other unspecified sources were quantified. Reported uncertainties in EXFOR contain counting statistics and detector efficiency. I would assume this contains statistics, PFNS and deadtime. Hence, I set statistical uncertainties to 0, PFNS to reported uncertainties and deadtime to 0. I took from the ^{235}U paper a 1% background uncertainty. Missing corrections: sample thickness, neutron flux variation, delayed gammas, false fissions, sample displacement. Uncertainties not provided (Delayed gammas, false fissions, angular distribution, sample thickness, sample displacement and impurity) were taken from the template.

Marini, 2021 Uncertainties called out by Paola: multiple scattering, limited E_{out} range (extrapolation), limited coverage of angular distributions. Explicitly given uncertainties: energy uncertainties, extrapolation, angular distribution, wrap-around background uncertainties. Uncertainties that are missing and I asked about: random coincidences, gamma background uncertainties, impurity uncertainties, and multiple-scattering uncertainties. The impurity level of ^{252}Cf was such that no impurity uncertainties apply. The purity level ^{239}Pu is 99.9% (rest Pu-240) comparable to Conde who cites 0.2% uncertainties while Julien states a 0.01% impact. I take the middle ground of 0.1%. They correct random coincidences by randomly triggering a gate and measuring it and claim no uncertainty. Zero uncertainties in this correction is not supported by literature. I take the template value. They apply the same gamma cuts to ^{239}Pu and ^{252}Cf, which also cut out some neutrons because they really want to get out gammas. I think that could bias the PFNS and there is also a difference between gammas from ^{239}Pu than from ^{252}Cf. So, there is a remaining uncertainty; I take the template value. Data are cut above 20 MeV after private communication with Paola who wrote: "We corrected for the forward boost of fission fragments when accounting for the angular distribution of neutrons. However I have to mention that, as we do not measure $E_{\text{out}} > 14$MeV, we trust our $\overline{\nu}$ values up to 20 MeV. Above this energy, the pre-equilibrium emission above 14 MeV [outgoing energy in the spectrum] becomes significant, so you should consider the $\overline{\nu}_p$ values only as a lower limit. I take multiple scattering uncertainties at uncertainties of 0.2% as Paola said the uncertainties are similar in size. As should be obvious from the discussion above private communication with authors took place.

Mather, 1965 This is a reasonably well-documented data sets. They were aware of many effects that need to be corrected for. I am worried by the fact that they use Pt backing foils that are known to lead to necessary Colomb corrections for (n,f) cross sections. Not sure if they studied it here. They were aware of deadtime issues with ^{239}Pu and tried to minimize it with PTFE slabs between samples. I wonder if that could lead to multiple scattering. They studied the effect via an experiment and concluded that the effect should be small. ^{240}Pu contamination (spontaneous fission) was studied by a beam-off measurement. It sounds like they are using ^{252}Cf(sf) $\overline{\nu}$ TOTAL as a monitor. They got the detector efficiency with that measurement. Strongly related to Mather1970 (same reference). Missing correction: delayed gammas, sample thickness and displacement of sample.

Mather, 1970 This is a reasonably well-documented data sets. They were aware of many effects that need to be corrected for. I am worried by the fact that they use Pt backing foils that are known to lead to necessary Colomb corrections for (n,f) cross sections. Not sure if they studied it here. They were aware of deadtime issues with ^{239}Pu and tried to minimize it with PTFE slabs between samples. I wonder if that could lead to multiple scattering. They studied the effect via an experiment and concluded that the effect should be small. ^{240}Pu contamination (spontaneous fission) was studied by a beam-off measurement. It sounds like they are using ^{252}Cf(sf) $\overline{\nu}$ TOTAL as a monitor. They got the detector efficiency with that measurement. Strongly related to Mather1965 (same reference). Missing correction: delayed gammas, sample thickness and displacement of sample.

Nurpeisov, 1975 They did a good job describing what was corrected. Their data agrees well with the bulk of other experimental data. An 80% detector efficiency is very reasonable. The gate is open for a very long time (100 μs). However, this is explained by the time the neutron spends inside the detector (50 μs) on average and seems to be a material-dependent quantity. They get the random coincidence (sometimes termed false-fission events) by measuring 250 ns after the fission pulse is detected which sounds reasonable. Multiple scattering effects were reduced by shielding. Detector efficiency was measured due to that PFNS uncertainties are replaced by detector efficiency uncertainties. They had problems with beam stability above 3.5 MeV. They did a good job at UQ and corrections. Explicit uncertainties are given for correction factors which will be used as uncertainties. Two effects they missed: delayed gammas and sample displacement where I take uncertainties from the $\overline{\nu}$ template. I added also impurity uncertainties as I don't have much information to go by.

Savin, 1970 The data lie systematically above the evaluation and have a wave-like structure that makes me wonder about their statistical uncertainties. One can calculate an energy uncertainty from the TOF length of 35 m and time resolution of 1 ns/m. I wonder if this data set could be correlated with Khoklov because they use the same flight-path length and Khoklov is the second author. Fission was detected by prompt gammas. They accounted for scattering in the sample holder/ backing (Pb) by doing measurements just with the sample holders/ backing. The neutron-detector efficiency assumes a value of 70%. That is not the best value but reasonable. The statistical uncertainty of the combined data set is 0.5-0.7%. The neutron-detection efficiency is given with 0.5% which replaces the PFNS uncertainty. Background uncertainty of 0.5% are given. Weirdly enough in EXFOR ERR-3 is given with 1% citing background uncertainties. It seems that the total uncertainties in EXFOR consist of neutron-detection efficiency uncertainties, background uncertainties and statistical uncertainties. Hence, the latter can be backed out. The journal article is in Russian. Hence, I cannot be sure what was corrected and what not. No mention of delayed gammas, deadtime, sample thickness, displacement of sample, energy spread and beam-stability monitoring was made in the EXFOR entry. Uncertainties taken from template: delayed gamma, false fission deadtime, angular distribution, sample thickness, sample displacement and impurity uncertainties.

Soleihac, 1970 This measurement used the same equipment as Frehaut 1983. They measured with mono-energetic neutron sources but also performed TOF for energy determination to distinguish spurious neutron groups. They used the ratio liquid-scintillator technique. A coincidence between fission fragments and prompt-fission gammas in the scintillator (doped with Gd) was used as a start of the counting gate. Most uncertainties are estimated with the template following the procedure for Frehaut data as they are missing or the template uncertainties are within a credible range given the corrections that Frehaut mentions in his journal articles.

Volodin, 1970 This data set is strongly correlated with Volodin_2. The latter set is given in ratio to one point (at 0.4 MeV) of this data set here. Data agree well with ENDF/B-VIII.0 and the bulk of the data. There is a wave-like structure from 1.1–1.5 MeV that could be more than statistics. Authors state in EXFOR that these data superseed 40033.003 by V.G. Nesterov with the following statement: "Previously measured data published in 70HELSINKI are considered as overruled due to strong disagreement with this measurement in energy range $0.4 < E_{\mathrm{inc}} < 1.3$ MeV caused by high ($\sim$10 times this one) admixture of ^{240}Pu in the sample used at the previous measurement." The start signal is from a fission-fragment measurement. Then neutron counting is in coincidence with the gate. They don't mention how long the gate was open nor the neutron-detection efficiency. EXFOR uncertainties consist of statistical uncertainties, correction uncertainties and those of individual measurement cycles. Total systematic uncertainties (called correction uncertainties) of 0.4-0.5%. I backed out statistical uncertainties with this information. The correction uncertainties contain those due to angular distributions, PFNS, coincidence losses (false fissions), background and deadtime. You can use that to counter-check the uncertainties you have from the template. The background was not exceeding 3%. So, we can estimate 0.3% alone due to background which is smaller. Delayed-gamma uncertainties are zero. If I sum up all template uncertainties for what is considered in their total correction uncertainties and assume 0.3% uncertainty for background, I end up with 0.42% systematic uncertainties which is a reasonable estimate. I still take the template uncertainties and just replace the background uncertainties coming out at a similar uncertainty value. Additional uncertainties from template: impurity, sample displacement, sample thickness. Fairly well-documented data set and agrees with our current knowledge.

Volodin, 1970 (2) This data set is strongly correlated with Volodin_1. The latter set is given in ratio to one point (at 0.4 MeV) of this data set here. The data agree well with ENDF/B-VIII.0 and the bulk of the data. There is a wave-like structure from 1.1–1.5 MeV that could be more than statistics. Authors state in EXFOR that these data superseed 40033.003 by V.G. Nesterov with the following statement: "Previously measured data published in 70HELSINKI are considered as overruled due to strong disagreement with this measurement in energy range $0.4 < E_{\rm inc} < 1.3$ MeV caused by high ($\sim$10 times this one) admixture of ^{240}Pu in the sample used at the previous measurement." The start signal is from a fission-fragment measurement. Then neutron counting is in coincidence with the gate. They don't mention how long the gate was open nor the neutron-detection efficiency. EXFOR uncertainties consist of statistical uncertainties, correction uncertainties and those of individual measurement cycles. Additional uncertainties from template: impurity, sample displacement, sample thickness. This is a fairly well-documented data set and agrees with our current knowledge. The monitor is their ^{239}Pu(n,f) $\overline{\nu}_p$ measurement at 400 keV from Volodin_1 which is a bit a circular argument. This particular measurement uses another neutron detector (Th-detector) than Volodin_1. Hence, delayed gamma uncertainties should be zero. I learned from the Volodin_1 measurement that template uncertainties approximate their uncertainties well except for the fact that background uncertainties should be smaller (0.3%) which I correct here and then take the template uncertainties to extract statistical uncertainties. The data are given in ratio to their own data at 0.4 MeV from Volodin_1 which I add in. The data are treated as absolute with the reference's uncertainties added in quadrature.

Walsh, 1970 The data agree partially with ENDF/B-VIII.0. Some of them are outlying but overall the agreement was fine. The counting gate was open for 40 μs which is reasonable. Many uncertainties were explicitly given. Background uncertainties seems low but that may be ok. The description of the measurement is very detailed and I do not see any red flags. They were aware of many pertinent effects.

Rejected Data Rejected because measured at lower energy than evaluation:

- Apalin (1965) measured at thermal.
- Boldeman (1980) measured at thermal.
- Frehaut (1980) measured from 22.79 to 28.28 MeV.
- Gwin (1984; 1) measured from 0.005 to 60 eV.
- Gwin (1984; 2) measured from 0.005 to 10 eV.
- Kalashnikova (1955) measured at thermal. Very little information.
- Nefedov (1983) measured at thermal.
- Nishiko (1988) measured at thermal.
- Sanders (1965) measured at thermal.
- Vorobyev (2016) measured at thermal.

Rejected data because superseeded:

- Gwin (1978): This data set seems superseeded by (Gwin, 1986). The 1978 data set was published only as an ORNL report in that year, while the NSE publications came out 1986. So, it seems he spent some time correcting the data. There was an issue in the ^{252}Cf(sf) $\overline{\nu}_p$ measurement for 1978. However, there is a much bigger variation in the data for 1986. It is not completely clear to me that one data set is better than another.

- Diven (1961): This data set seems superseeded by (Hopkins, 1963). The 1961 data set was published only as a proceeding in that year, while the Nucl. Phys. publications came out 1963 with essentially the same two authors with switched order. So, it seems he spent some time correcting the data. Also, Diven gave a value at 3.415 and Hopkins at 3.9 MeV. Hopkins gave more data.

Rejected data sets because either clearly outlying, or for physics reasons, too large uncertainties or insufficient uncertainty information provided both in EXFOR or the literature:

- Johnstone (1965): The gate was open too long (500 μs). Hence, they measured a lot of background. The monitor is also not properly described in the EXFOR entry. It looks like natural uranium, not ^{235}U. The statistical uncertainty is huge (8.8%). The data will likely have no impact at all and are rejected. Not surprisingly, given the problems above, the data are clearly outlying. Missing corrections: attenuation, sample thickness, angular distribution of fission fragments, forward boost (14 MeV), geometry, displacement of sample.
- Huanqiao (1980): While many important corrections were undertaken, the detector efficiency is below 60%. This low detector efficiency makes it very likely that biases happen. Their data are also systematically lower than other data highlighting that indeed there could be an issue. Also, the journal article is in Chinese and cannot be found. Comment: Phil Young doubled the uncertainties.
- Leroy (1960): The gate was open too long (200 μs). Hence, they possibly measured a lot of background. The monitor is also not properly described in the EXFOR entry. It seems to be natural uranium rather than ^{235}U. The statistical uncertainty is huge (10%). The data point will likely have no impact at all and is rejected. Not surprisingly that data are clearly outlying by up to 5% (even more so than Johnstone). Missing corrections: displacement of sample, neutron flux variation, delayed gammas, sample roughness, foward-boost likely.
- Nesterov (1970): The neutron-detector efficiency is at 20%! The correction necessary is so big that it is very likely to introduce a bias. Not surprisingly, the data are outlying by up to 3% from ENDF/B-VIII.0 and clearly from the bulk of the data. Comment: Phil Young doubled the uncertainties. In the Volodin EXFOR entry 40148.001, they clearly state that these data are superseeded. They wrote: "Previously measured data published in 70HELSINKI are considered as overruled due to strong disagreement with this measurement in energy range 0.4 $<$ En$<$ 1.3 MeV caused by high ($\sim$10 times this one) admixture of ^{240}Pu in the sample used at the previous measurement."
- Smirenkin (1959): Two data points are given. One at 4 MeV, another at 15 MeV. The one at 4 MeV looks reasonable. The one at 15 MeV differs by 6% from the evaluated mean value. I was tempted to reject the second data point given that rather large outlying behavior, especially considering recent CEA experimental data. However, I found several issues in the data: $\overline{\nu}$ is measured by a coincidence of two fission halves in an ionization chamber. One sees the neutron flux by detecting fission fragments which is the start signal. Another counts the neutrons being emitted from the fission event by detecting again fission events. Between the two halves is a Pt foil that could lead to scattering effects thanks to known Coloumb scattering effects on fission fragments (bad choice from todays' perspective). That, however, does not explain why one data point (4 MeV) is fine while the one at 15 MeV has a major issue. The coincidence counting was 3–5 mins which is very long. Background was consequently overwhelmingly large by 30-50%. With a 10% uncertainty that would lead to 3-5% uncertainty which would lead to an overlap between evaluation and experiment, but effectively de-weights the data. Not corrected for angular distribution of FF and forward boost which should be substantial at 15 MeV. Many important effects are not corrected or the necessary corrections are huge!